Investigating Dark Matter: Insights from Stars

Ilídio Lopes

Center for Astrophysics and Gravitation

Instituto Superior Técnico
University of Lisbon

13th IDPASC SCHOOL

IDPASC

DiFC

INFN
LNS

AISF associazione italiana studenti di fisica

TÉCNICO LISBOA

centra
30th Anniversary

Outline

- Dark Matter in the Universe
  – Evidence in the Universe and Milky Way
  – Status of the Standard Model and Candidates for Dark Matter
- How Dark Matter affects Stars
  – Capture, Evaporation, Annihilation and transport of energy.
- Dark Matter Constraints
  – Axions, WIMPs, Asymmetric Dark Matter, Annihilating Dark Matter
- Conclusion
  – What we know, and what we can learn

Dark Matter in the Universe

TÉCNICO LISBOA

Dark Matter in the Universe

Energy density

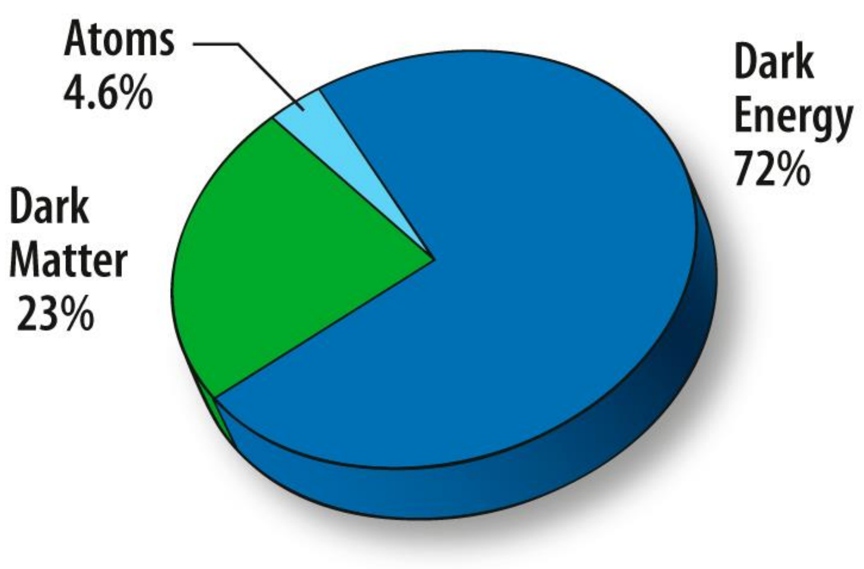

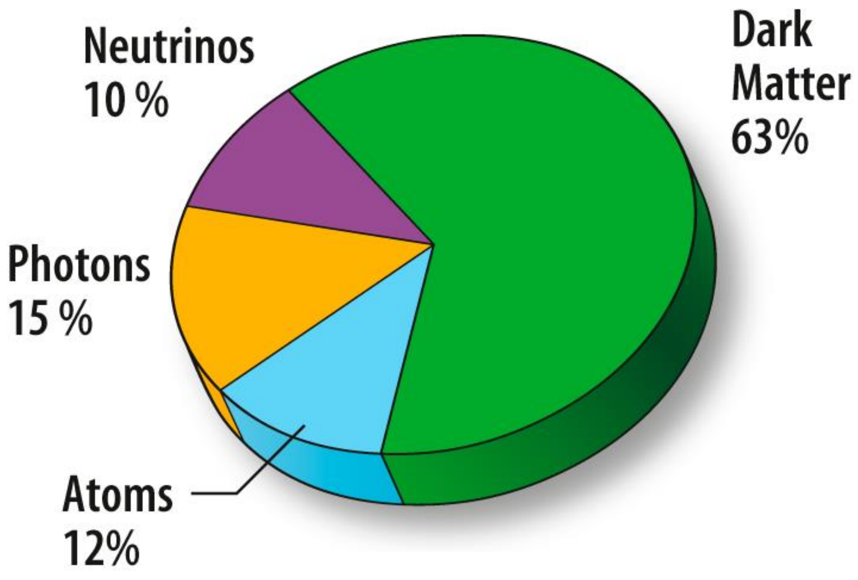

Today **~ 380 000 years (CMB)**

https://wmap.gsfc.nasa.gov/universe/uni_matter.html **Nature of Dark Matter:** cold weakly interacting particles

Lambda-CDM Model: The dark matter creates the gravitational web for the formation of structures that reproduces the observed present baryonic structure of the Universe, i.e., stars, stellar clusters, galaxies, galaxy clusters.

Dark Matter in the Universe

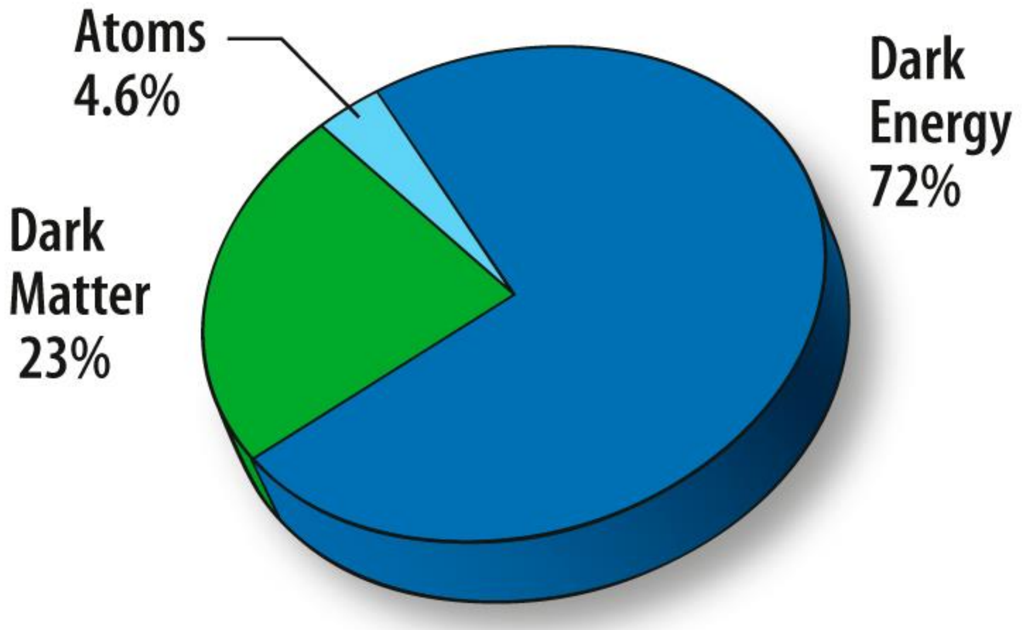

Today

CL0024+17 cluster of galaxies (HST, 2004): Gravitational lensing, the bending of light rays by gravity, can also give us a cluster's mass.

Observational Evidence: This HST optical image of the galaxy cluster CL 0024+17 shows the gravitational lensing of faraway galaxies by the nearby galaxies. The gravitational lensing is created by dark matter clustered around each galaxy.

Dark Matter in the Universe (Zoom in)

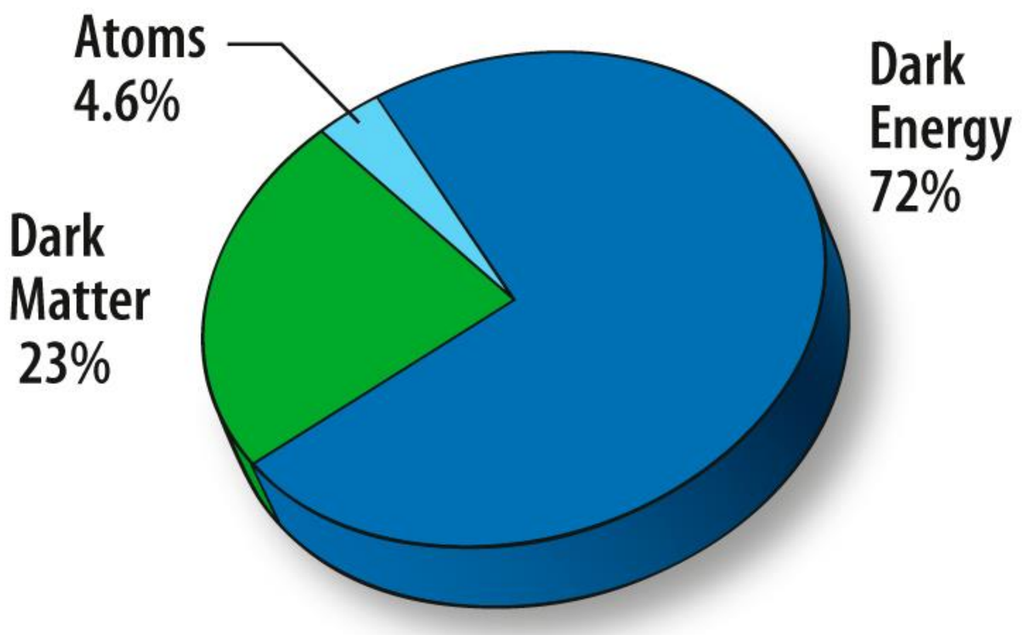

Today

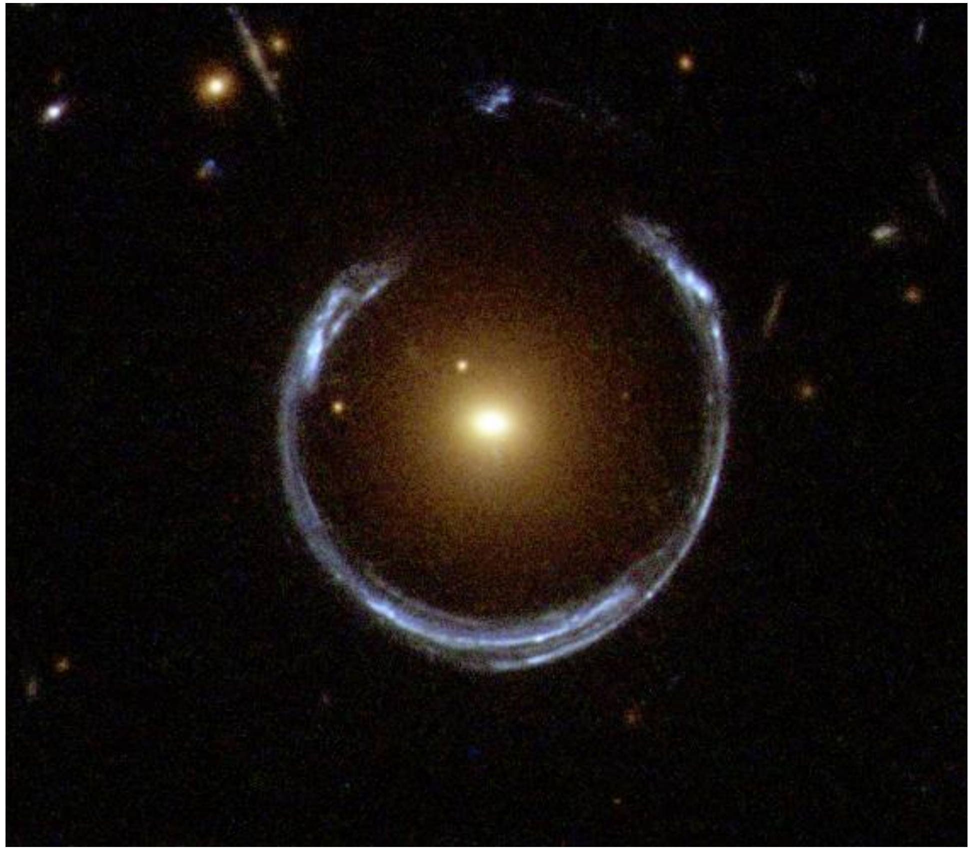

Image LRG 3-757 (HST): the gravitational field of an orange luminous galaxy gravitationally distorted the light from a much more distant blue galaxy. The almost perfect alignment between Earth and galaxy (blue) gives rise to the resulting image that is an **almost complete Einstein ring** (Belokurov et al. ApJ 2007).

Observational Evidence: This HST optical image of the galaxy cluster CL 0024+17 shows the gravitational lensing of faraway galaxies by the nearby galaxies. The gravitational lensing is created by dark matter clustered around each galaxy.

TÉCNIC

Dark Matter in the Universe

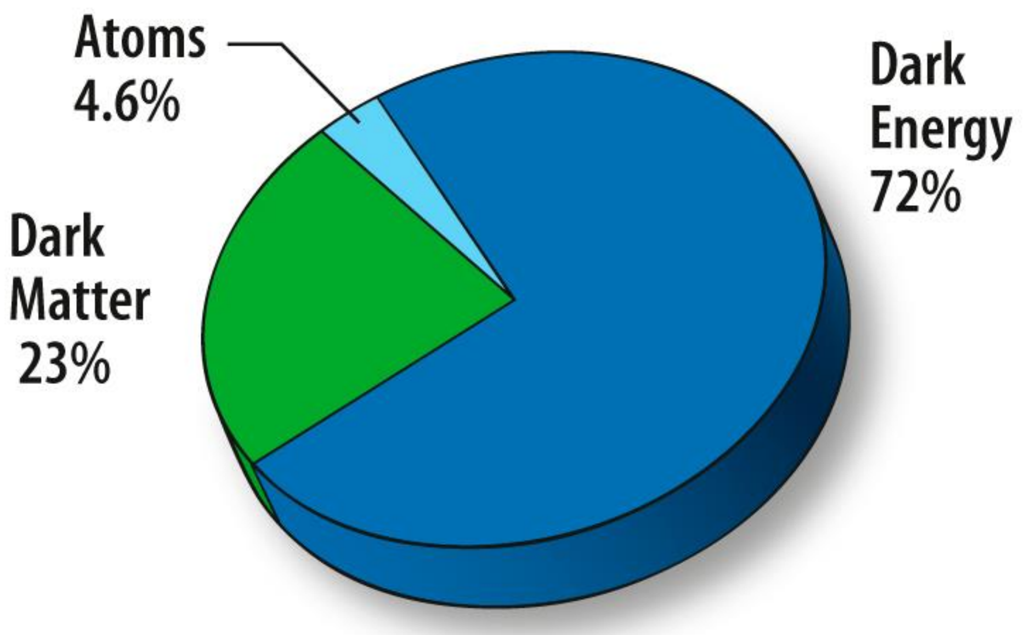

Today

The gravity map super-imposed on the HST image which shows a dark matter distribution in the central region and a thick ring.

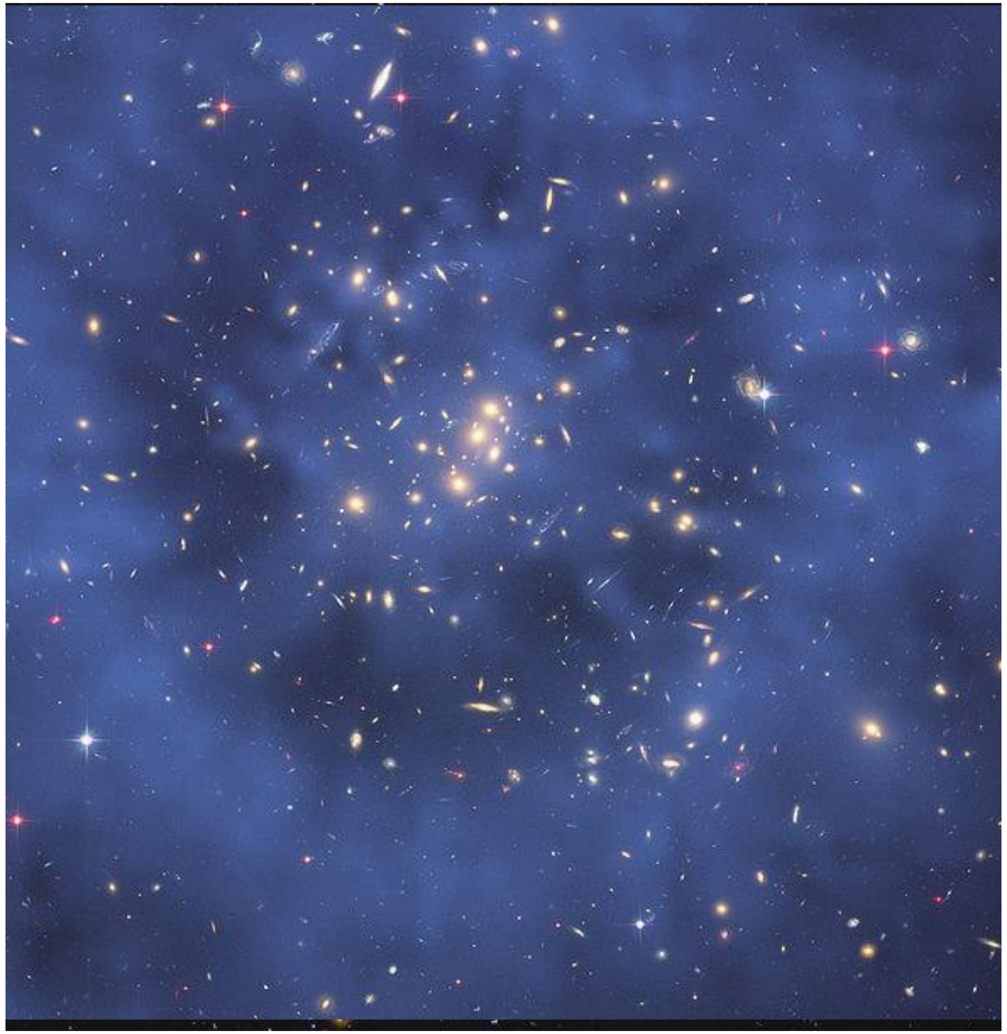

CL0024+17 cluster of galaxies (HST, 2004): Gravitational lensing, the bending of light rays by gravity, can also give us a cluster's mass.

Observational Evidence: A strong evidence of dark matter is the HST image of the galaxy cluster CL0024+17 as shown in this Figure. Because of their mutual gravitational attraction, dark matter and visible material are generally expected to be together, however in this image the dark matter distribution does not match with that of the stars

TÉCNIC

Dark Matter in the Universe

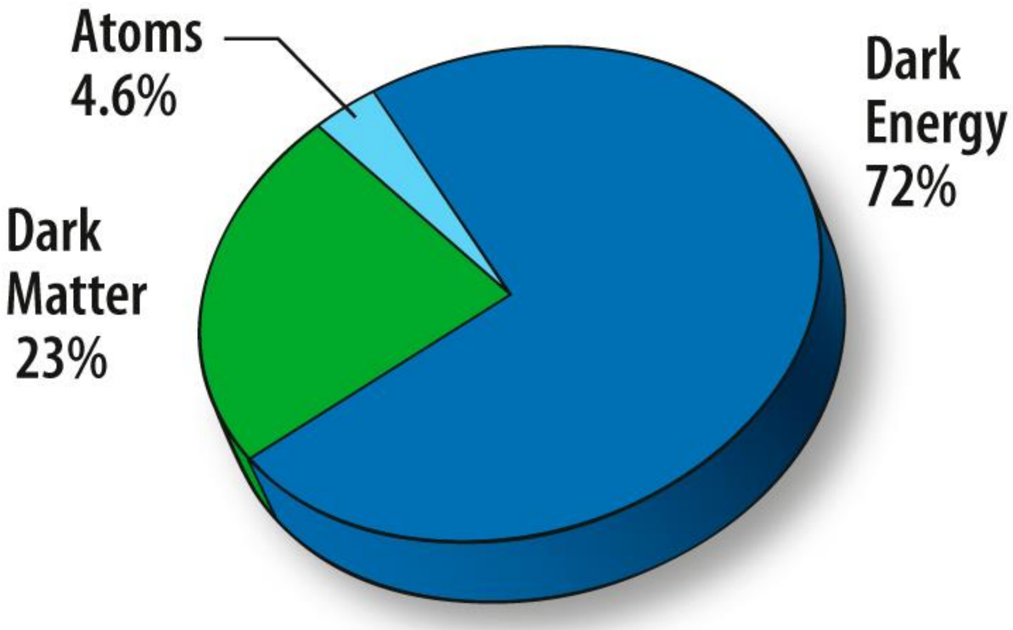

Today

Bullet cluster of galaxies 1E 0657-56

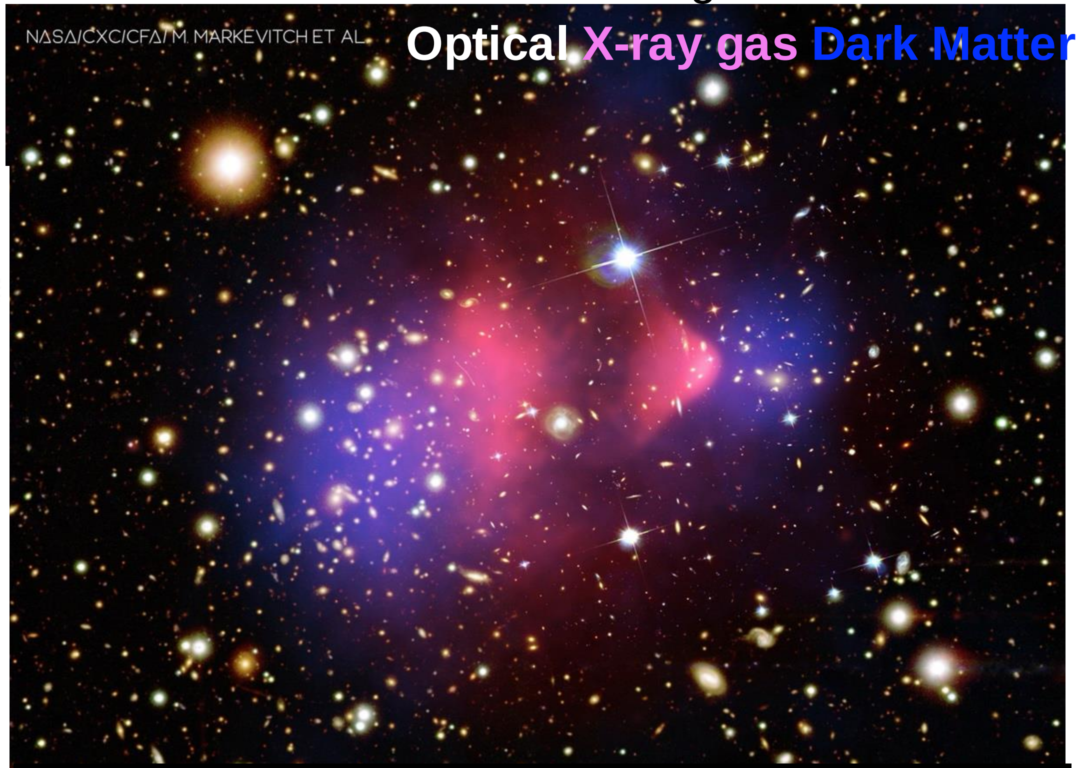

Image: optical, pink: X-ray gas, blue: lensing

$M_{total}: M_{gas}: M_{star} \sim 70:10:1$

Clowe, Gonzalez & Markevitch ApJ 2004

+ 72 bullet clusters by Harvey et al. Science 2015

Observational Evidence: This image of the bullet cluster is a composite of optical (HST:white), X-ray (Chandra X-ray Observatory: pink), and a reconstructed mass map (lensing mass: blue). It shows that the total mass of the system (galaxies +dark matter) is not where is the X-ray gas. This fixes a bound for **dark matter self-interaction cross section:** $\sigma/m < 8.3 \times 10^{-25}$ cm^2/GeV **at 95% CL**

TÉCNIC

Dark Matter in the Universe

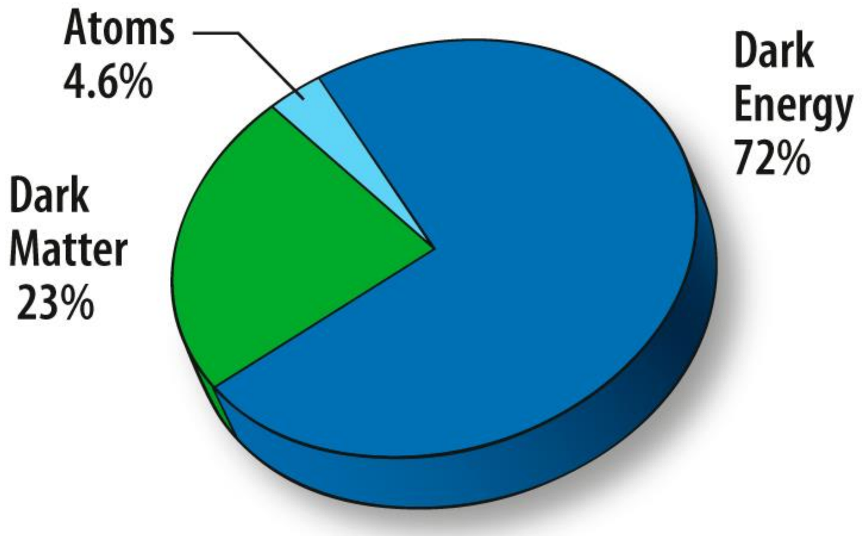

Today

visible matter + dark matter

Vera Rubin et al., 1976, ApJL

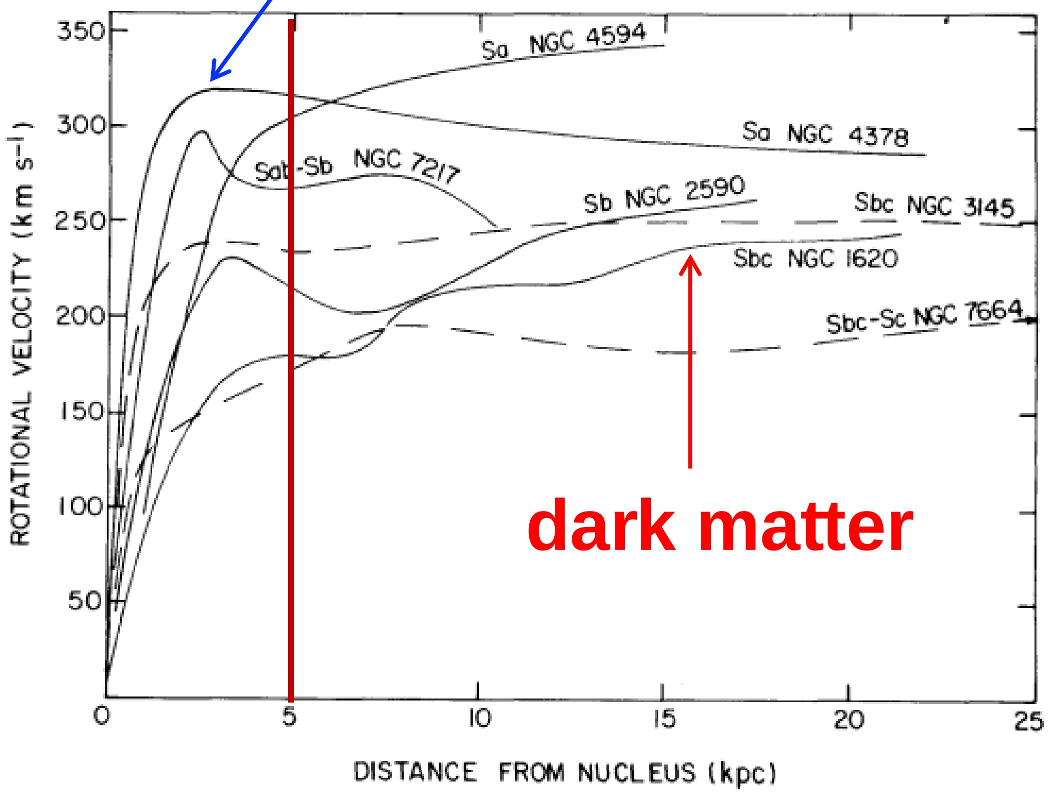

Vera Rubin and Kent Ford have made these critical observations in **1975.**

The radius of 90% of the enclosed "visible matter" is shown as the vertical red line.

Observational Evidence: Inner galactic core (Milky Way), the comparison of the observed rotation curve (data from gas and stars kinematics) with the predictions of baryonic models strongly support the existence of dark matter (Iocco et al. 2015).

Dark Matter in the Universe

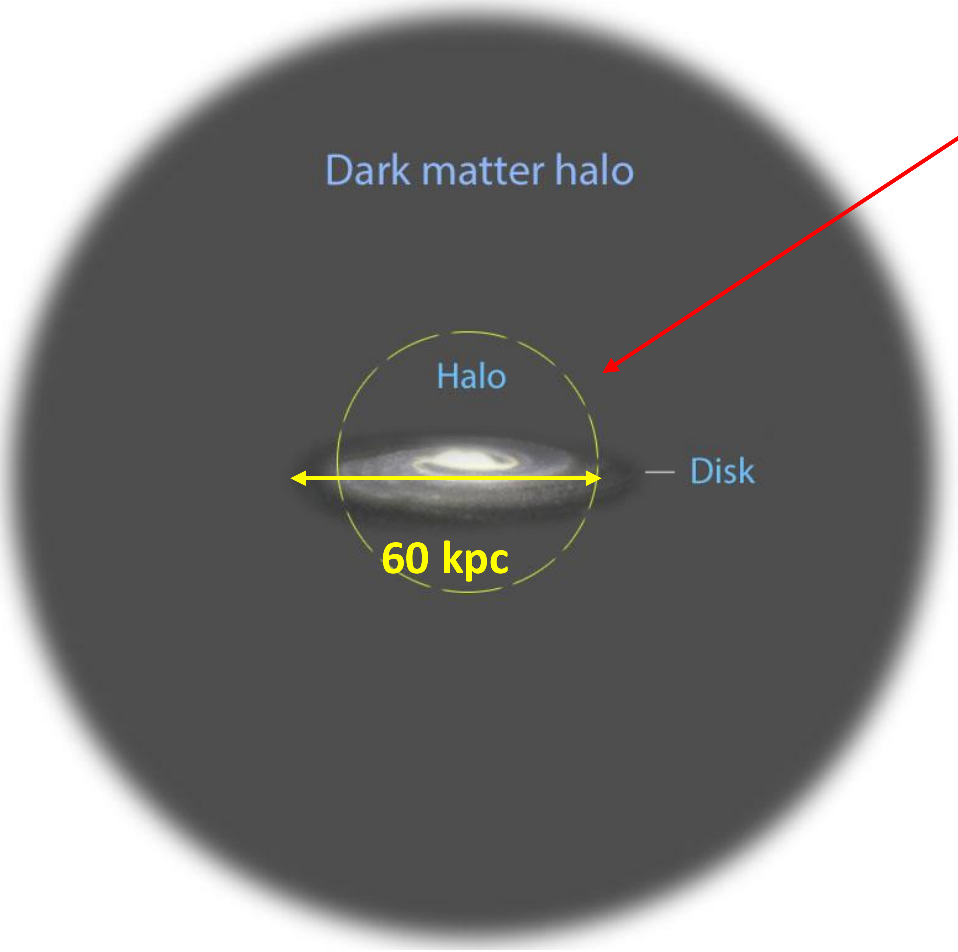

Star s

Milky Way: Standard DM Halo

visible matter + dark matter

Vera Rubin et al., 1976, ApJL

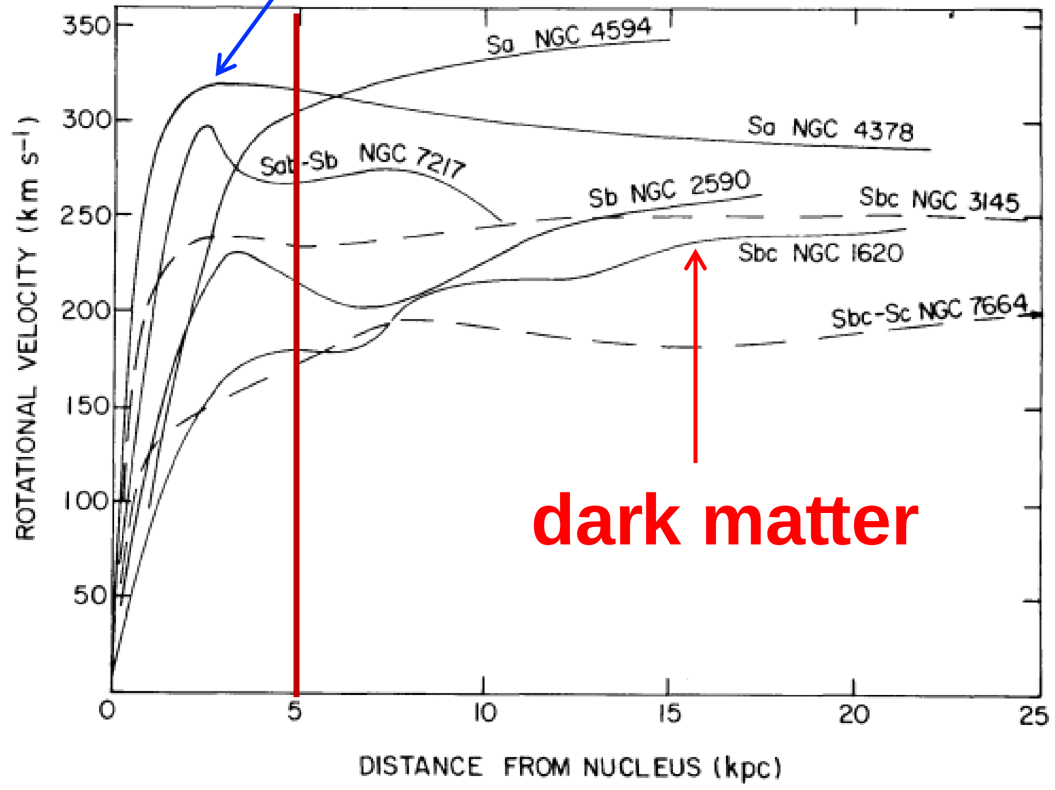

Observational Evidence: In the standard cosmological model, **the dark matter halo** of a galaxy like the Milky Way forms from the merger and accretion of smaller sub-halos. These sub-units also harbour stars, typically old and metal-poor, that are deposited in the inner galactic regions by disruption events.

Dark Matter in the Universe

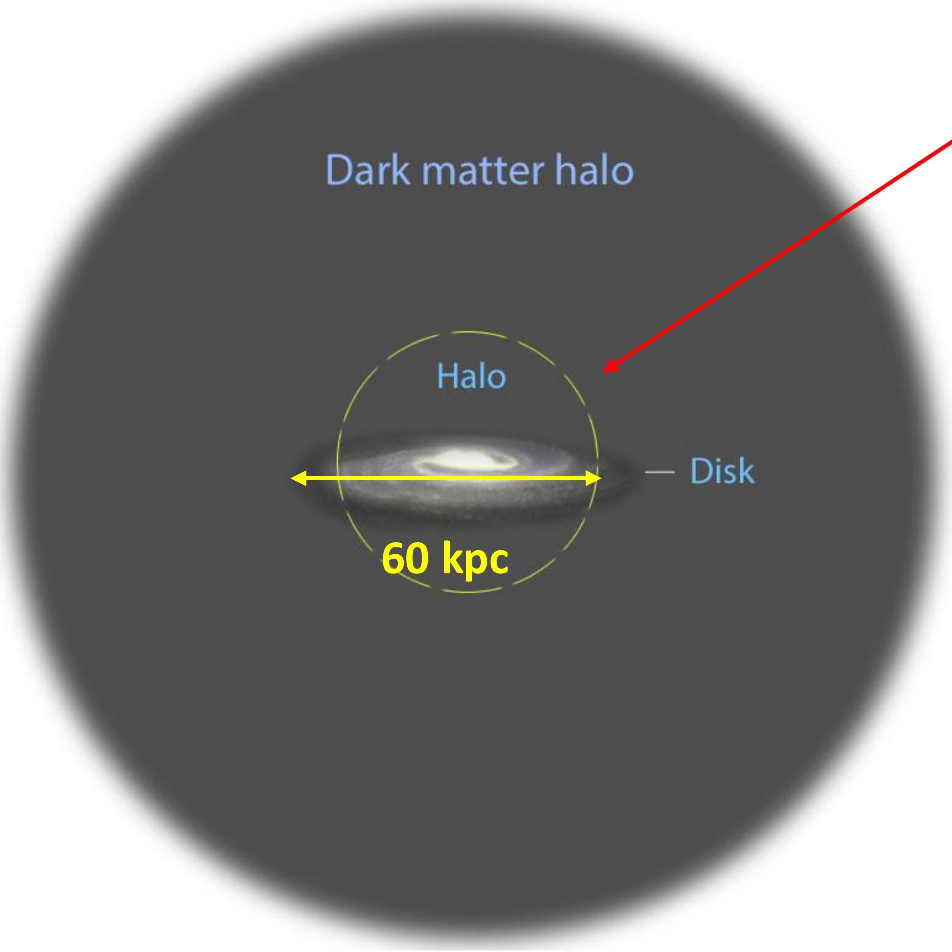

Milky Way: Standard DM Halo

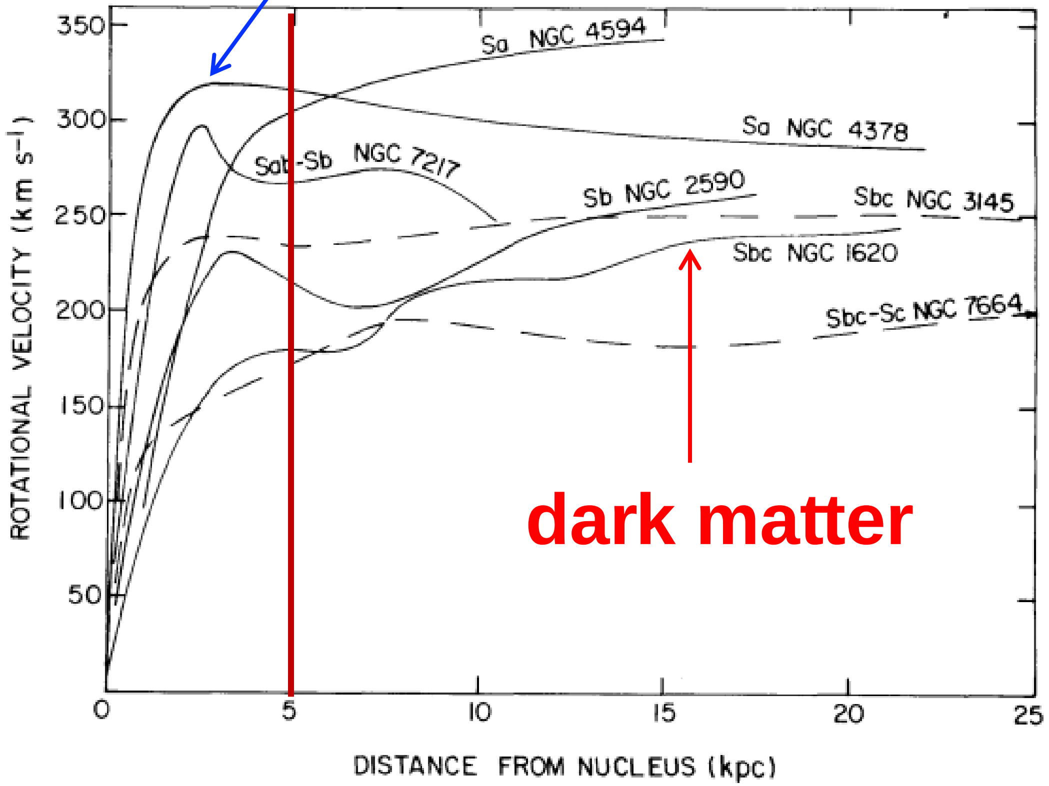

Dark Matter content of the Milky Way: Among other authors, Posti and Helmi (2019), using GAIA data (globular cluster motions), estimated that the total mass of the Milky Way within the region of 20 Kpc to be $1.91 \pm 0.17 \times 10^{11}$ M☉ of which 70% is dark matter.

Important point: numerical simulations predict 90% - 95 % of the Milky Way mass is dark matter (up to 200 Kpc).

Dark Matter in the Universe

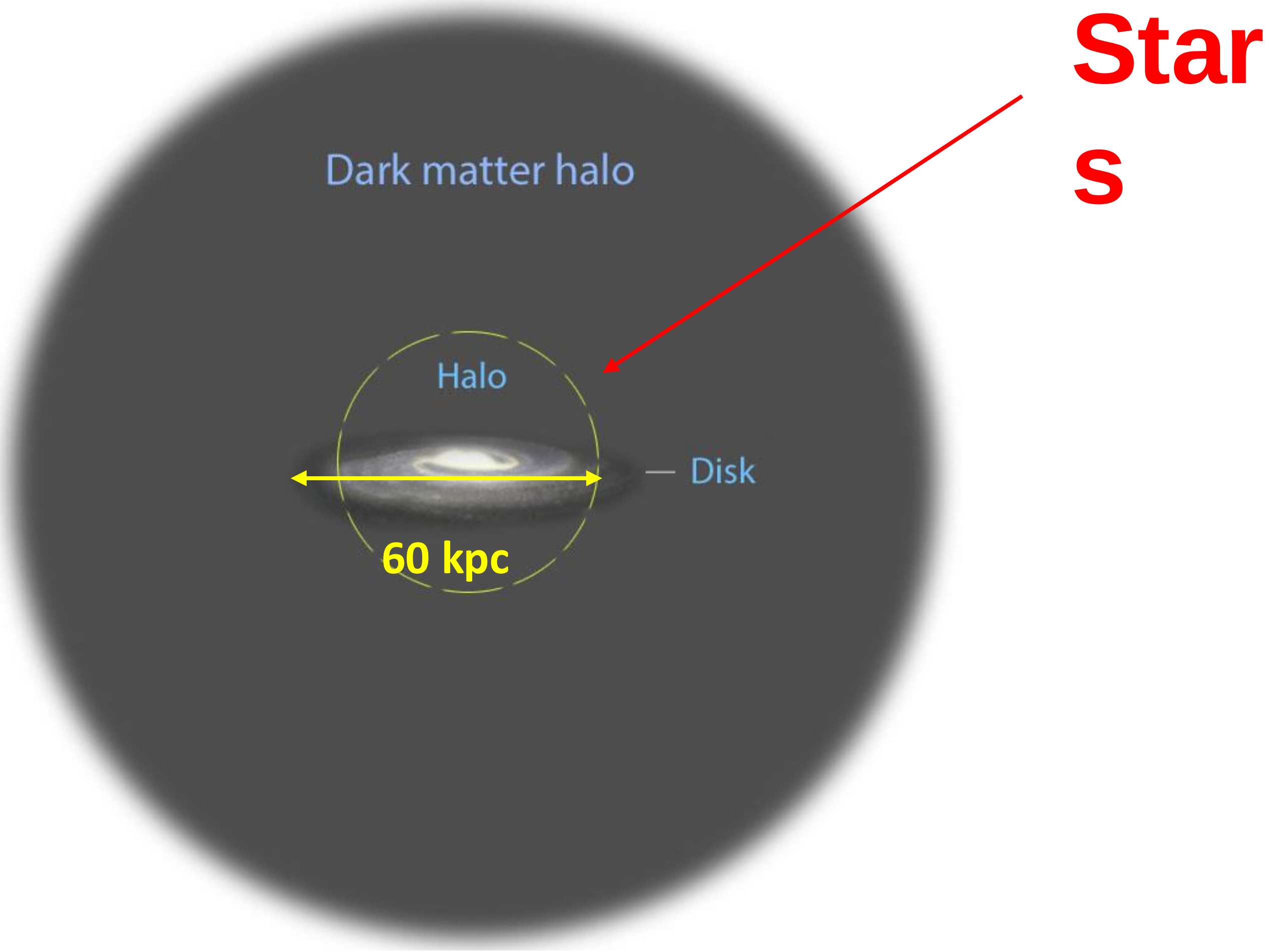

Milky Way: Standard DM Halo

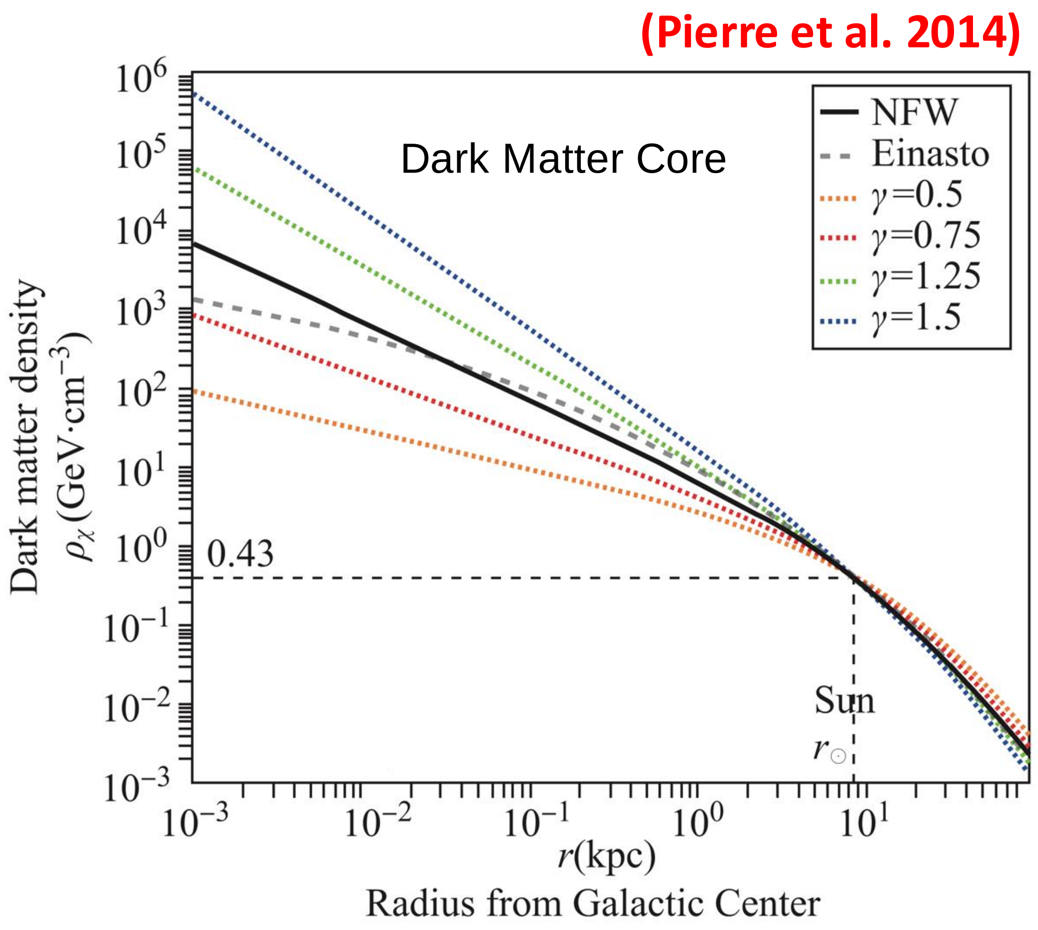

dark matter density at the Sun's position is ~ 0.4 GeV/cm^3

Dark Matter content of the Milky Way: In light of the uncertainty in the DM distribution in the Inner Galaxy and the dependence of the signal on it, there is a range of possible density profiles. The most common benchmarks are NFW and Einasto profiles.

Dark Matter in the Universe

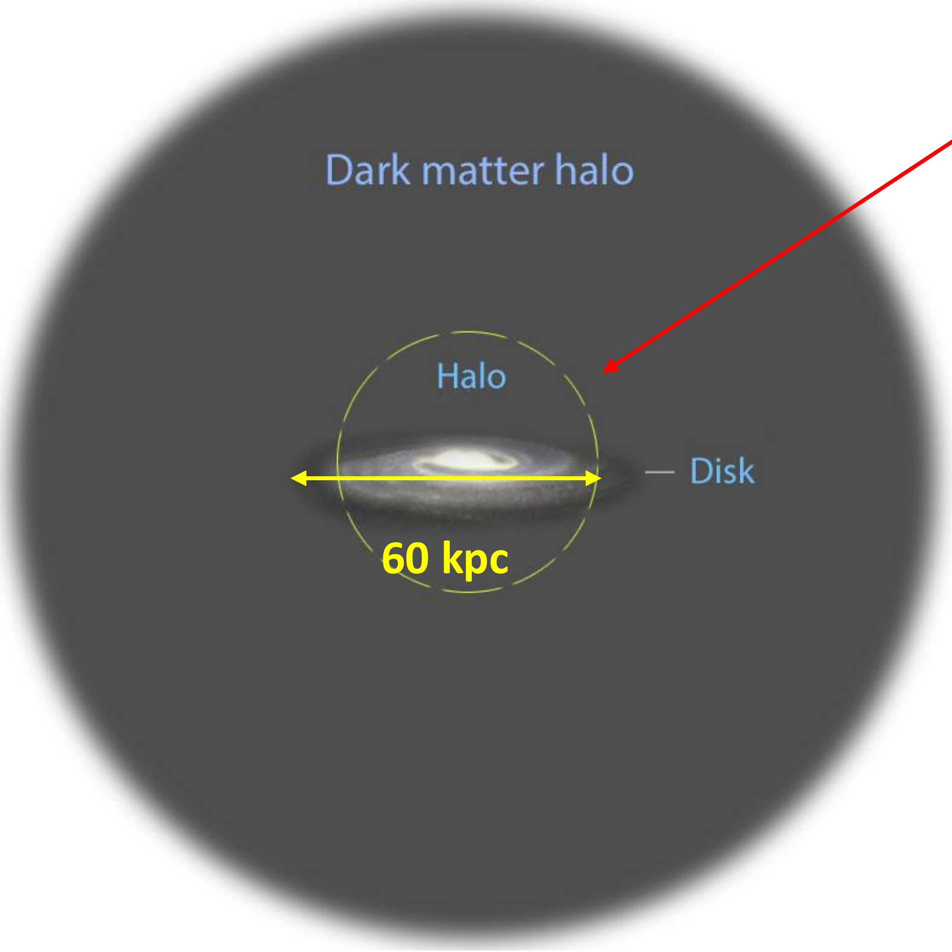

Star s

(Balaji et al. 2023, Gondolo & Silk 99)

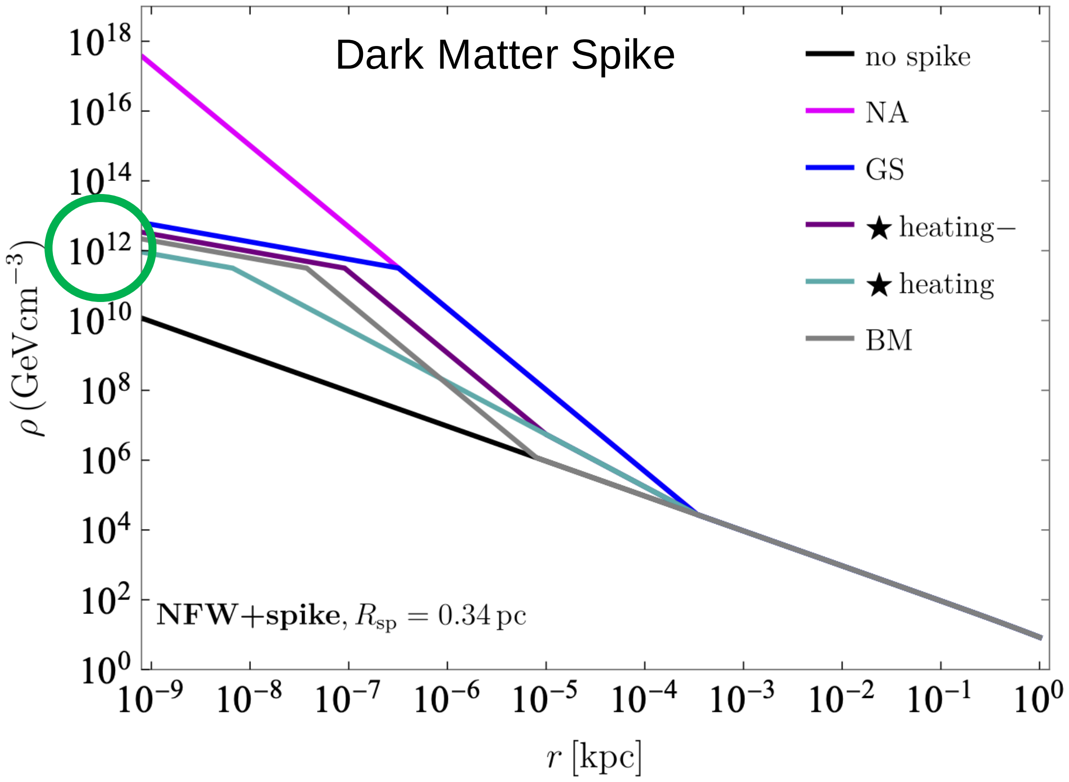

Milky Way: Standard DM Halo

dark matter density at the Sun's position is ~ 0.4 GeV/cm^3

Dark Matter content of the Milky Way: In light of the uncertainty in the DM distribution in the Inner Galaxy and the dependence of the signal on it, there is a range of possible density profiles. The most common benchmarks are NFW and Einasto profiles.

The density of the most metal-poor stellar population exhibits the same dependence on the radius as the DM near the Sun's position (Herzog-Arbeitman et al. 2018).

Dark Matter in the Milky Way

A large amount of the total mass of the Milky Way is dark matter

Dark Matter in the Universe

(What is dark matter made of ?)

What is dark matter made of?

Standard Model of Elementary Particles

This graph shows the mass distribution of elementary particles, along with important energy scales. The exact masses of neutrinos are unknown; their placement indicates the maximum possible value (Zupan 2019).

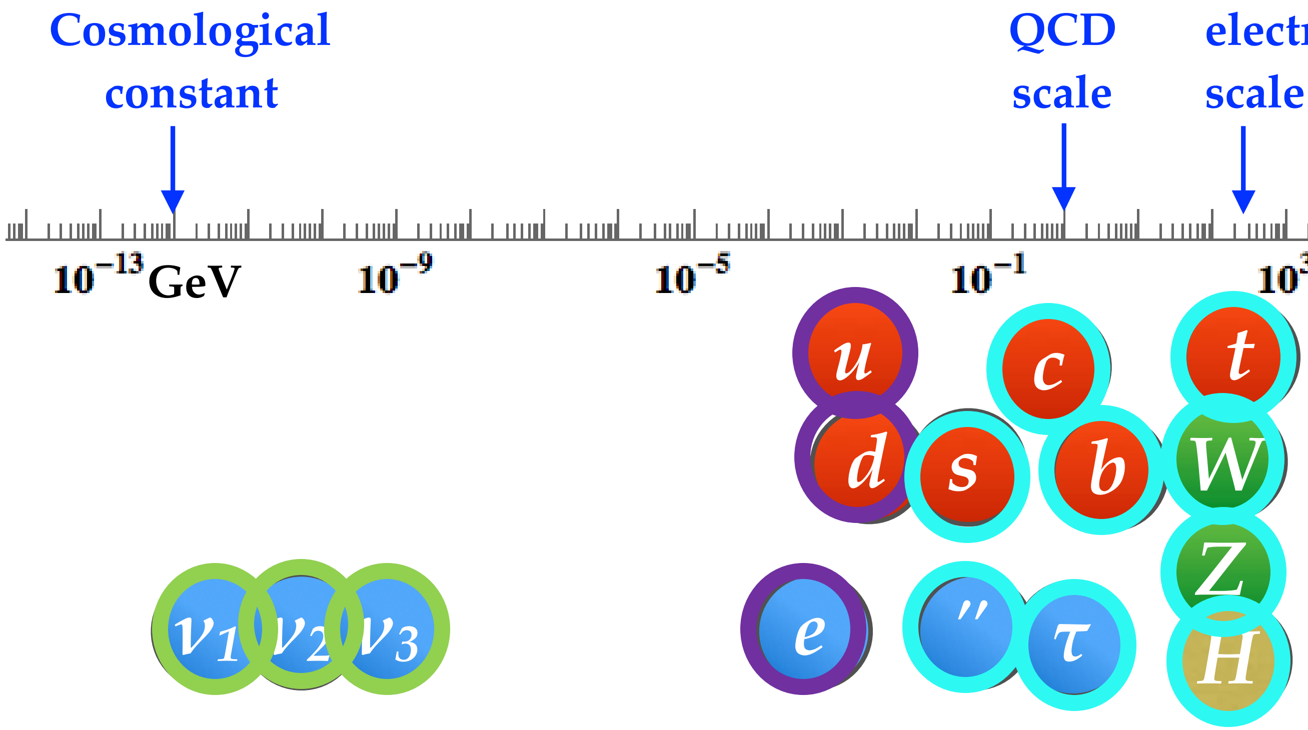

Bosons (mass zero):

Gluon (g) and Photon (γ)

Couples to the plasma

Disappears too quickly

Hot dark matter

This table of elementary particles (with its rules) explains the origin of all known matter of the Universe (that corresponds to 4% of the cosmological density).

What is dark matter made of?

Standard Model of Elementary Particles

This graph shows the mass distribution of elementary particles, along with important energy scales. The exact masses of neutrinos are unknown; their placement indicates the maximum possible value (Zupan 2019).

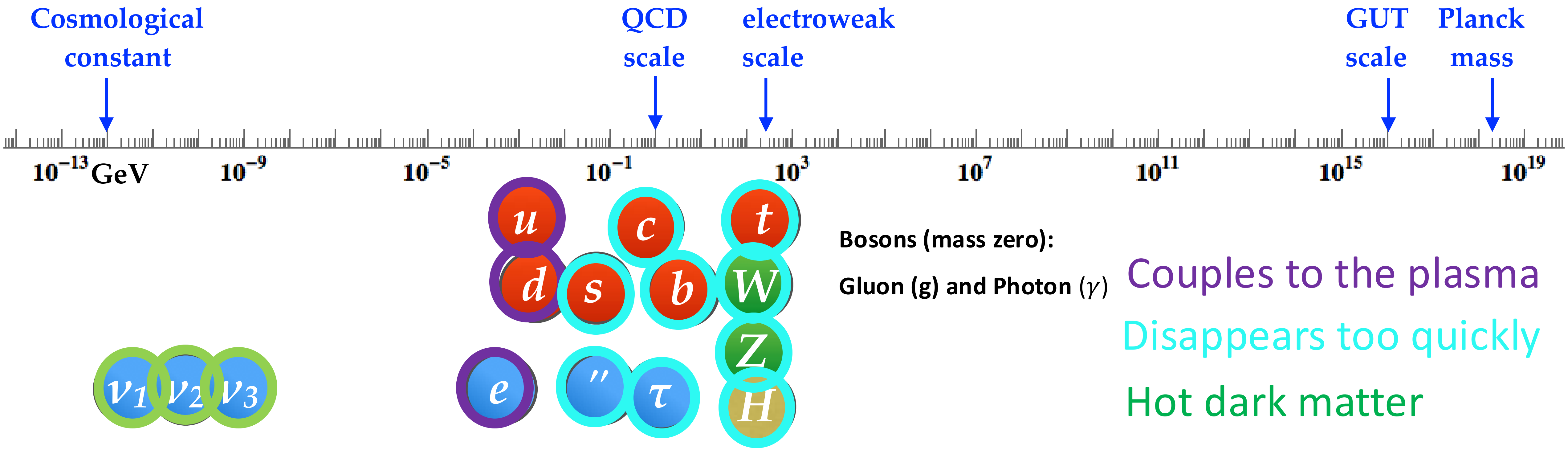

Bosons (mass zero):

Gluon (g) and Photon (γ)

Couples to the plasma

Disappears too quickly

Hot dark matter

This table of elementary particles (with its rules) explains the origin of all known matter of the Universe (that corresponds to 4% of the cosmological density).

None of these particles can be constituents of dark matter.

If not standard particles, then how to proceed …

What is dark matter made of?

Standard Model of Elementary Particles

This graph shows the mass distribution of elementary particles, along with important energy scales. The exact masses of neutrinos are unknown; their placement indicates the maximum possible value (Zupan 2019).

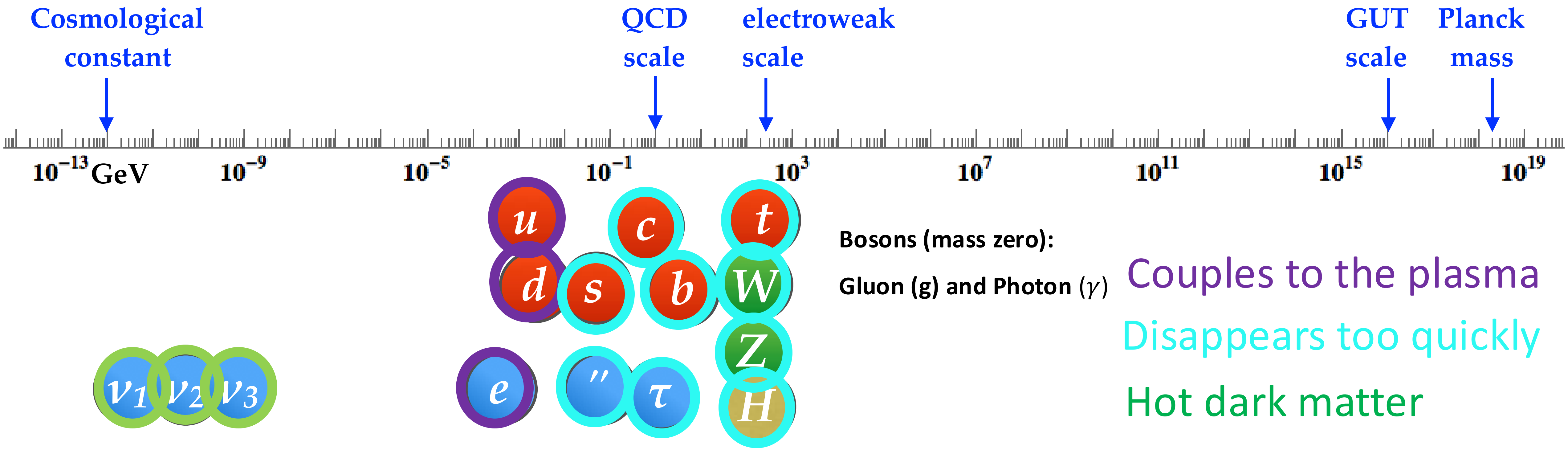

As the standard model is quite successful in explaining all the known interactions (other than gravity), let us now consider that these new particles have somehow identical properties to the ones found in the standard particles.

What is dark matter made of?

Standard Model Extend

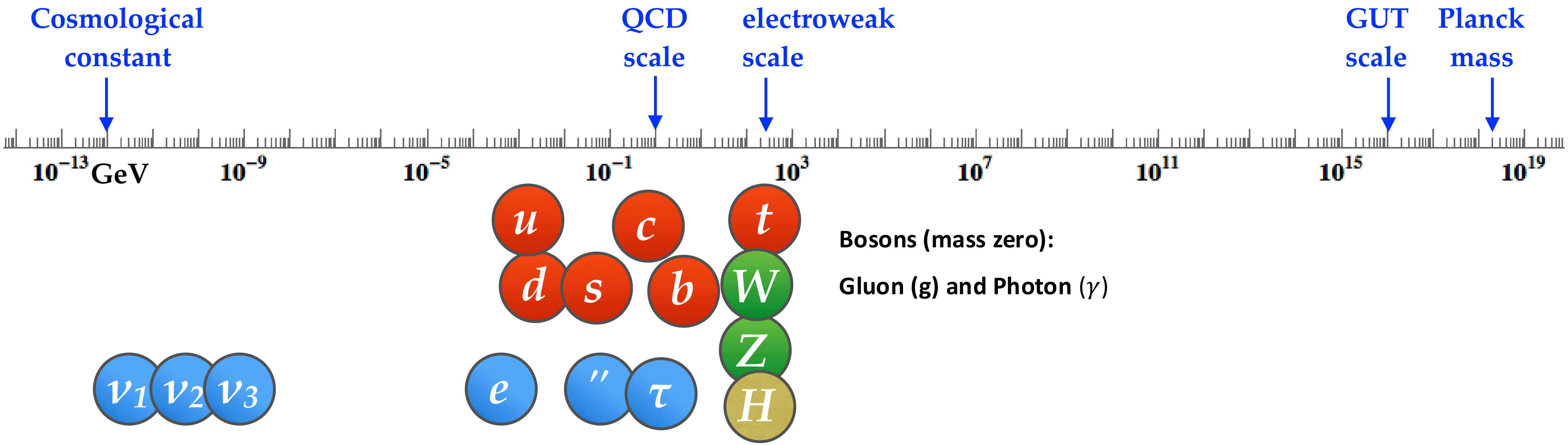

As the standard model is quite successful in explaining all the known interactions (other than gravity), let us now consider that these new particles have somehow identical properties to the ones found in the standard particles.

What is dark matter made of?

Standard Model Extended

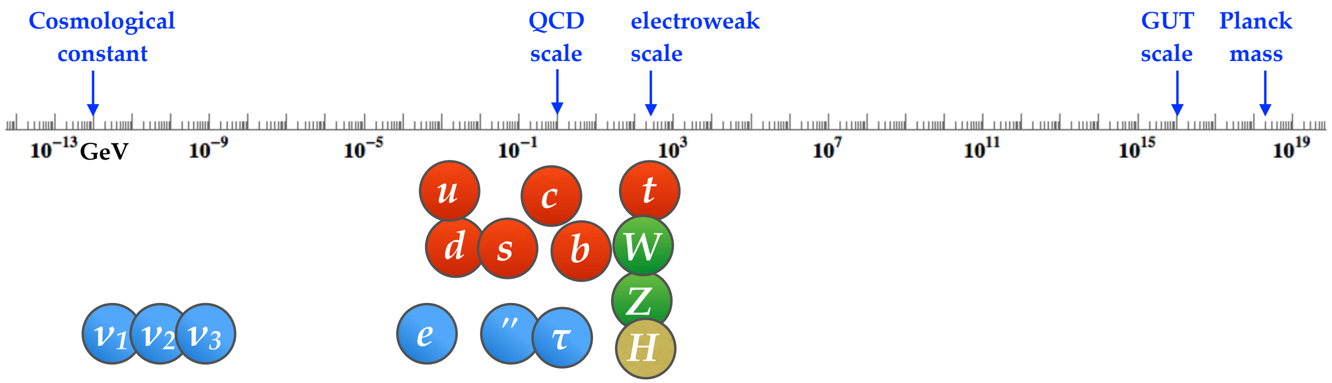

+ new fermions

new bosons

New particles

Visible sector **Dark (matter) sector**

Expected properties of the Dark Matter particles: They should have the cosmic dark matter density, have mass, weak interacting with ordinary matter, be non-relativistic, **be stable or very long-lived;** compatible with bounds coming from experimental (direct an indirect) detectors,

What is dark matter made of?

Standard Model Extend

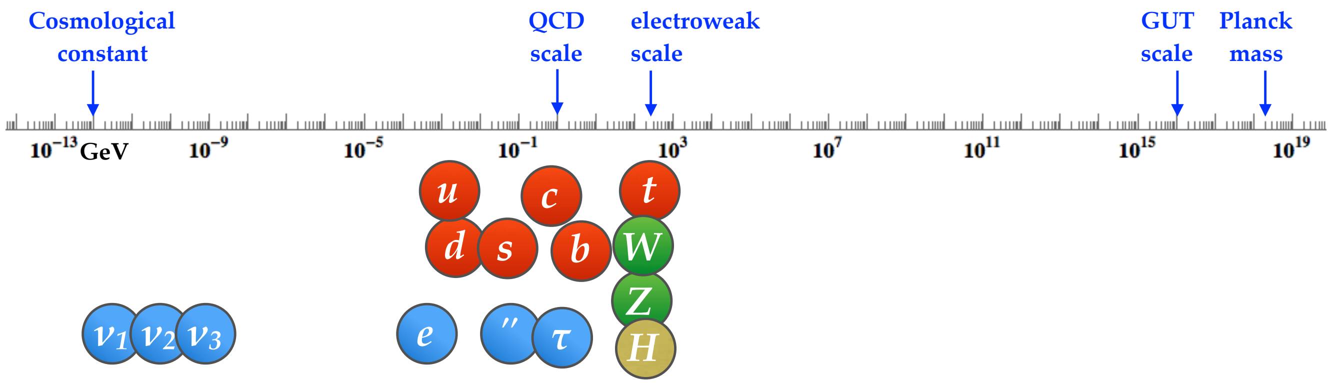

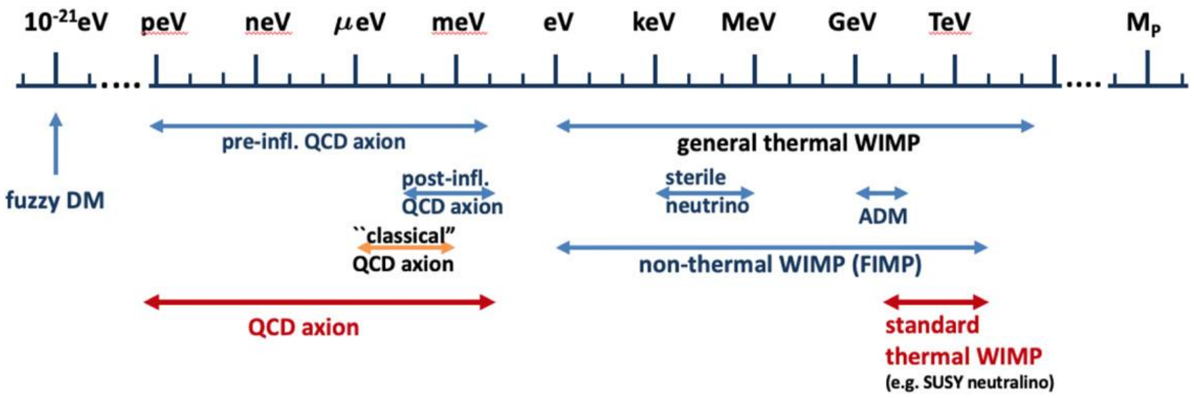

+ new fermions

new bosons

Visible sector

Dark (matter) sector

Expected properties of the Dark Matter particles: They should have the cosmic dark matter density, have mass, weak interacting with ordinary matter, be non-relativistic, **be stable or very long-lived;** compatible with bounds coming from experimental (direct an indirect) detectors,

What is dark matter made of?

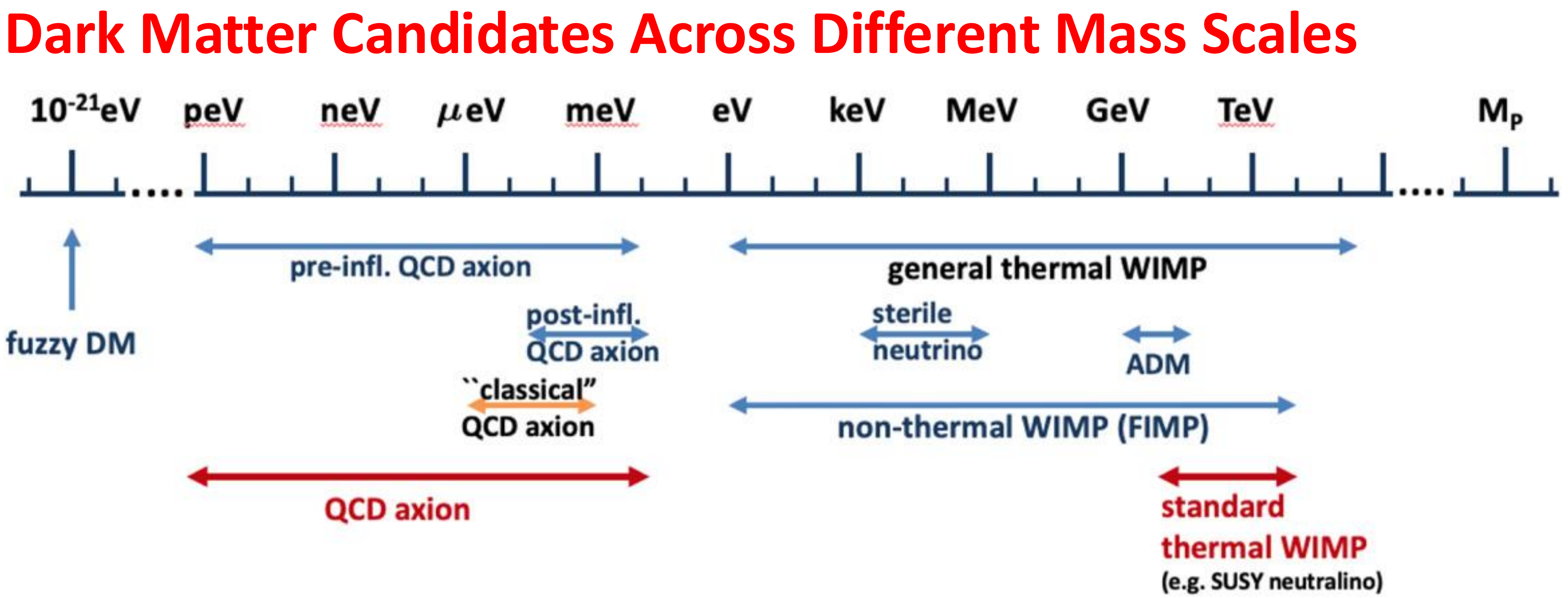

Julien Billard et al. 2022

The mass spectrum of dark matter candidates ranges from extremely low masses: 10^{-21} eV to very high masses, potentially approaching the Planck mass Mp (= 10^{28} eV)

It categorises these candidates into different types and their corresponding mass ranges: Axion Like Particles, General Thermal WIMP (Annihilating DM), Sterile Neutrinos and Asymmetric Dark Matter.

The best motivate dark matter candidates are the non-relativistic **(cold) particles.**

What is dark matter made of?

Dark Matter Candidates: Theory

Picobarn=10^{-36} cm^2

Heros (2020)

Cold particles (blue, cyan, green)

Warm particles (pink)

Hot particles (red)

The candidates span a range of 35 orders of magnitude in mass and 50 orders of magnitude in the scattering cross-section with baryons.

Popular candidates of dark matter are indicated by their mass and strength of interaction with ordinary matter.

The best motivate dark matter candidates are the non-relativistic **(cold) particles.**

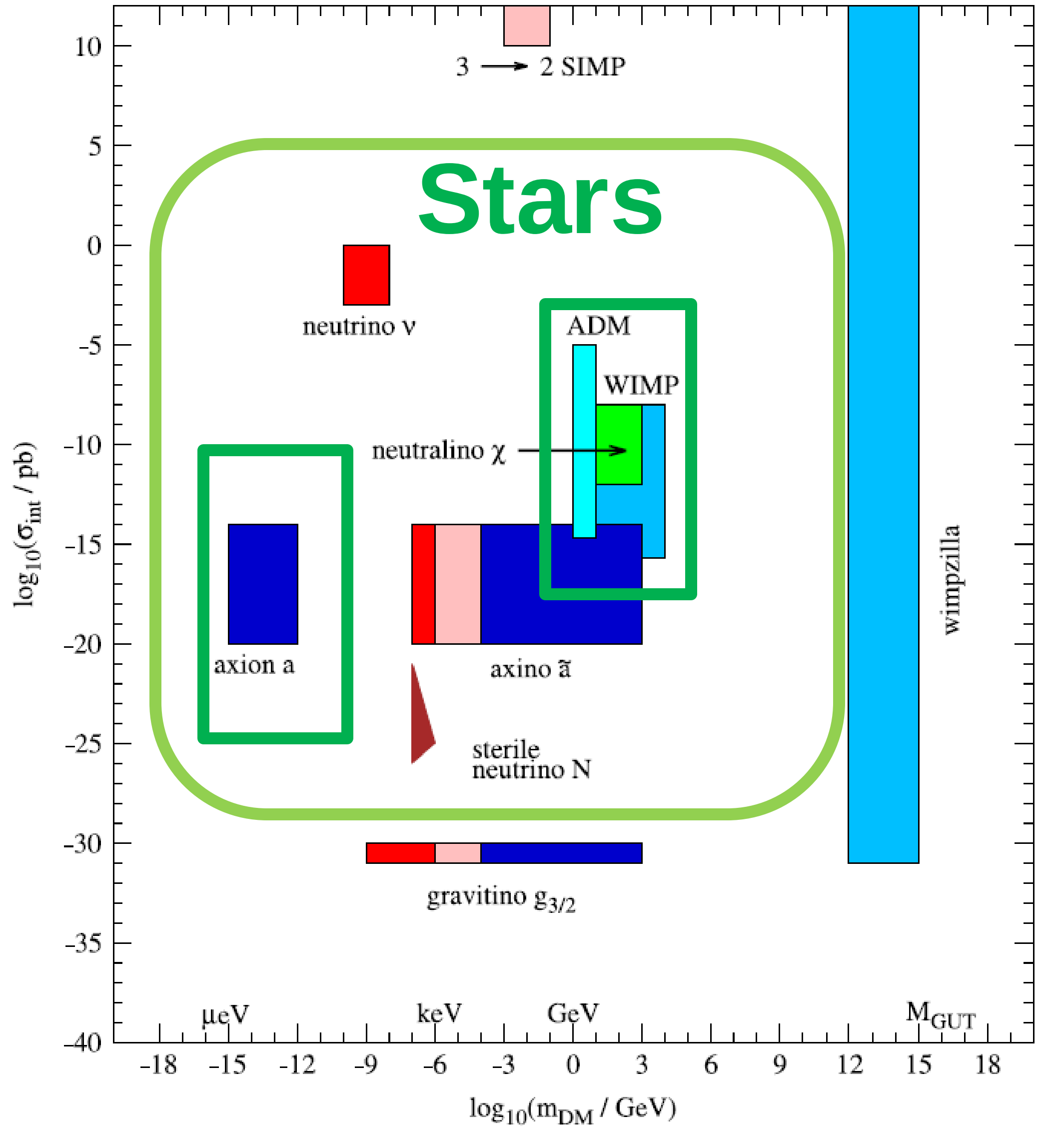

What is dark matter made of?

Dark Matter Candidates: Experimental Bounds

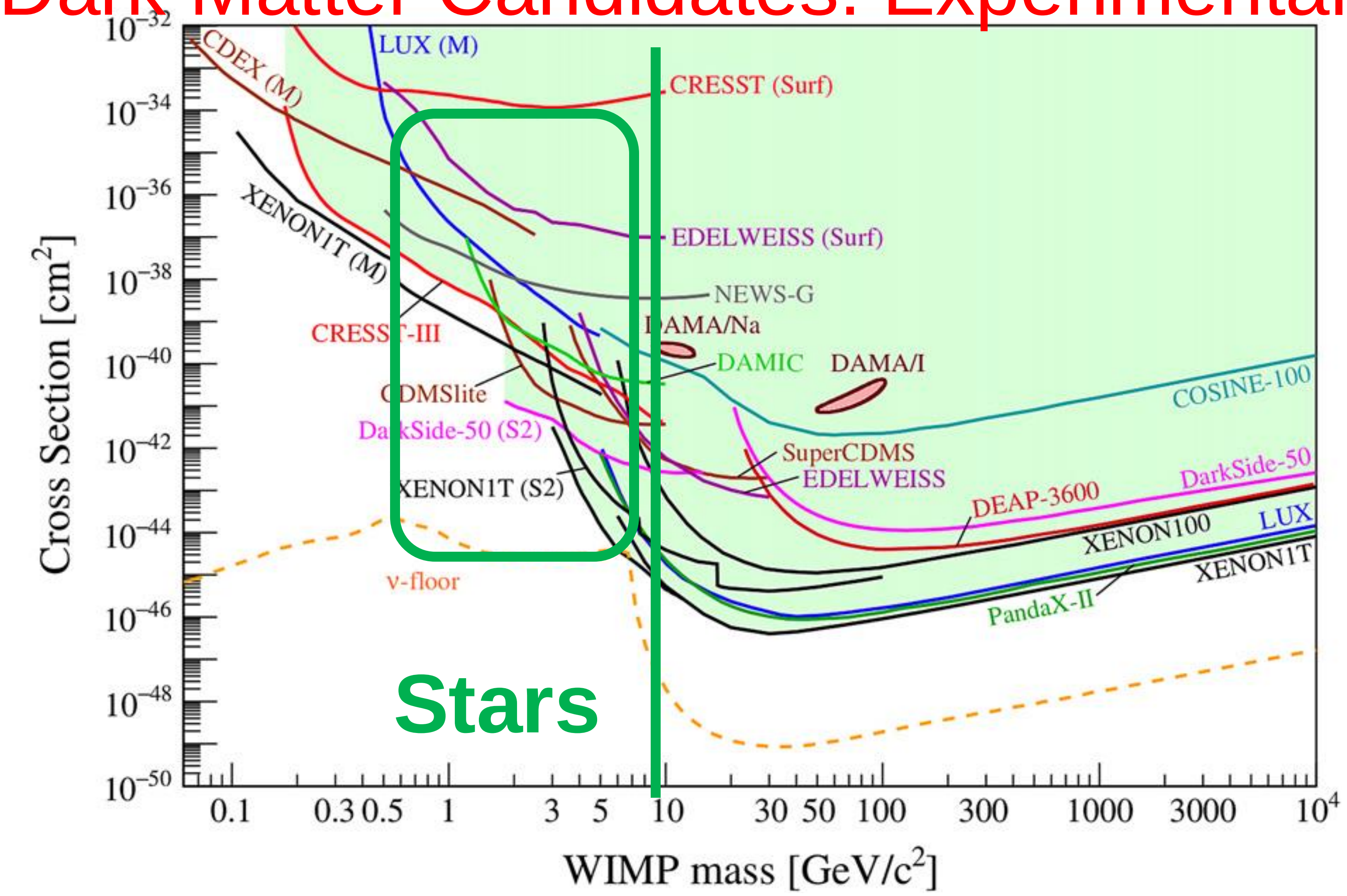

Billard et al. (2022)

Stars located in regions of high dark matter density: DM Galactic core ($\sim 10^4$ GeVcm^{-3}) and/or DM spikes ($\sim 10^{12}$ GeVcm^{-3}, Balaji et al. 2023)

The region below of 20 GeV shown as the **vertical green** line is difficult to probe by experimental detectors and corresponds to **dark matter candidates that most affect stars.**

Expected properties of the dark matter particles: Current and future limits on DM direct detection: spin-independent cross section as a function of DM mass.

What is dark matter made of?

Dark Matter Candidates: Axions

Batkovic et al. (2021)

The candidates span a range of 19 orders of magnitude in mass m_a and 25 orders of magnitude in the coupling constant $g_{a\gamma}$ with baryons.

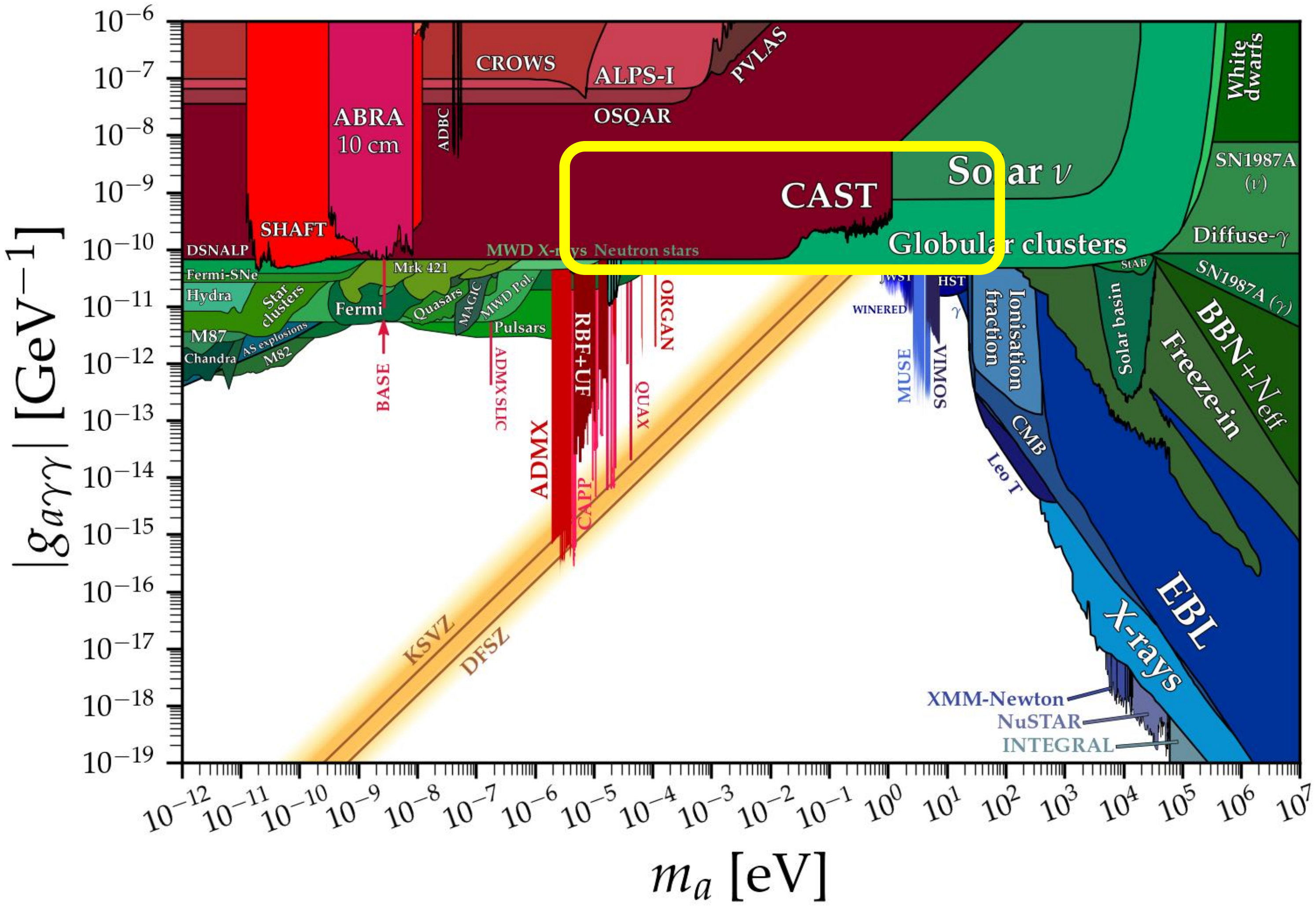

Sun and Stars

Important Point

The Sun and stars are sensitive to several type of dark particles which are difficult to probe by direct dark matter detection experiments.

Stellar Astrophysics and Constraints

(Helio- Asteroseismology)

TÉCNICO LISBOA

Pulsating stars in the HR diagram

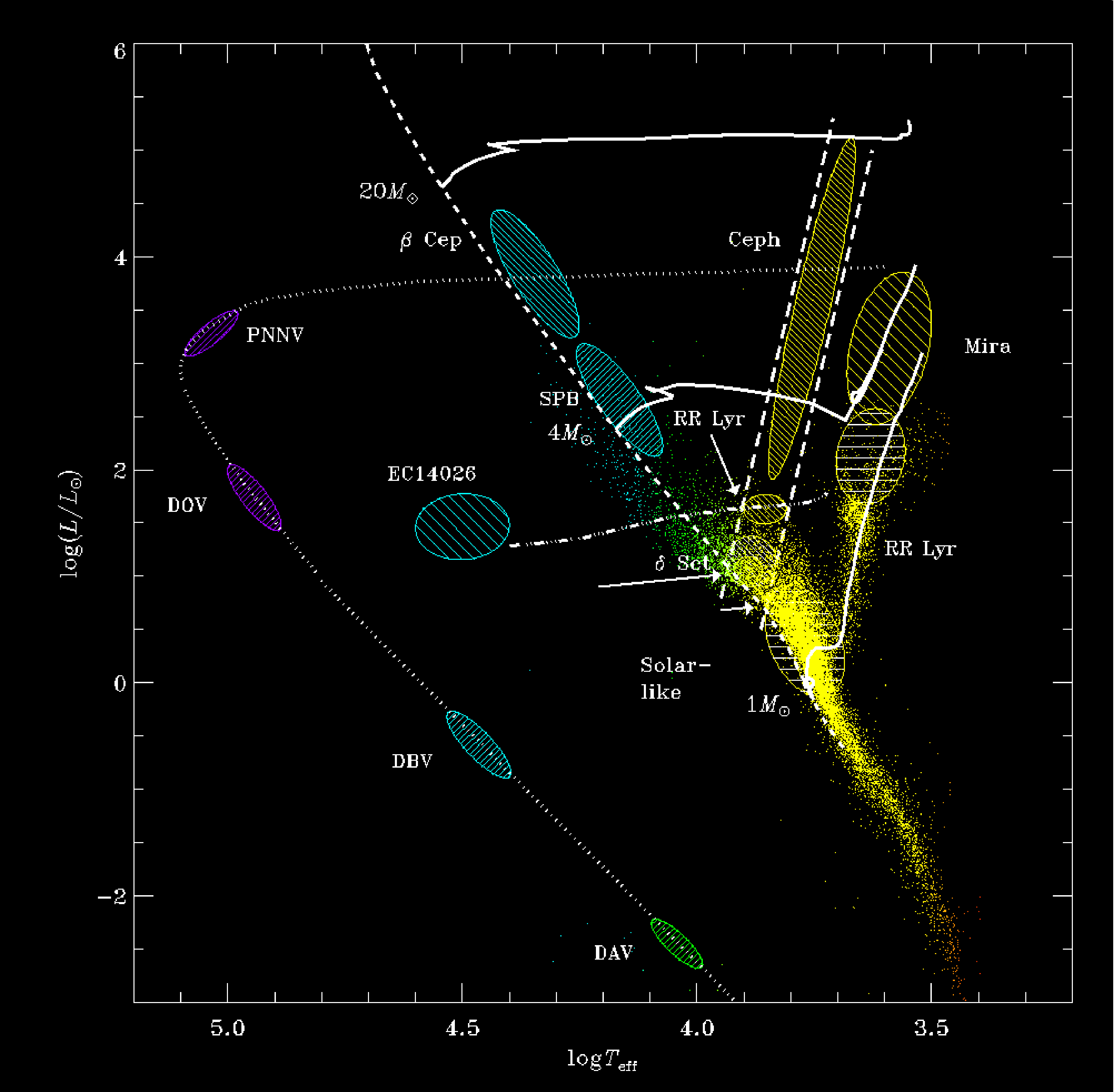

$$\tau_{\rm dyn} \simeq \sqrt{\frac{R^3}{GM}} \simeq \sqrt{\frac{1}{G\,\overline{\rho}}},$$

$$\tau_{\rm th} \simeq \frac{GM^2}{RL},$$

Stellar oscillations: solar type oscillations

p-mode spectra of several solar-like stars.

Linear adiabatic oscillation

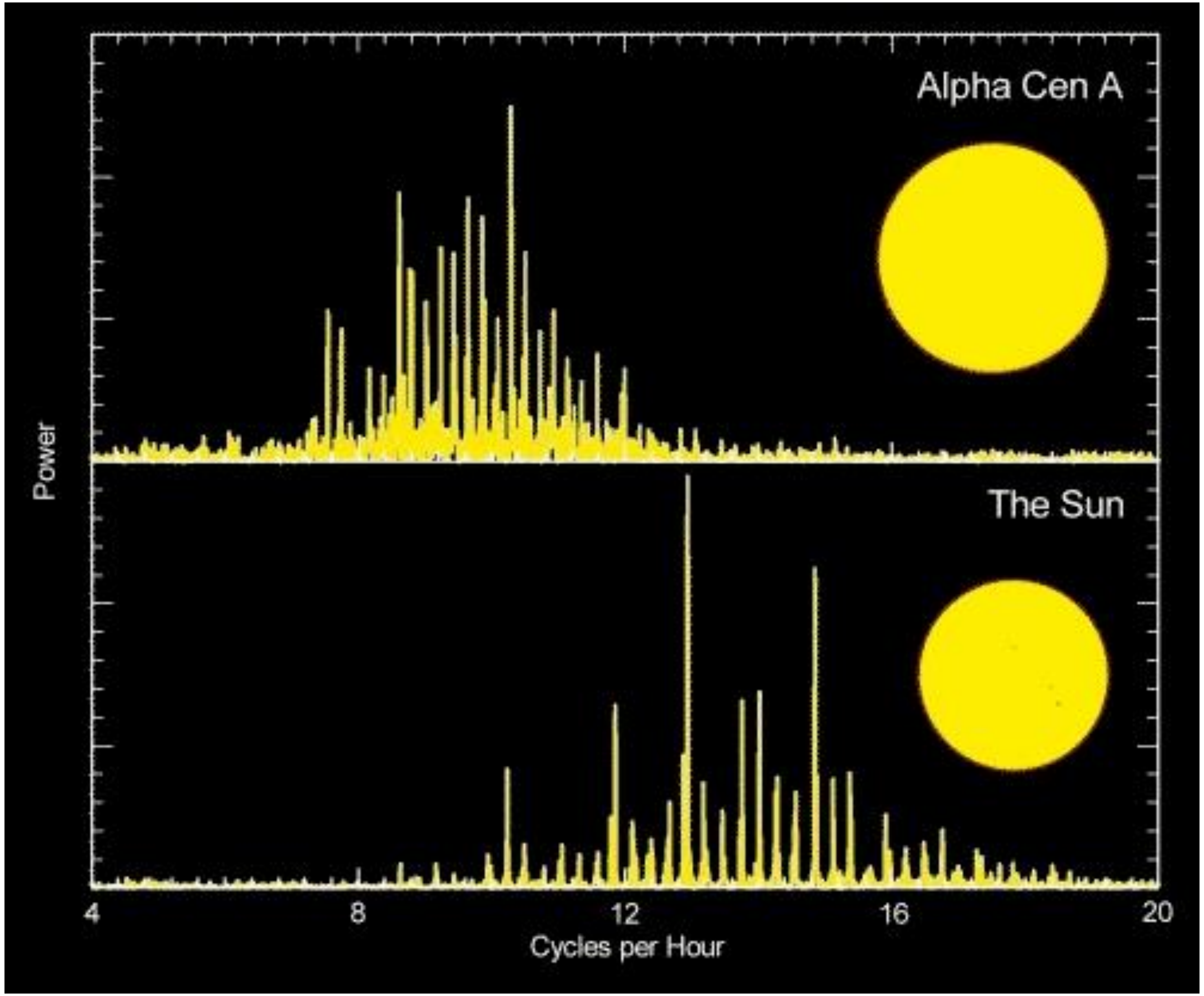

OBSERVING THE SUN FROM SPACE: GOLF/SOHO ACOUSTIC MODES

Lazrek et al. (1997)

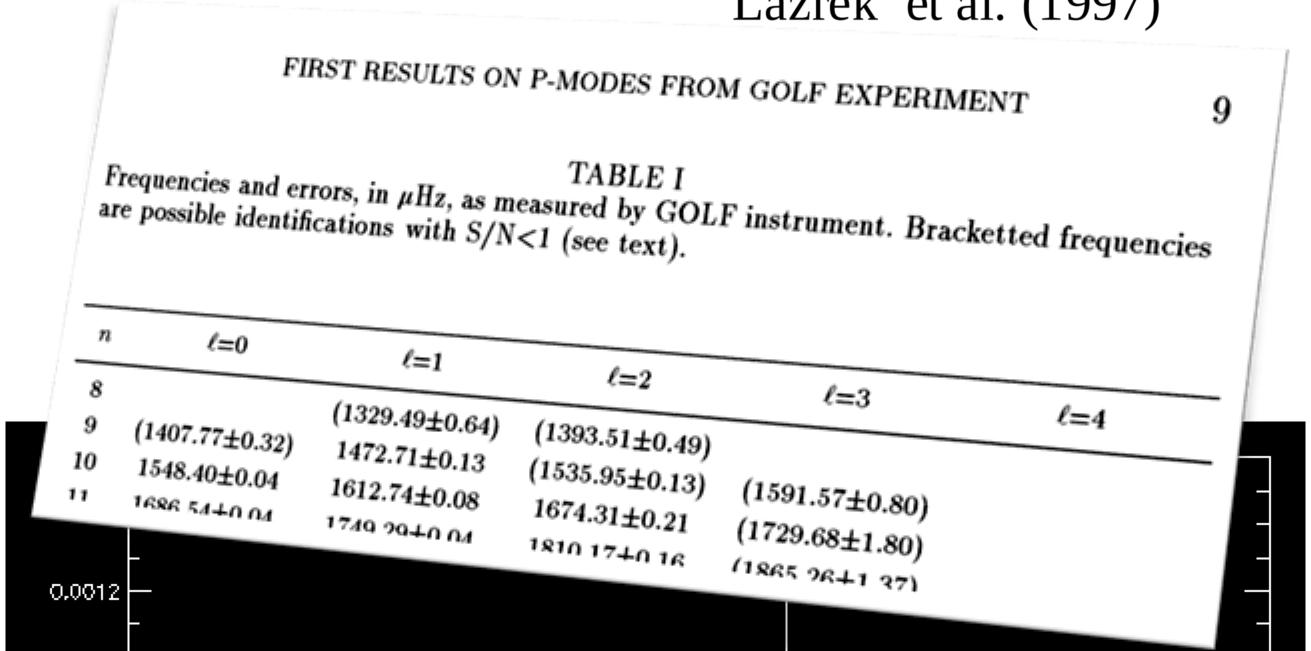
FIRST RESULTS ON P-MODES FROM GOLF EXPERIMENT 9

TABLE I

Frequencies and errors, in μHz, as measured by GOLF instrument. Bracketted frequencies are possible identifications with S/N<1 (see text).

n	$\ell=0$	$\ell=1$	$\ell=2$	$\ell=3$	$\ell=4$
8		(1329.49±0.64)	(1393.51±0.49)		
9	(1407.77±0.32)	1472.71±0.13	(1535.95±0.13)	(1591.57±0.80)	
10	1548.40±0.04	1612.74±0.08	1674.31±0.21	(1729.68±1.80)	
11	1686.54±0.04	1749.29±0.04	1810.17±0.16	(1865.26±1.37)	

I. Lopes Co-I GOLF Team

The p-mode Fourier spectrum from GOLF, using a 690-day time series of calibrated velocity signal, which exhibits an excellent signal to noise ratio.

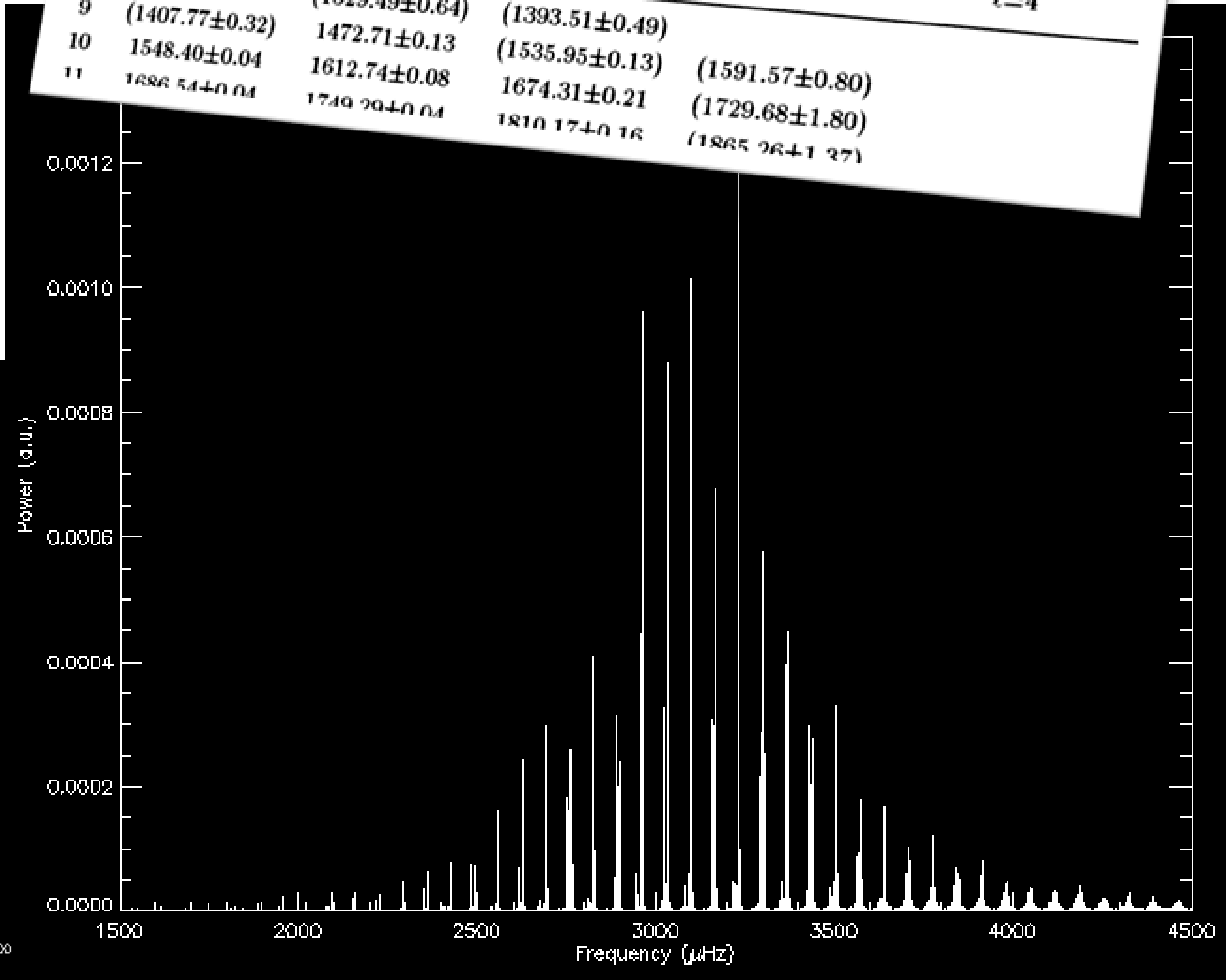

The low-frequency range of the P-modes from above spectrum, showing low-n order modes.

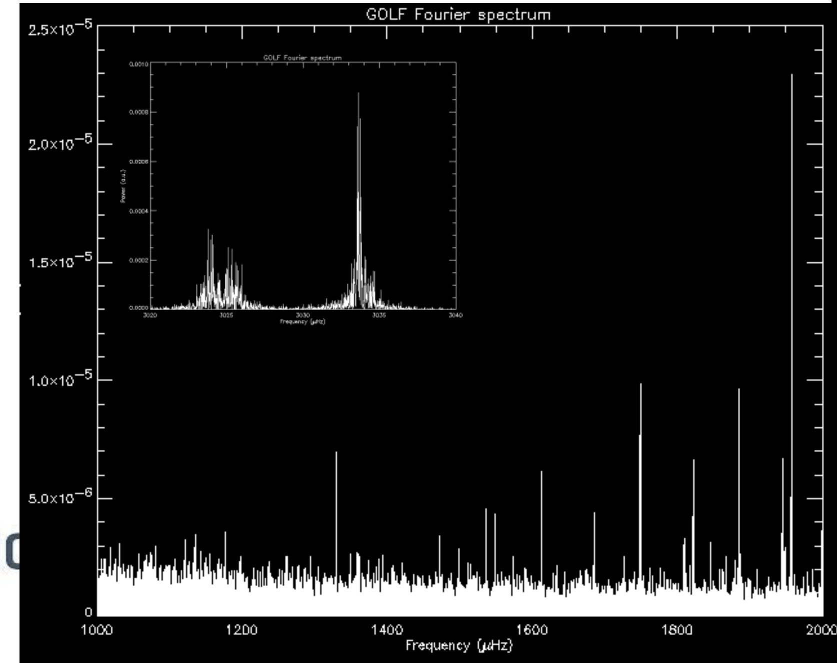

TÉCNIC

Stellar oscillations:
solar type oscillations

Linear adiabatic oscillation

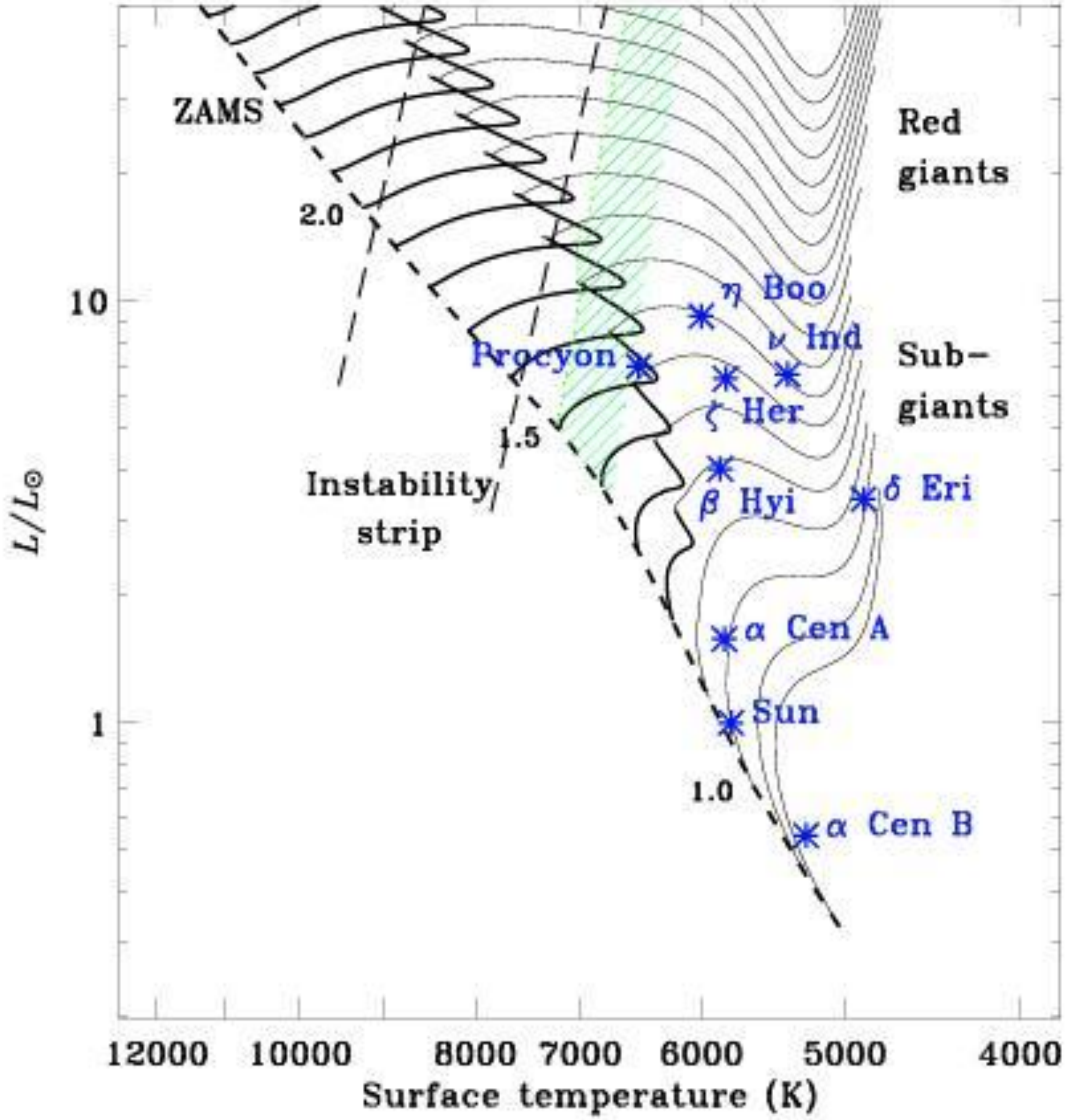

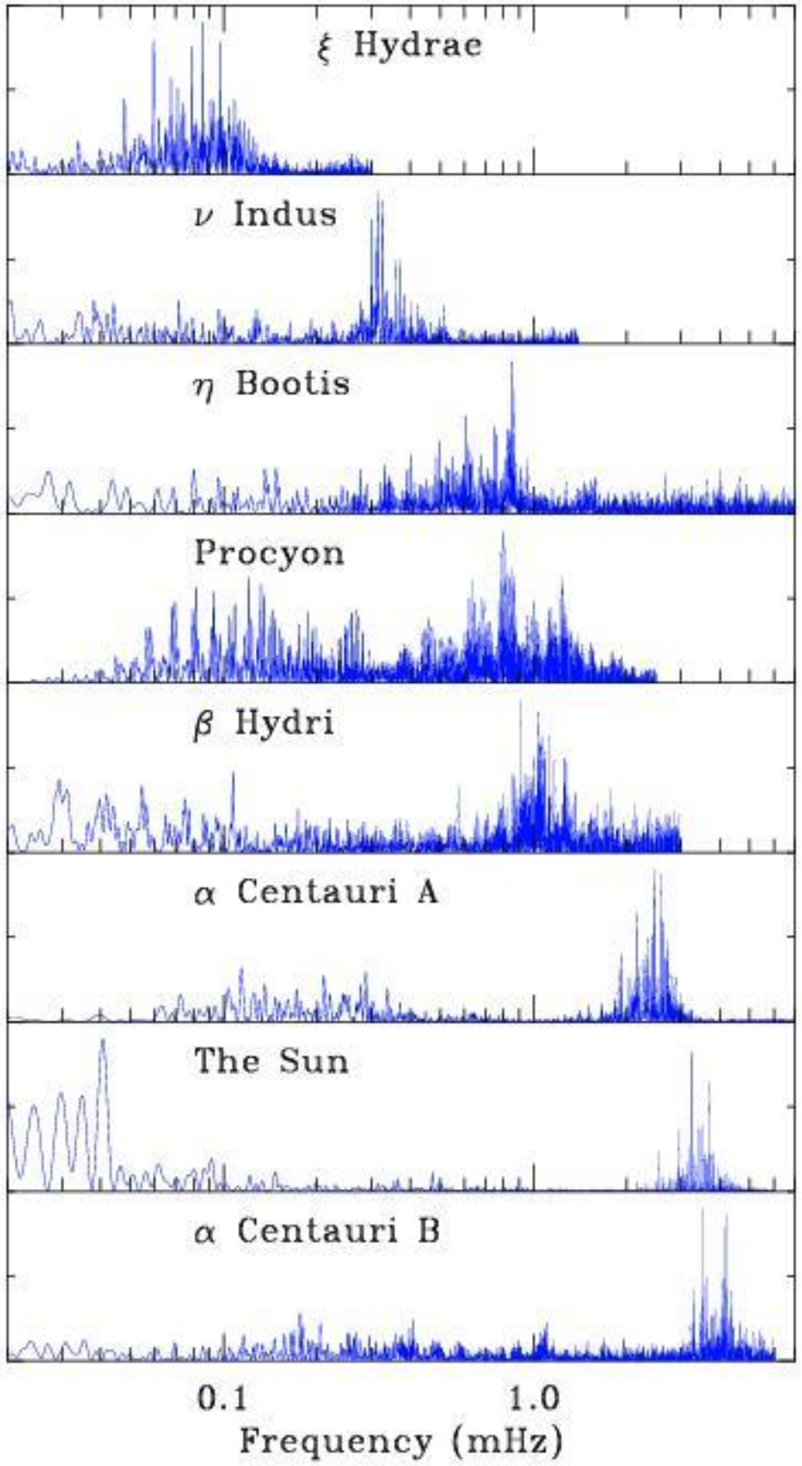

TÉCNIC

Asteroseismology

Huber (2014)

Sun-like oscillations…

Stochastically excited oscillations in stars with a convective envelope

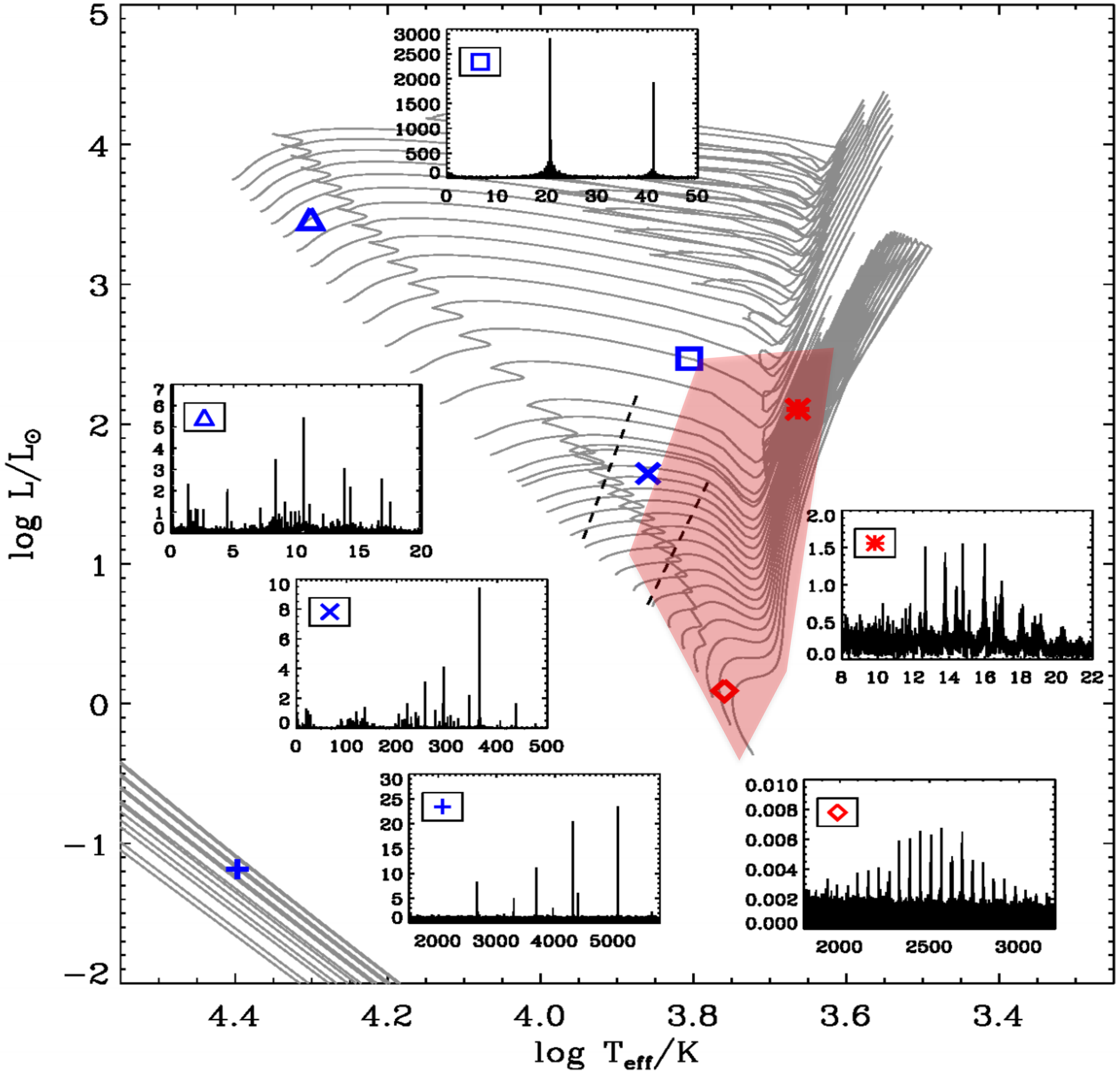

TÉCNICO LISBOA

Asteroseismology

Kepler observations

Solar-like oscillations

Main sequence and subgiant stars (~ 1M$_\odot$)

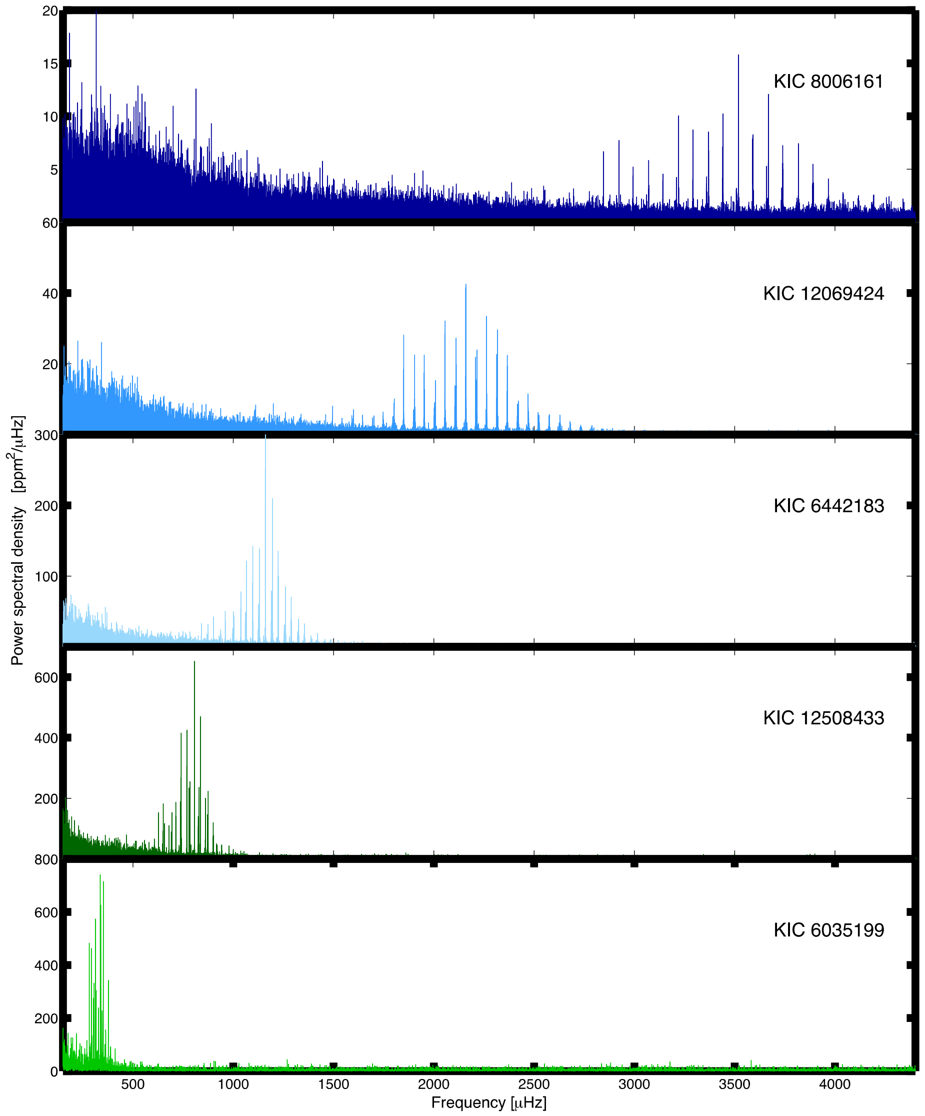

Red giant stars (~ 1M$_\odot$)

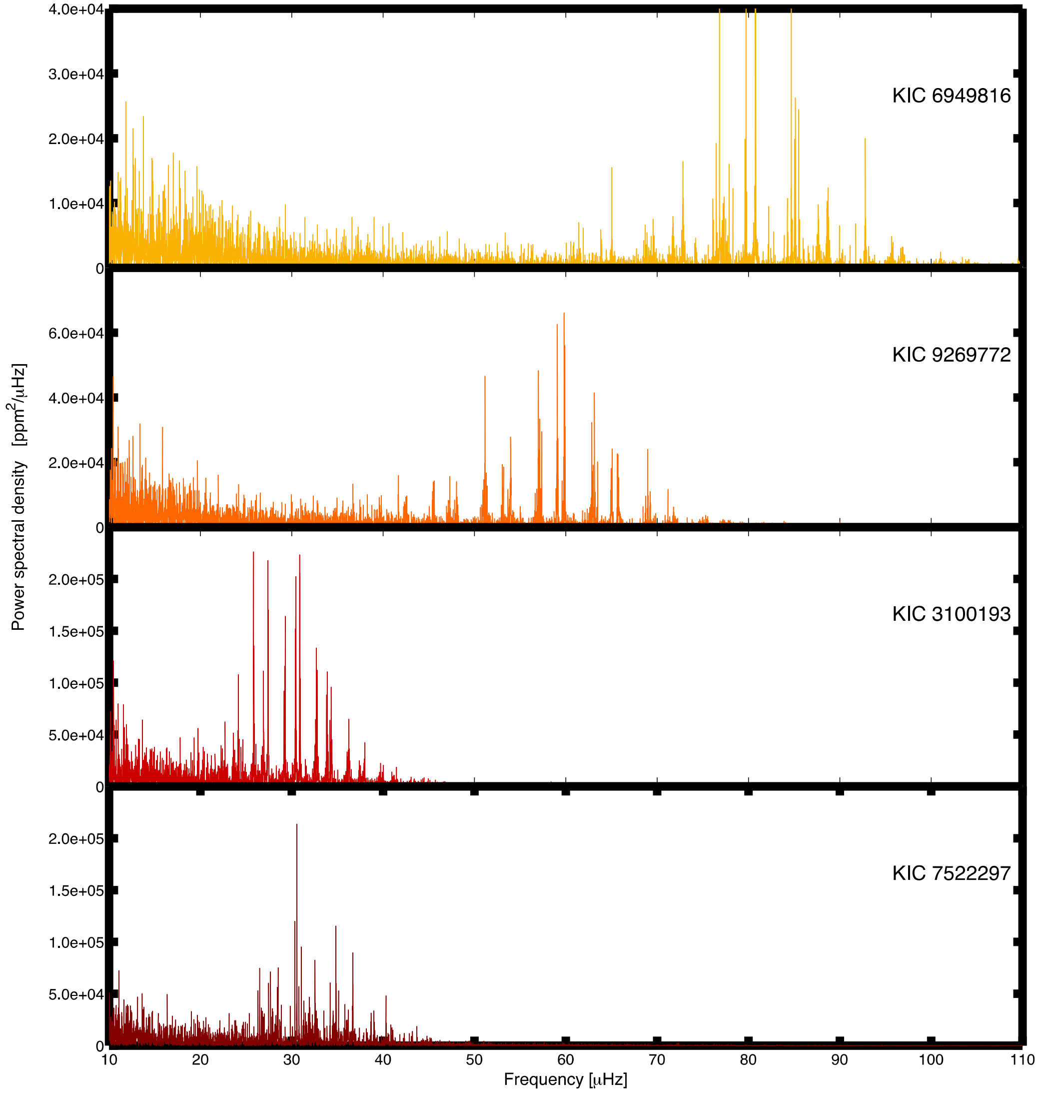

TÉCNICO

Asteroseismology

Chaplin & Miglio. (2014)

Hertzsprung-Russell diagrams showing populations of stars with detected solar-like oscillations (Detections made by the Kepler mission): The large coloured circles mark the stars whose spectra are plotted in the left Figure. Solid lines in both panels follow evolutionary tracks (Ventura, D'Antona & Mazzitelli 2008).

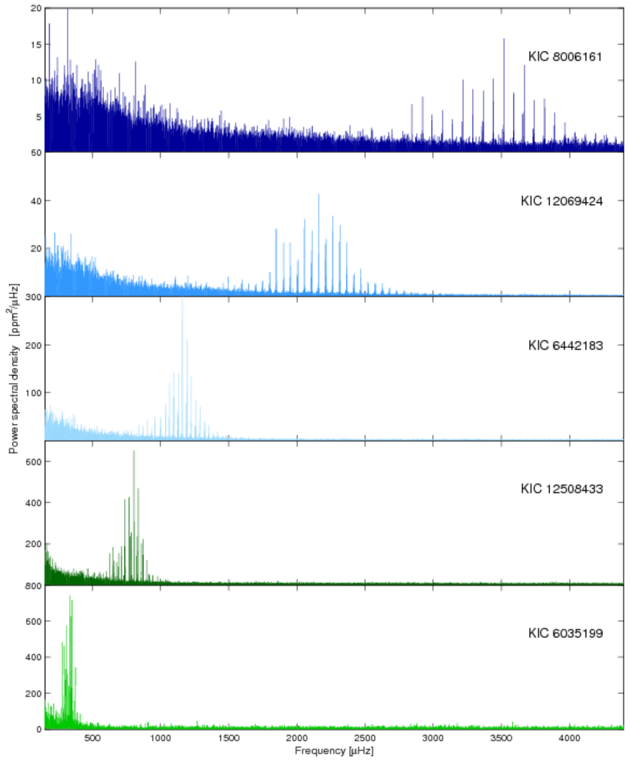

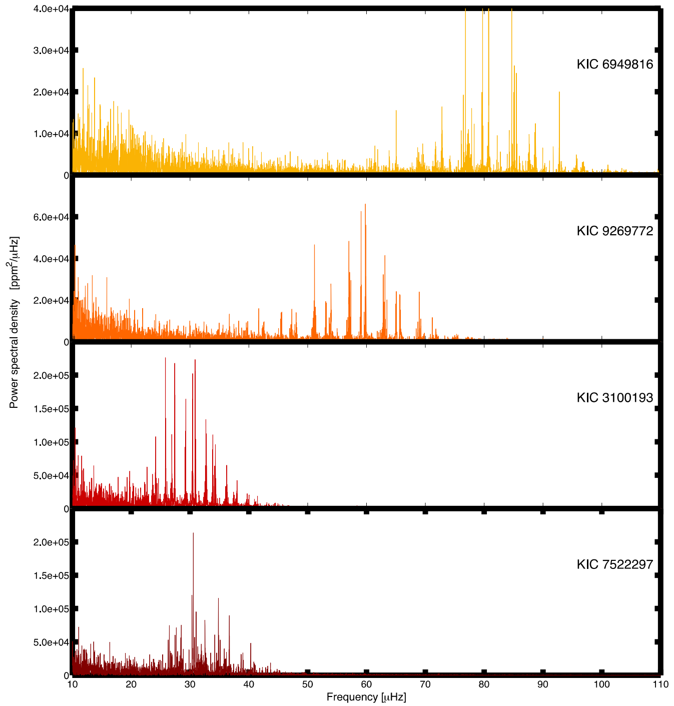

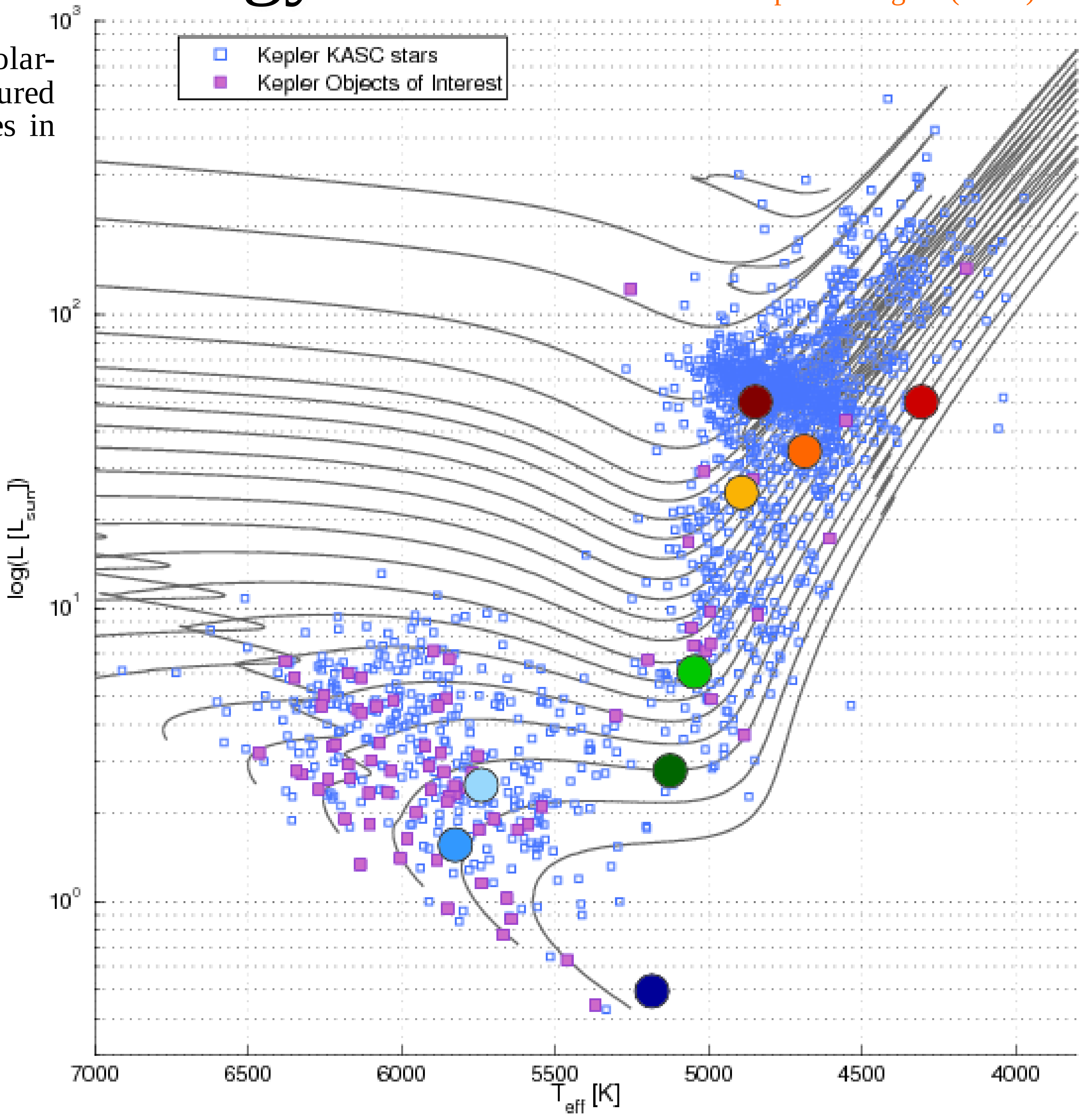

PLATO observing strategy

Baseline observing strategy:

- 6 years nominal science operation
- 2 long pointings of 2-3 years + step-and-stare phase (2-5 months per pointing)

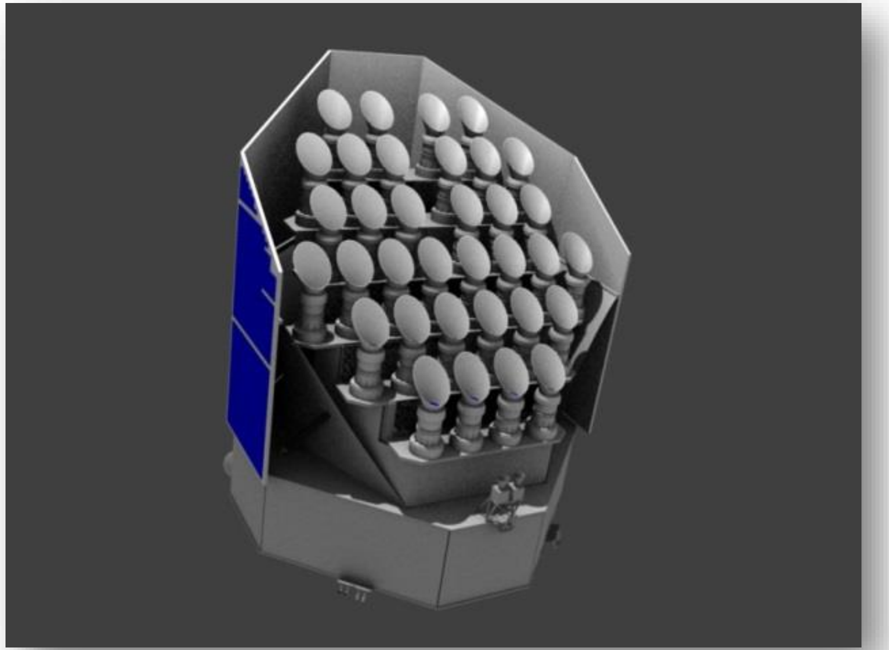

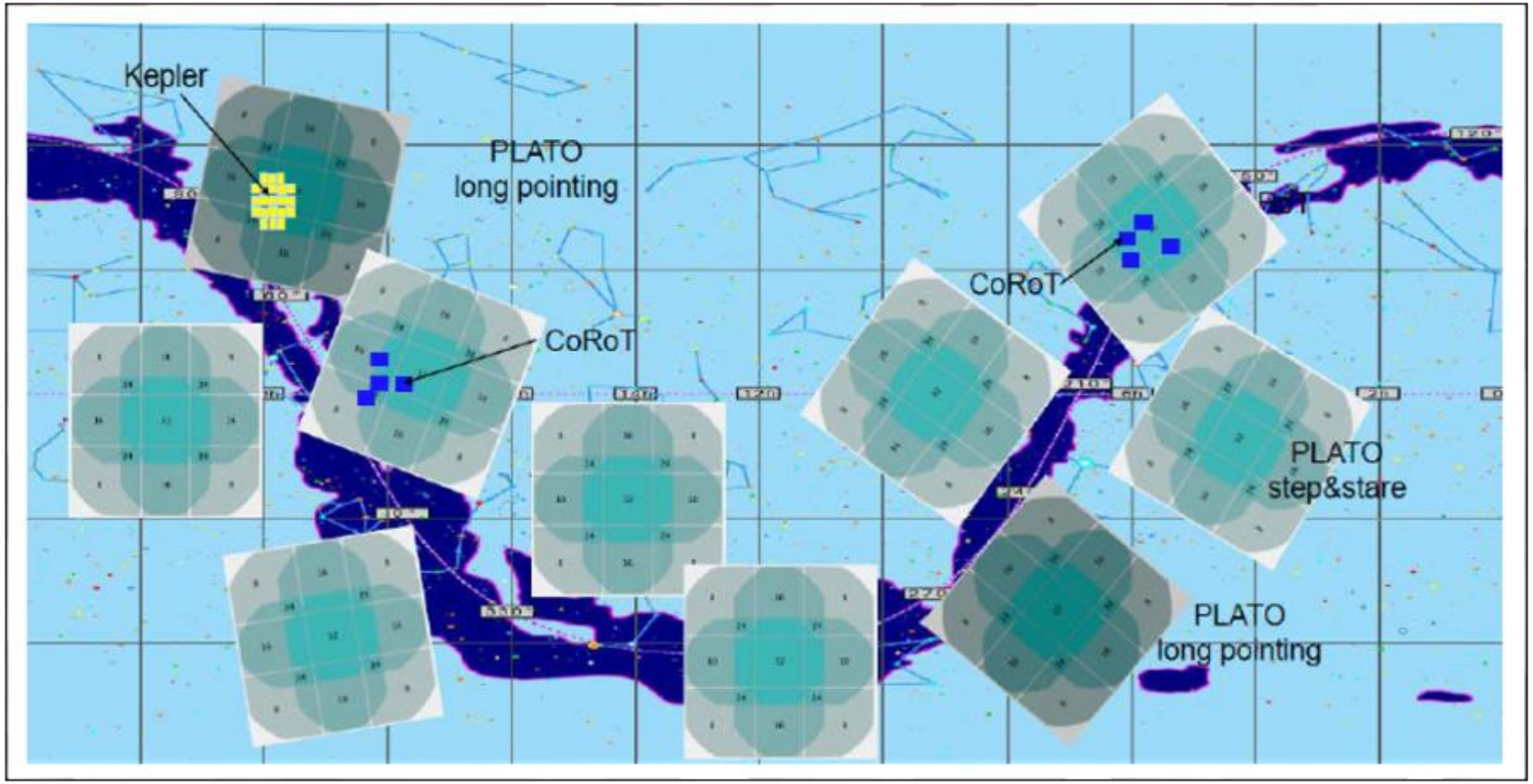

How Dark Matter affects Stars

How does dark matter influence stars?

Pioneer Works:

Cosmions as a solution to the solar neutrino problem and dark matter problem [Steigman et al. (83), Spergel and Press (85), Krauss et al. (85), Gilliland et al. (86), Dearborn et al. (91), Faulkner et al. (86), Dappen et al. (86)]

Dark matter impact in Stars (Sun and red giant stars, . . .) [Gould, Bouquet, Dearborn, Edsjö, Freese, Raffelt, Salati, Silk. , . . .]

Sun, Solar neutrinos and helioseismology: constraints low-mass DM candidates [Bottino, Bertone, Casanellas, Cumberbatch, Kouvaris, Frandsen, Guzik, Lopes, Iocco, Panci, Meynet, Ricci, Sarkar, Scott, Silk, Vicent, Taoso, Turck-Chièze, Watson, Vincent]

Stars and asteroseismology: Constraints on low-mass DM candidates [Casanellas, Lopes, Silk, Brandão, Lebreton, Bramante, Lebreton,. . .]

Neutron stars: Constraints on DM candidates (including Axions) [Kouvaris, Tinyakov, Ivanytskyi, Sagun, Lopes, Panotopoulos, Rincón, Perez-García, Silk, Kokkotas.]

Stars in the Galactic Center: Constraints on low-mass DM candidates [Casanellas, Lopes, J. Lopes, Edsjö, Silk, Sakstein, Acevedo, Leane, Linden, John, Smirnov]

Advantages of Using Stars to Study Dark Matter

Experimental detectors – Stars (including asteroseismology), Compact Stars, Cosmological Tests

Studying dark matter (DM) properties is greatly advanced using helio- and asteroseismology, as well as solar neutrino datasets in sun-like stars, subgiants, and red giants, rather than in compact stars like neutron stars, for several key reasons:

– Sun-like stars (“known Physics”) and their evolved forms offer for studying dark matter (DM) interactions. This is in contrast, to cosmological studies and neutron star constraints, which are affected by **uncertainties** in the equation of state and the presence of intense gravitational and magnetic fields.

– Asteroseismology (and helioseismology) allow precise measurements of these stars' internal structure and dynamics, revealing detailed insights into potential DM-induced signatures.

– Solar neutrino data provide direct evidence of processes in the cores of the Sun, helping to constrain DM particles interacting with nuclear matter.

– The extensive observational data from these types of stars, such as the approximately 30 frequencies of low-degree eigenmodes measured with a precision of $\sim 0.1\ \mu\mathrm{Hz}$ in sub-giant stars, enhance statistical reliability and reduce uncertainties in DM property estimations.

Star’s Dector: These reasons collectively make sun-like stars, subgiants, and red giants,

Excellent “Laboratories” for DM research.

How does dark matter influence stars?

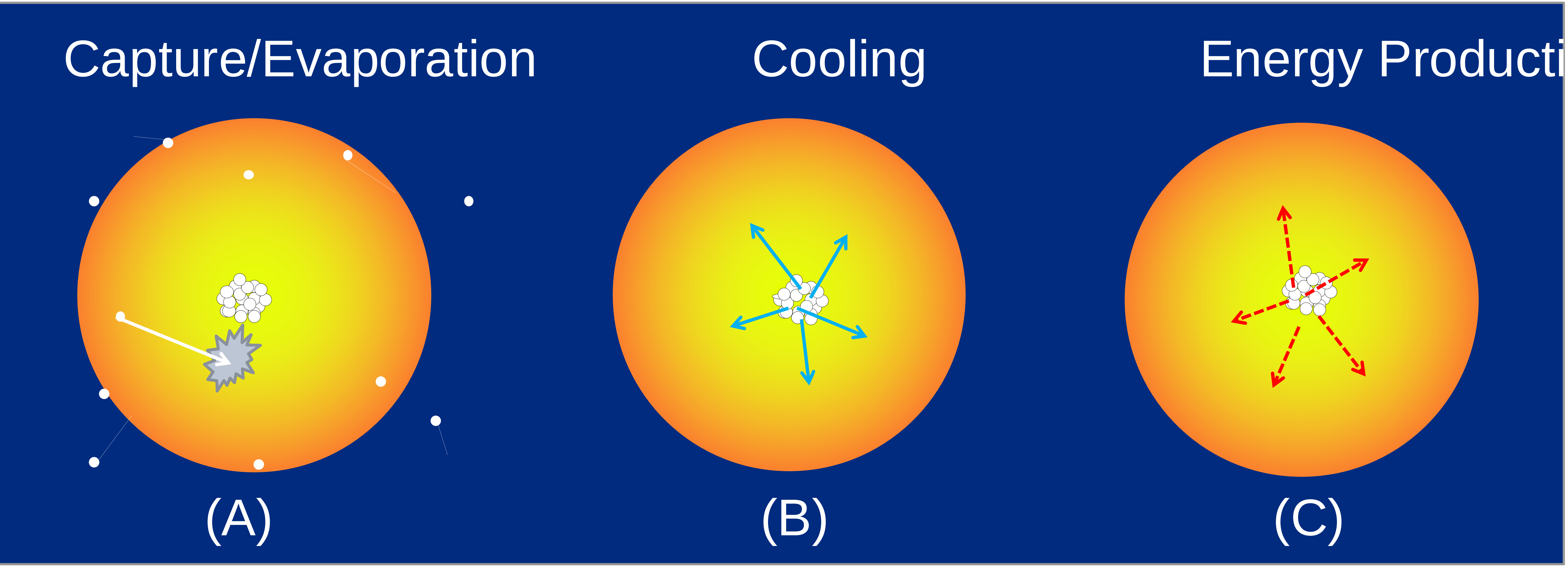

C_χ and $A_\chi \propto f(\chi, \star)$

$L_{transp,\chi} \propto f(C_\chi, m_\chi)$

$L_{prod,\chi} = f_\chi \cdot C_\chi \cdot m_\chi$

Generic properties

Interaction of dark matter particles with stars: The interaction of dark matter with baryonic matter inside stars follows three basic processes: **capture (A)**, C**ooling (B)** and Energy Production **(C)**

How does dark matter influence stars?

$m_\chi \quad \sigma_\chi$

$\rho_\chi \quad \bar{v}_\chi$

$v_\star \quad n_i$

$$E = \sum_i \int_0^{R_*} \mathrm{d}r 4\pi r^2 \int_0^{v_{\rm esc}(r)} \mathrm{d}w f_\chi(w) \Omega_i(v_{\rm esc}, \infty; w)$$

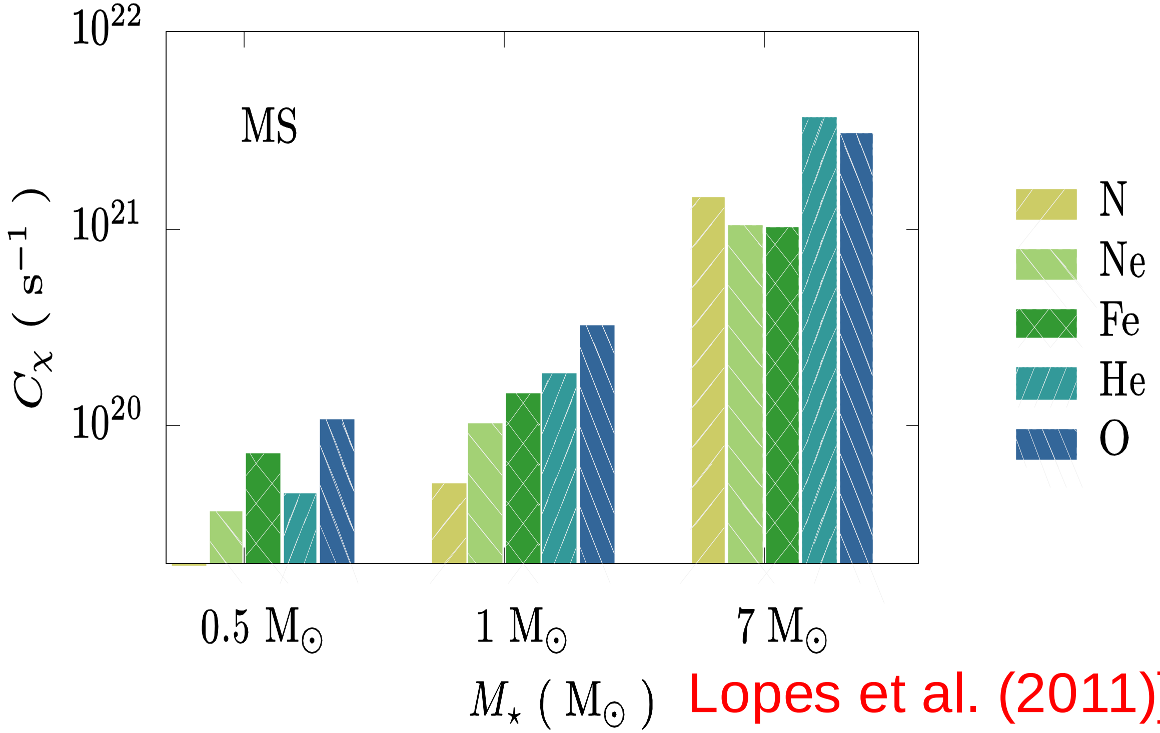

Lopes et al. (2011)]

Interaction of Dark Matter particles with stars: The interaction of dark matter with baryons depends on several factors that influence the capture and interaction dark matter with baryons on the star, properties of the dark matter particle, dynamics of the DM halo and internal properties of the star (including dynamical ones).

How does dark matter influence stars?

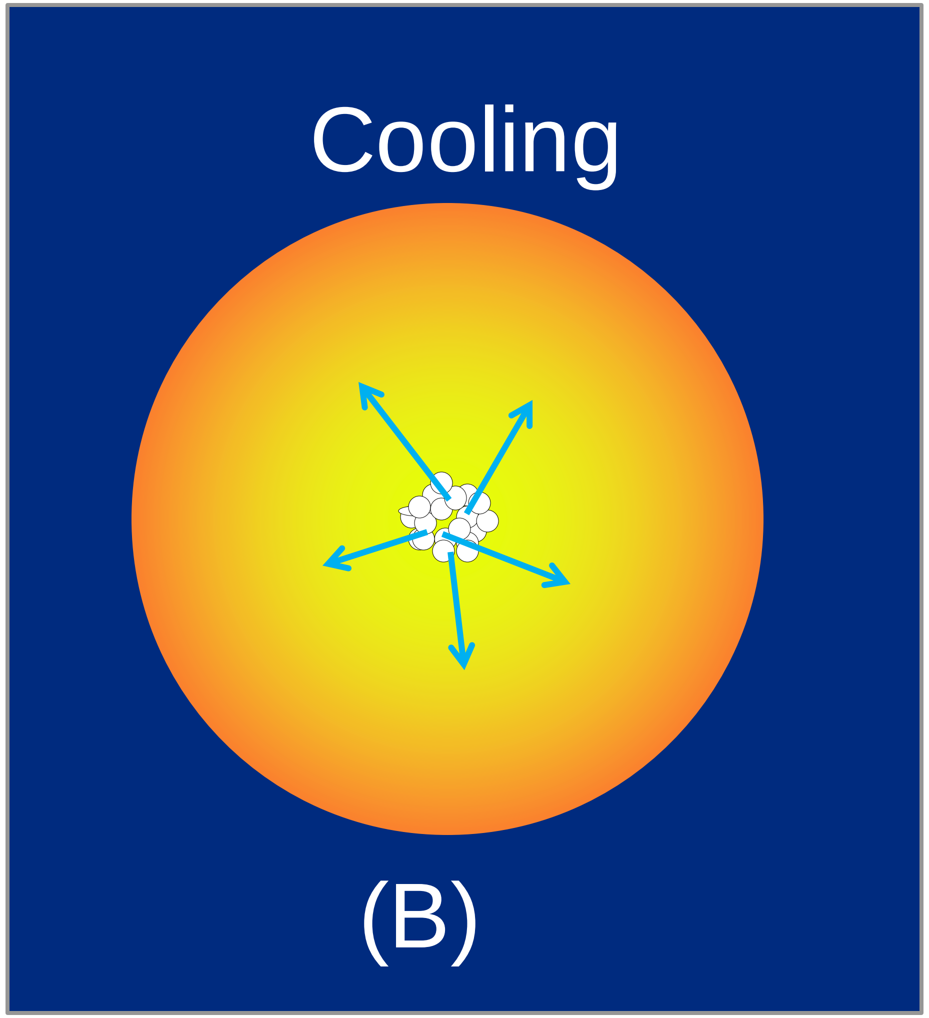

Reduction of the star’s core temperature

Cooling mechanisms:

- **Dark Matter Energy Transport:** Dark Mater Particles (i.e., WIMPs) can transport energy from the core to the outer layers of the star or even outside the star.

- **Axion emission:** Axions and ALP particles, can carry energy away from the star's core without requiring particle capture.

How does dark matter influence stars?

Cooling

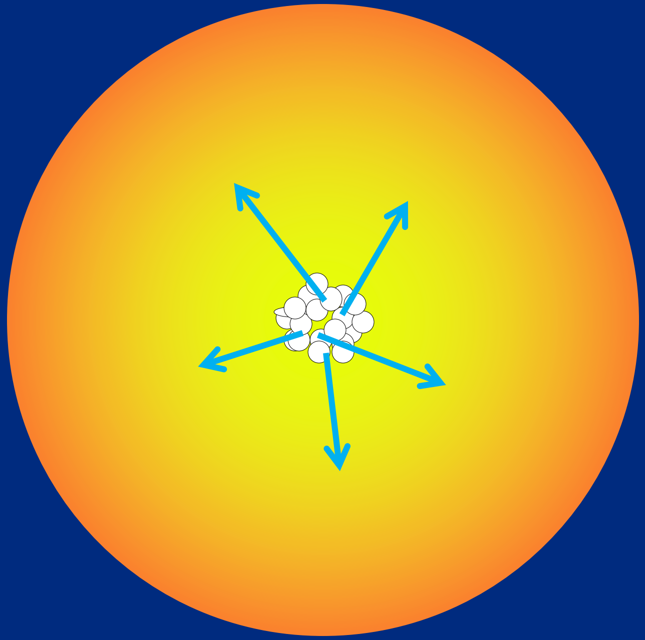

(B)

Energy Transport (by ADM particles)

Sun

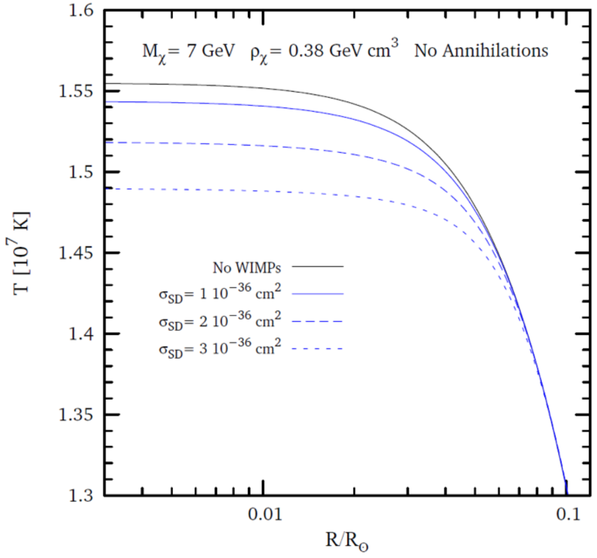

Taoso et al. (2010)

Subgiant Star

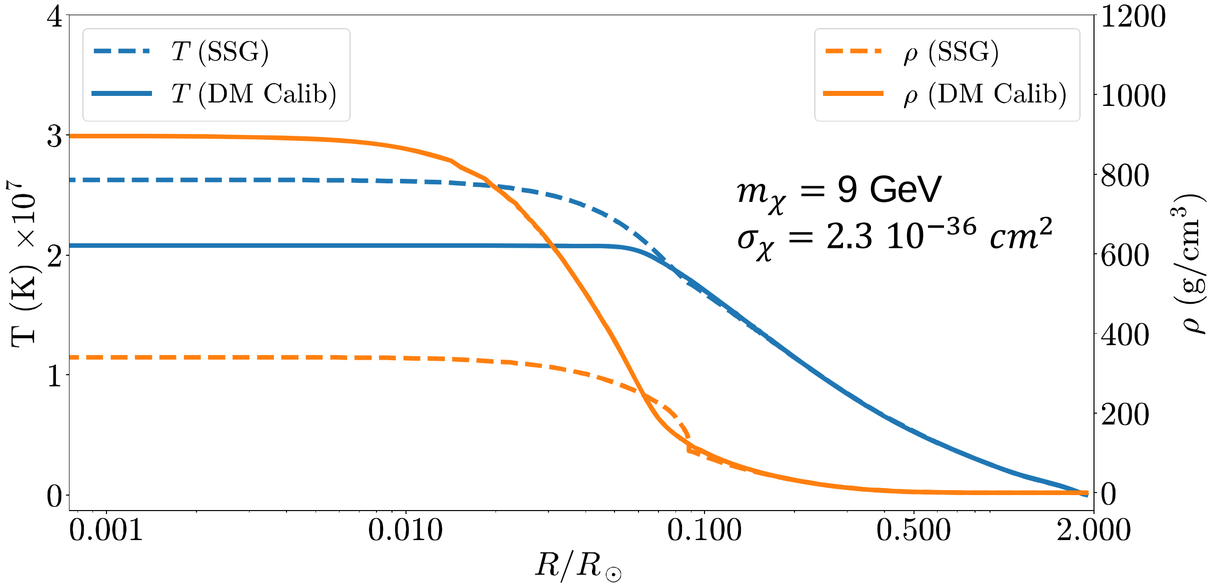

Pato, Lopes & Lopes (2021)

Reduction of the star's core temperature

Interaction of dark matter particles with stars: The presence of dark matter inside the star facilitates the energy transport outside of the core, leading to a reduction of the temperature in the centre. In extreme cases of the strong interaction of DM with baryons, it can lead to the creation of an isothermal core (Lopes & Silk 2002).

How does dark matter influence stars?

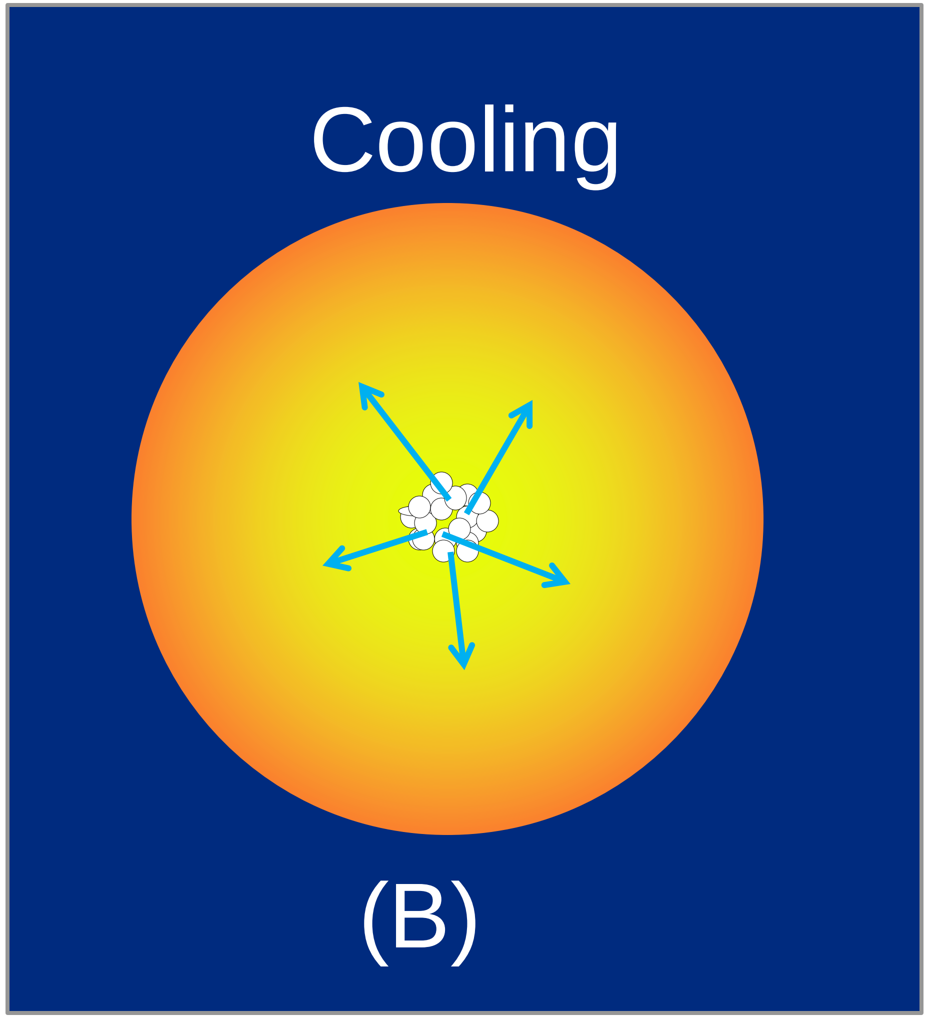

Axion Emission (subgiant and supergiant stars)

$$\varepsilon_a = 283.16 \times g_{10}^2 T_8^7 \rho_3^{-1} \xi^2 f(\xi^2)\ \mathrm{erg/g/s}$$

Raffelt (1999)

Subgiant Star

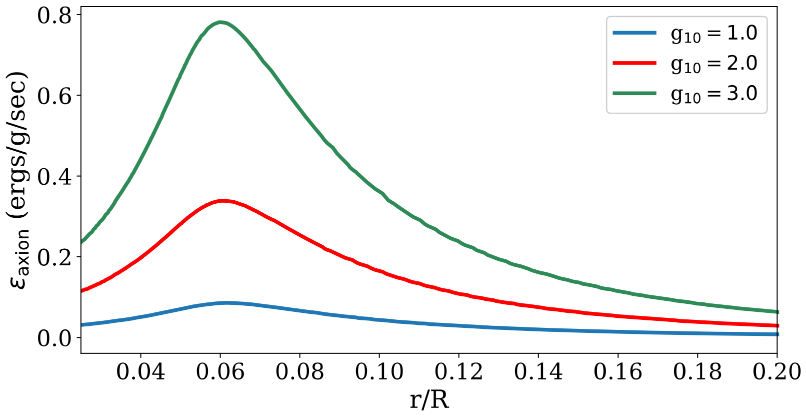

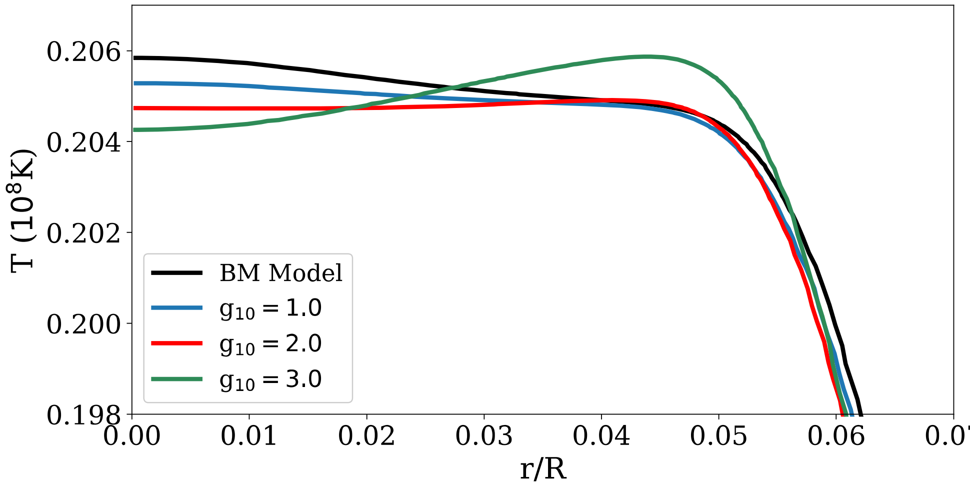

Fordham & Lopes (2024)

Reduction of the star's core temperature

The **axion emission (like neutrinos)** in the cores of main-sequence stars leads to a decrease in the core temperature. In other stars, such as subgiants, once energy production occurs off-centre, in the nuclear energy layer just above the helium core, the emission of particles occurs in that region. The cooling of stellar cores due to axion emission is identical to the cooling by neutrino emission (**Fordham & Lopes 2024).**

How does dark matter influence stars?

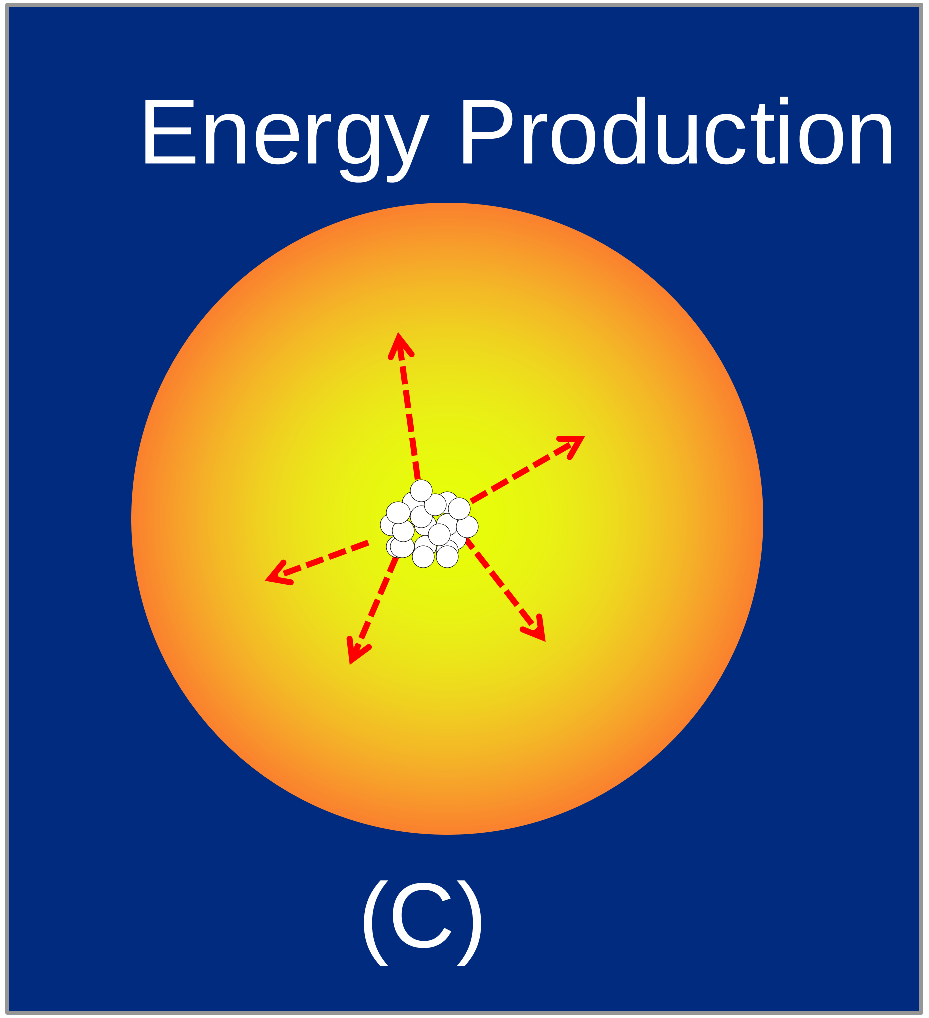

$\sigma_\chi \rho_\chi = 10^{-32} GeV cm^{-3}$

$\sigma_\chi = 10^{-36}\ cm^2$

$\rho_\chi = 10^4\ GeV cm^{-3}$

$\langle \sigma v \rangle_\chi = 3\ 10^{-26} cm^3 s^{-1}$

Red Giant S

Lopes & Lopes (2021)

WIMP impact in low-mass RGB stars ($0.8 - 1.4\ M_\odot$

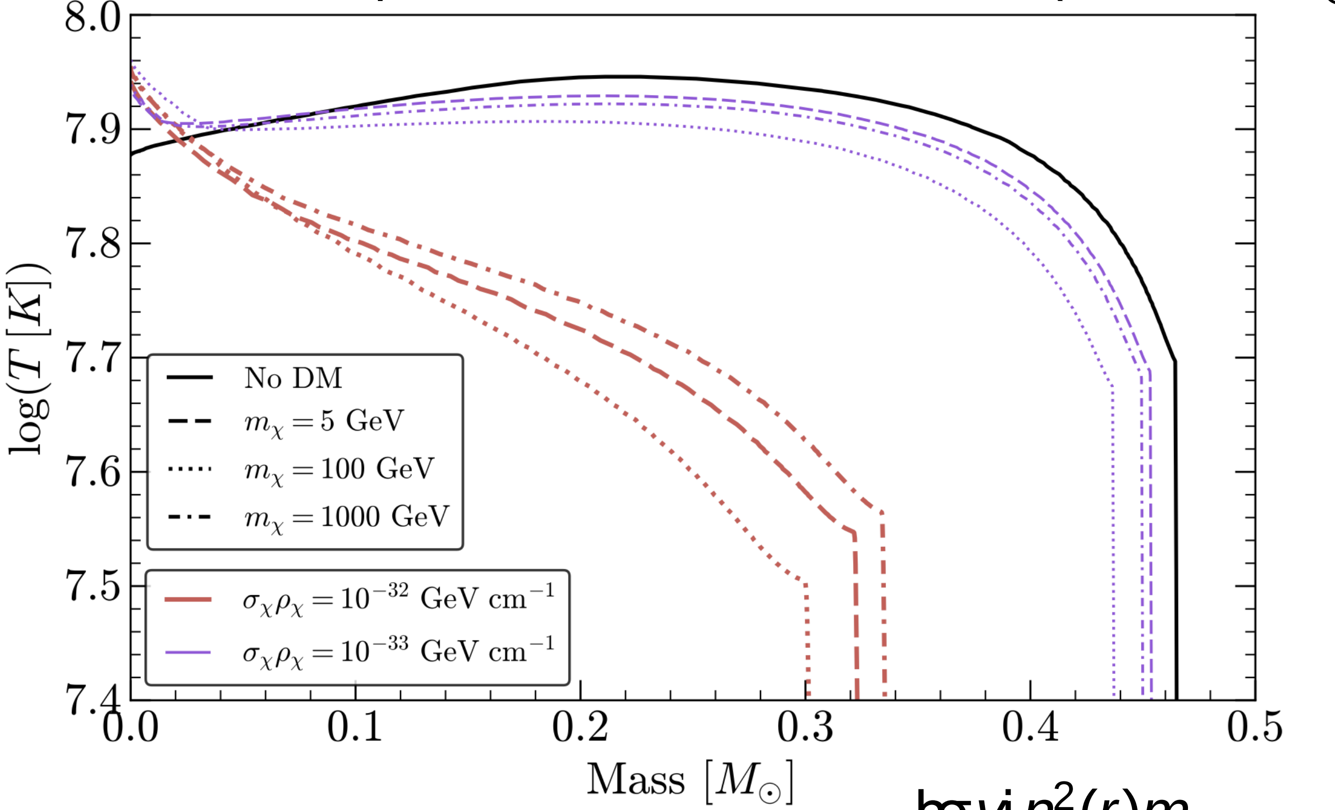

Energy Production inside stars

Energy produced by DM annihilation: $\epsilon_\chi(r) = f_\chi \frac{\langle \sigma v \rangle n_\chi^2(r) m_\chi}{\rho(r)}$

Temperature profile for a solar mass RGB star just before the onset of He^4 burning.

In stars without dark matter, helium ignition happens off-center. However, in stars with dark matter, the energy from dark matter annihilation causes helium ignition to start at the core.

How does dark matter influence stars?

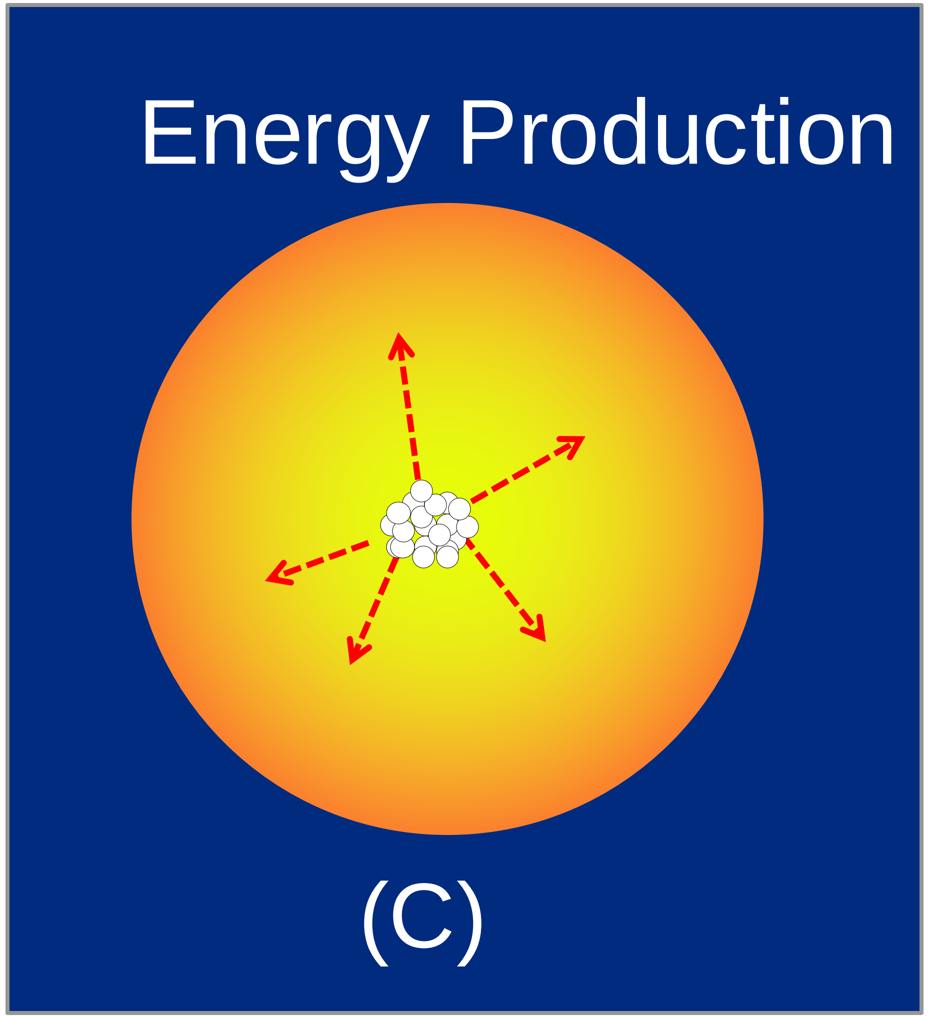

Stellar Cluster

Casanellas & Lopes (2011

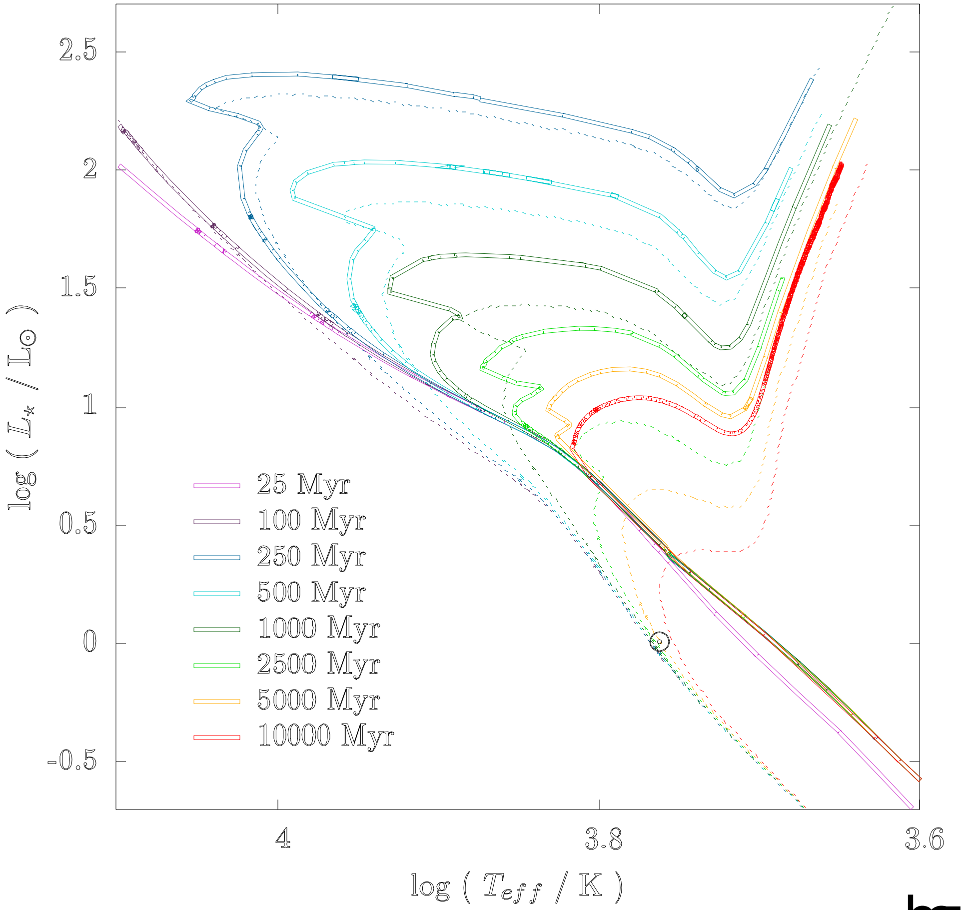

Energy Production inside stars

Energy produced by DM annihilation: $\epsilon_\chi(r) = f_Q \dfrac{\langle \sigma v \rangle n_\chi^2(r) m_\chi}{\rho(r)}$

The annihilation of dark matter as an energy source for stars in the Milky Way, will only reduce the efficiency of the cooling mechanism.

Stars formed in the dense dark matter halos (primordial Universe) have their lives extended (slower evolution in the HD diagram), due to the energy produced by dark matter (Lopes & Silk

How does dark matter influence stars?

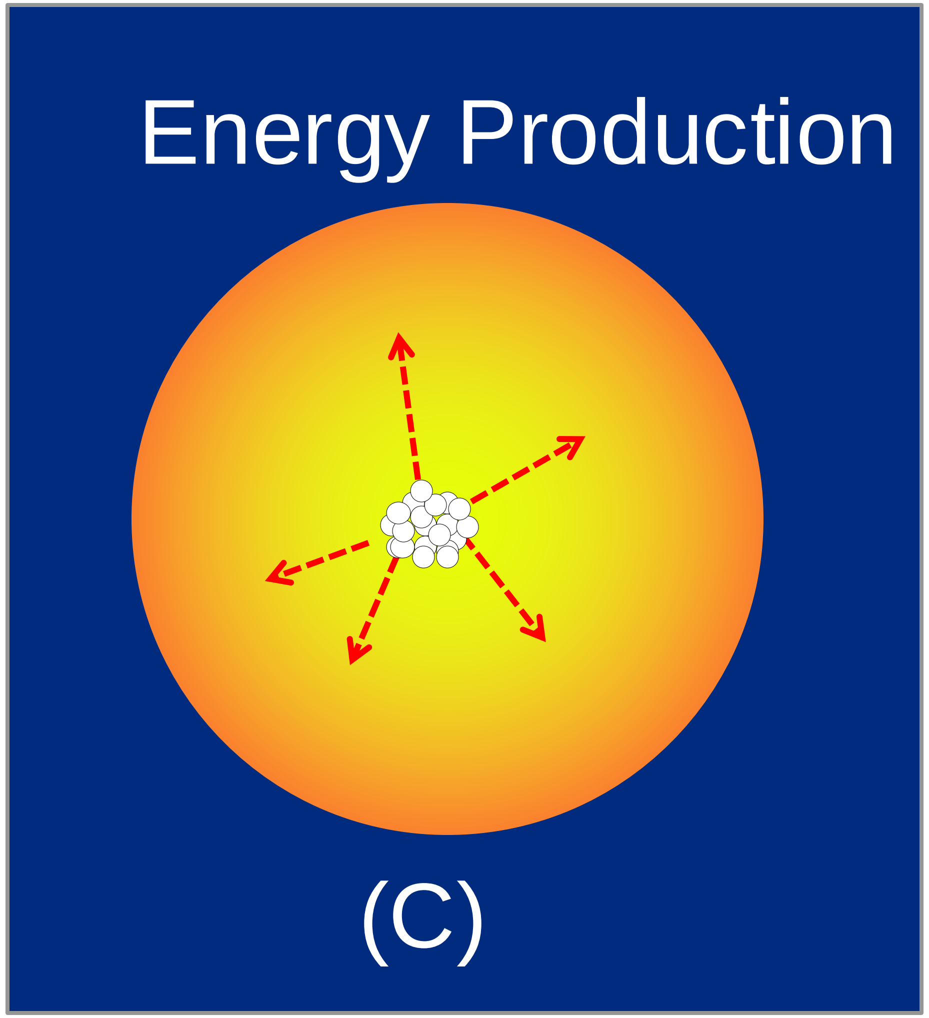

Stellar Cluster

Casanellas & Lopes (2011

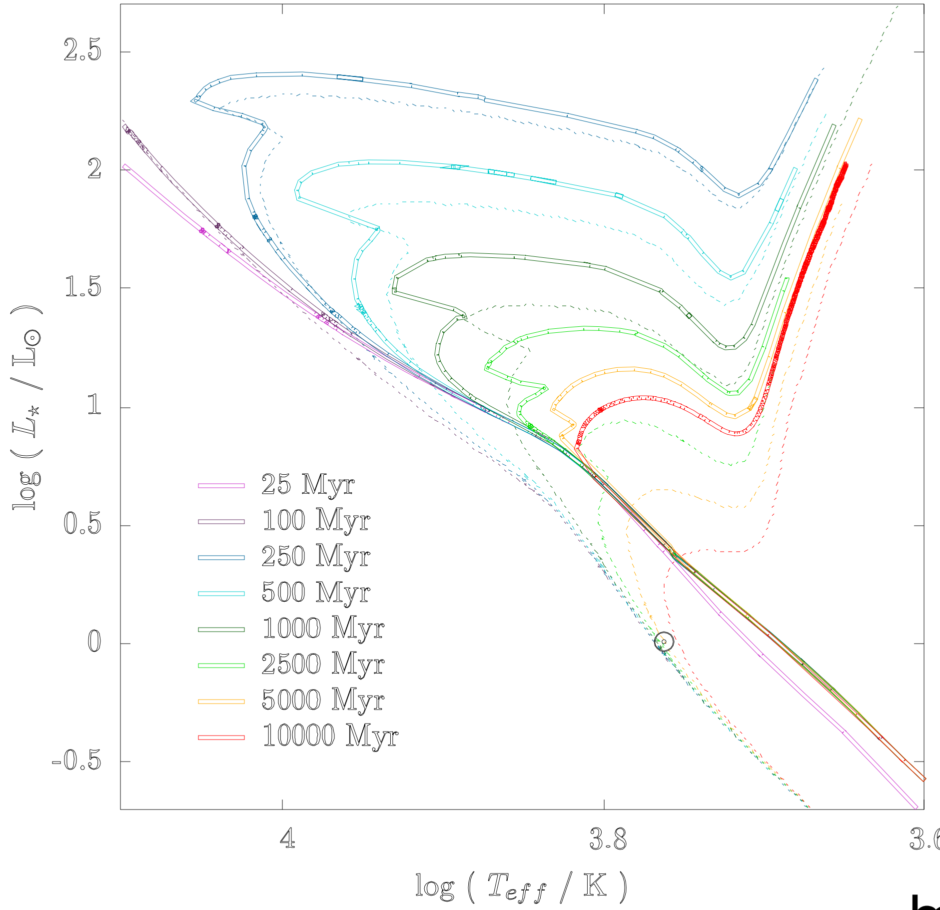

Energy Production inside stars

Energy produced by DM annihilation: $\varepsilon_\chi(r) = f_\chi \dfrac{\langle\sigma v\rangle n_\chi^2(r) m_\chi}{\rho(r)}$

For a cluster of stars (0.7-3.5 M⊙) in a DM halo (ρ ~ fixed, continuous lines) and a standard HR diagram (dashed lines), a DM halo with particles of ~100 GeV and $\boldsymbol{\sigma_\chi = 10^{-36}\ cm^2}$ significantly alters the location of the main sequence in the HR diagram (Casanellas & Lopes

Dark Matter Constraints using Stellar Observables (6 case-studies)

TÉCNICO LISBOA

Dark matter constraints using stellar observables

Constraints on Asymmetric Dark Matter interaction with Hydrogen

Helio- and Asteroseismology

TÉCNICO LISBOA

Helioseismology: limits to the DM characteristics

Dark Sector: DM particle (long range interaction) - interaction between a DM particle (with mass $\boldsymbol{m_\chi}$ and charge $\boldsymbol{Z_\chi\ g_\chi}$) and a nucleus (with mass $\boldsymbol{m_n}$ and electric charge $\boldsymbol{Ze}$). The scattering cross section $\boldsymbol{\sigma_{\chi n}}$ depends of the relative velocity $\boldsymbol{v_{rel}}$ of the particles, and there specific properties:

$\boldsymbol{\sigma_{\chi n}(v_{rel}\ Z_\chi\ ,\ m_\chi,\ g_\chi,\ Z, m_n \ldots)}$

(Pierre et al. 2014)

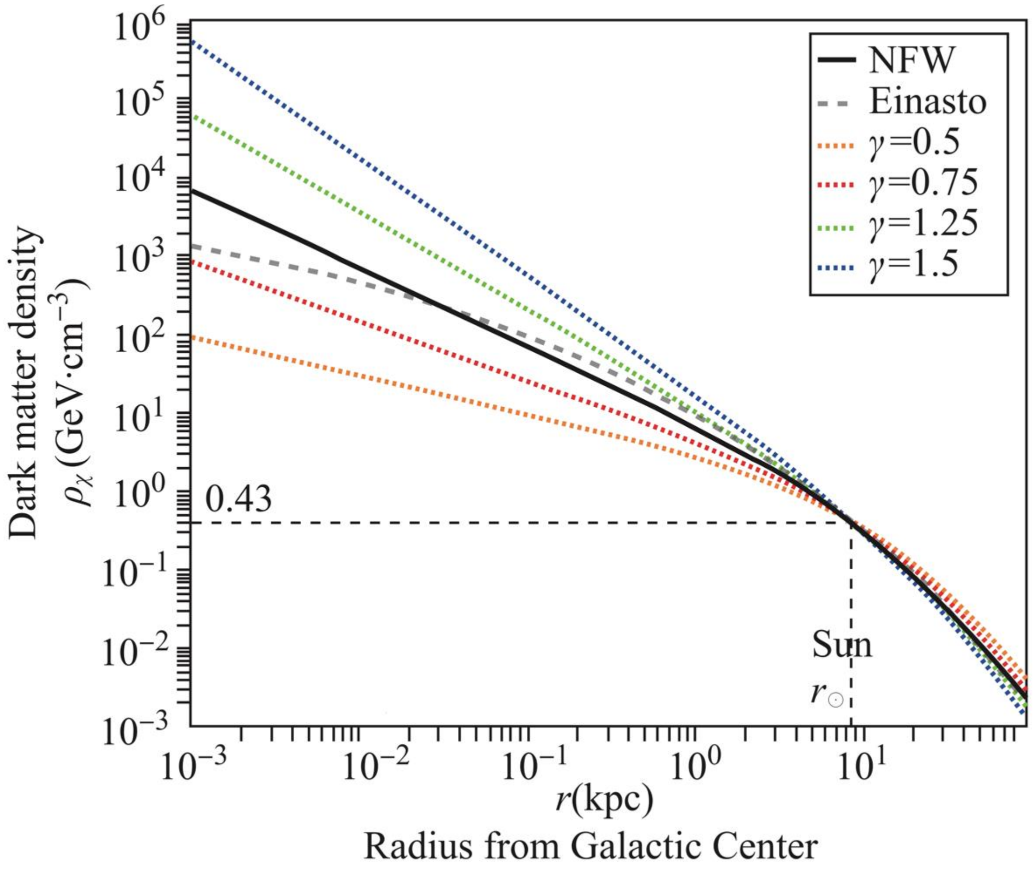

Motivation: Observational consequences (Galaxies cores): Resolves the **cusp halo problem** – DM becomes collisional: as a consequence the core of galaxies is in agreement with observations (see e.g. de Blok 2010), unlike numerical simulations (see e.g. Navarro et al. 2010).

TÉCNICO

Helioseismology: limits to the DM characteristics

Dark Sector: DM particle (long range interaction) - interaction between a DM particle (with mass m_χ and charge $Z_\chi\, g_\chi$) and a nucleus (with mass m_n and electric charge Ze). The scattering cross section $\sigma_{\chi n}$ depends of the relative velocity v_{rel} of the particles, and there specific properties:

$$\sigma_{\chi n}(v_{rel}\; Z_\chi\; , m_\chi,\, g_\chi,\, Z, m_n \ldots)$$

Popolo & Pace 2016 found that a baryonic clumps-DM interaction performs better than the one based on supernova feedback.

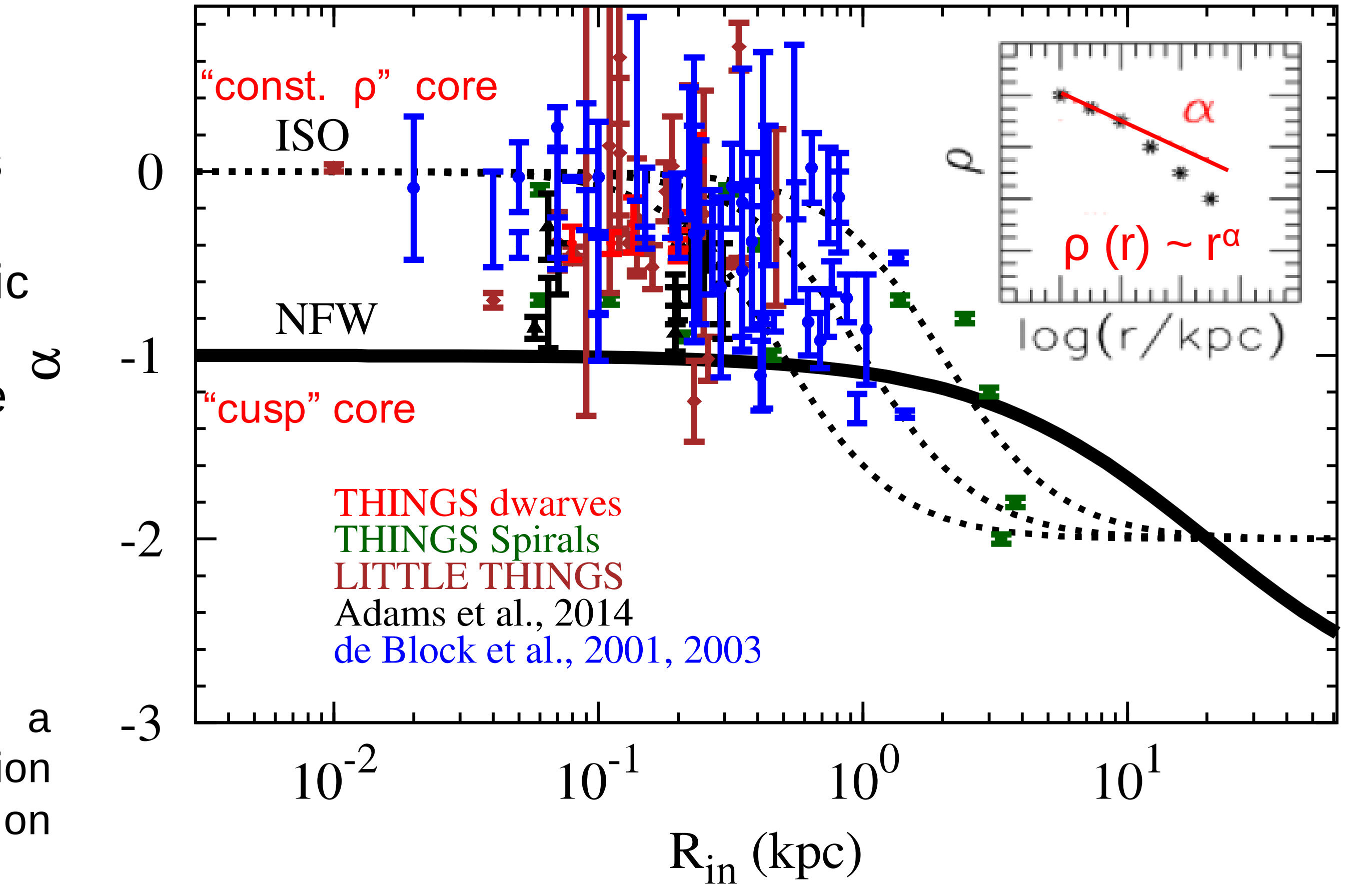

Experimental Detection evidence: These DM models can also "explain" the controversial positive results of direct detection experiments: DAMA. CoGeNT, CRESST and CDMS-Si experiments, and the constraints coming from null results (CDMSGe, XENON100 and very recently LUX);

Motivation: Observational consequences (Galaxies cores): Resolves the cusp halo problem – DM becomes collisional: as a consequence the core of galaxies becomes in agreement with observations (see e.g. de Blok 2010), unlike numerical simulations (see e.g. Navarro et al. 2010).

Helioseismology: limits to the DM characteristics

Dark Sector: DM particle (long range interaction) - interaction between a DM particle (with mass m_χ and charge $Z_\chi\ g_\chi$) and a nucleus (with mass m_n and electric charge Ze). The scattering cross section $\sigma_{\chi n}$ depends of the relative velocity v_{rel} of the particles, and their specific properties:

$\sigma_{\chi n}(v_{rel}\ Z_\chi\ , m_\chi, g_\chi, Z, m_n \ldots)$

Lopes, Panci and Silk (2014)

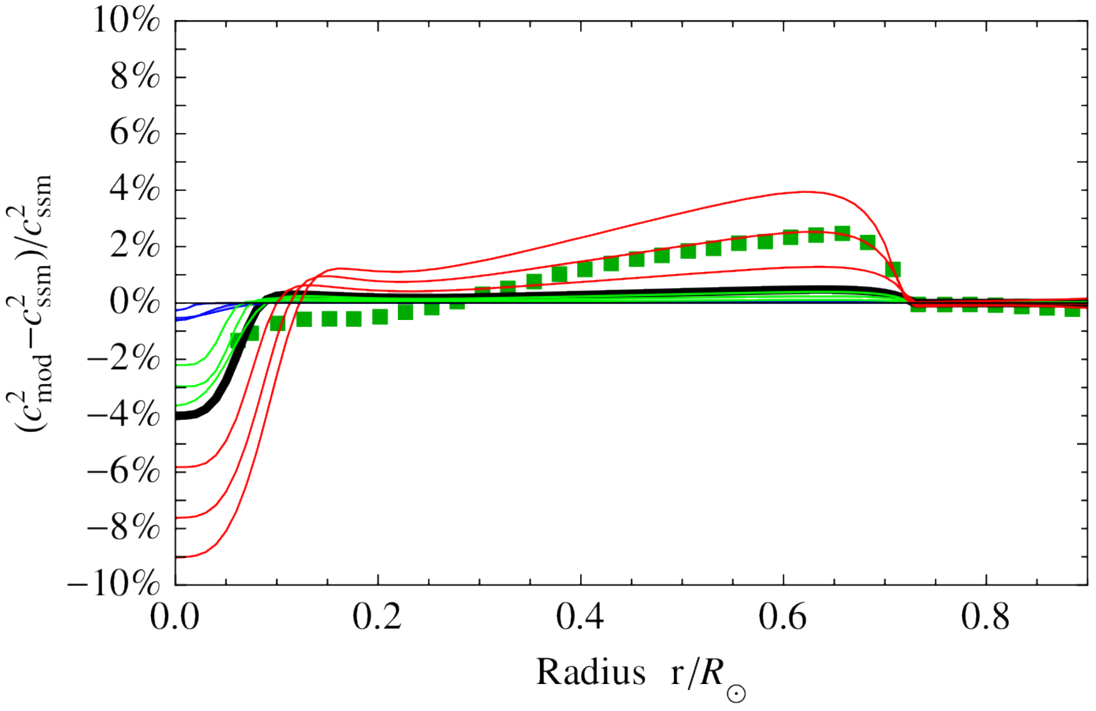

Max δc^2_{obs} [$=(c^2_{obs}-c^2_{ssm})/c^2_{ssm}$] $\simeq$ 3%

Max δc^2_{dm} [$=(c^2_{dm}-c^2_{ssm})/c^2_{ssm}$] $\simeq$ 3%

Helioseismology: DM particles with a mass of **10 GeV and a long–range interaction with ordinary matter mediated by a very light mediator (below roughly a few MeV**), can have an impact on the Sun's sound speed profile without violating the constraints coming from direct DM searches.

TÉCNIC

Helioseismology: limits to the DM characteristics

Dark Sector: DM particle (long range interaction) - interaction between a DM particle (with mass $\boldsymbol{m_\chi}$ and charge $\boldsymbol{Z_\chi\, g_\chi}$) and a nucleus (with mass $\boldsymbol{m_n}$ and electric charge $\boldsymbol{Ze}$). The scattering cross section $\boldsymbol{\sigma_{\chi n}}$ depends of the relative velocity $\boldsymbol{v_{rel}}$ of the particles, and their specific properties:

$$\boldsymbol{\sigma_{\chi n}(v_{rel}\ Z_\chi\ ,\ m_\chi,\ g_\chi,\ Z, m_n \ldots)}$$

Vincent et. al. (2015)

Max $\boldsymbol{\delta} c^2_{obs}$ $[=(c^2_{obs}-c^2_{ssm})/c^2_{ssm}] \simeq$ 3%

Max $\boldsymbol{\delta} c^2_{dm}$ $[=(c^2_{dm}-c^2_{ssm})/c^2_{ssm}] \simeq$ 3%

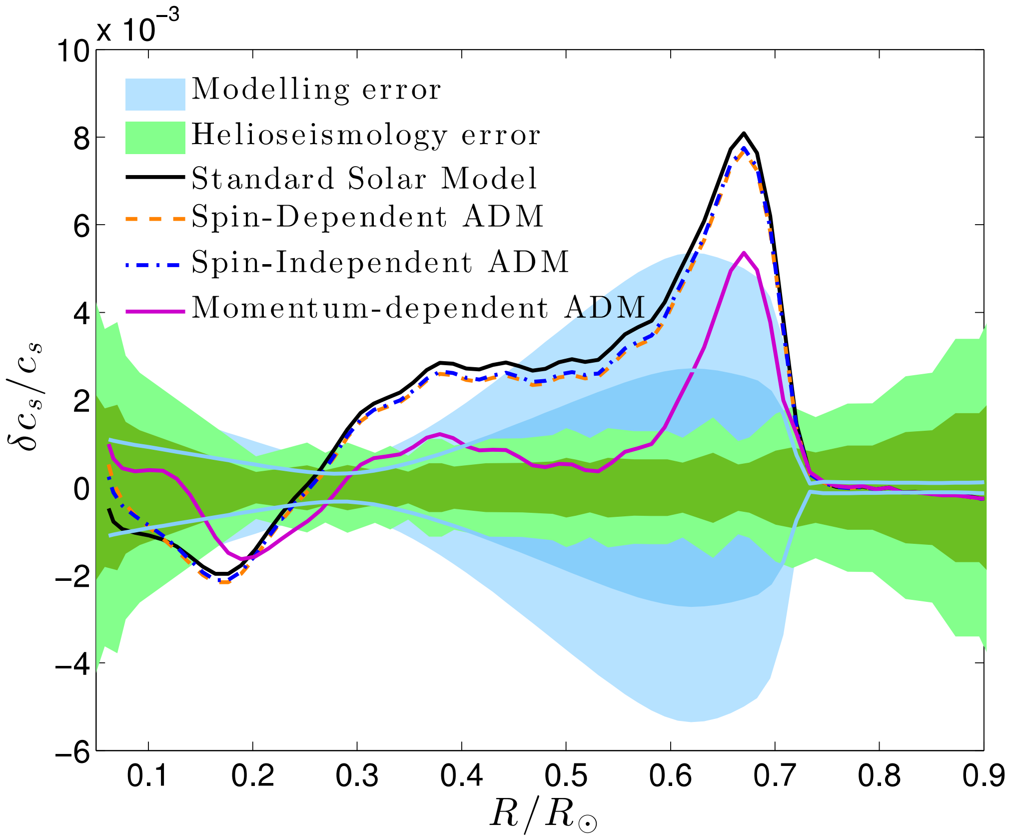

Helioseismology: Asymmetric dark matter coupling to nucleons has the square of the momentum q exchanged in the collision. Agreement with sound speed profiles, etc . . . . The best model corresponds to a dark matter particle with a **mass of 3 GeV**. Possible **solution** to the **solar metallicity problem.**

TÉCNIC

Helioseismology: limits to the DM characteristics

Dark Sector (magnetic dipole dark matter): interaction between DM particle (with mass m_χ and magnetic dipole moment μ_χ) and a baryon, this leads to the following expression for cross section: $\sigma_{\chi n}(\ m_\chi, \mu_\chi\ , \ldots)$

Lopes, Kadota & Silk (2014)

Max δc^2_{obs} [$=(c^2_{obs}-c^2_{ssm})/c^2_{ssm}$] $\simeq$ 3%

Max δc^2_{dm} [$=(c^2_{dm}-c^2_{ssm})/c^2_{ssm}$] $\gtrsim$ 3%

μ_χ is the magnetic dipole moment

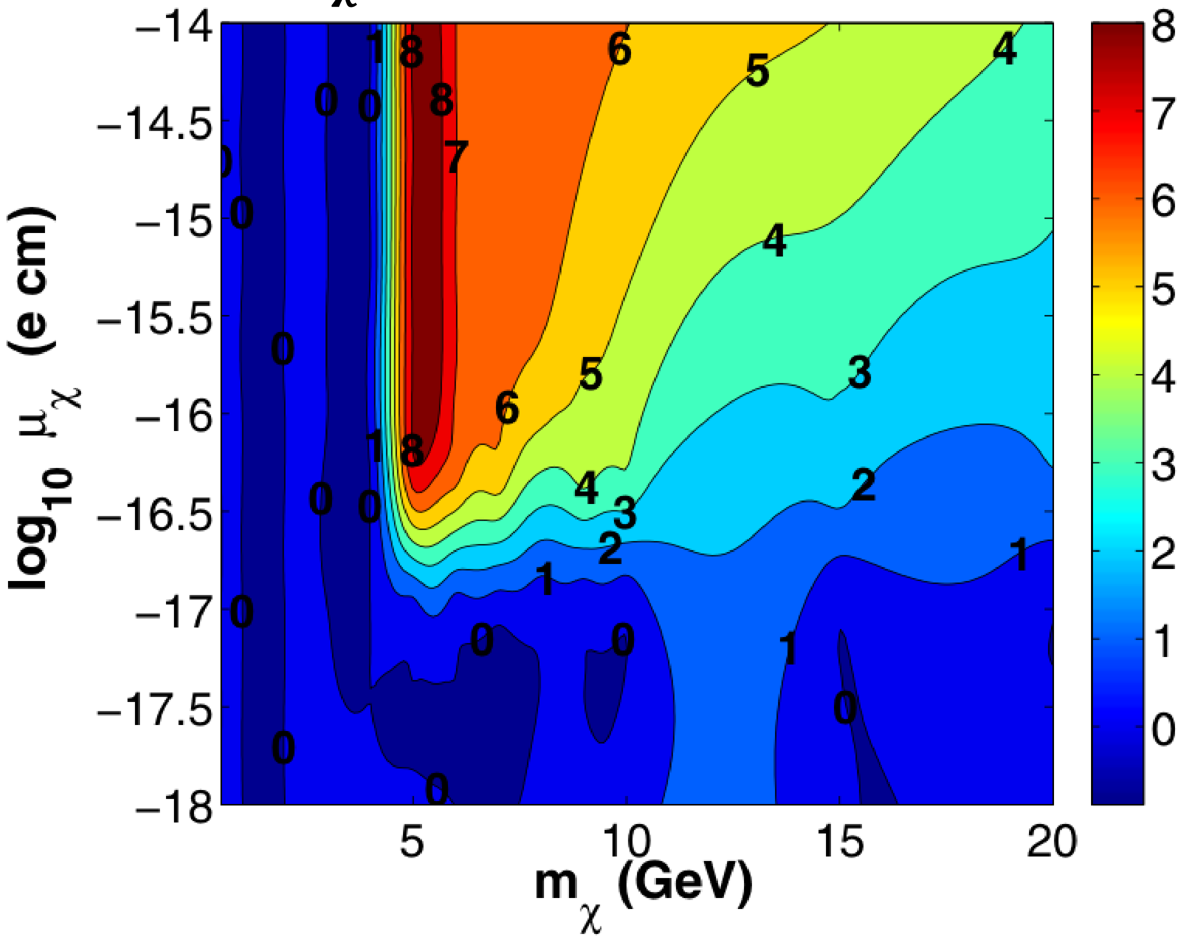

Helioseismology: The dipole interaction can lead to a sizable DM scattering cross section even for light DM, and asymmetric DM can lead to a large DM number density in the Sun. We find that solar model precision tests, using as diagnostic the sound speed profile obtained from helioseismology data, exclude dipolar DM particles with a mass larger than 4.3 GeV and magnetic dipole moment larger than 1.6×10^{-17} e cm.

TÉCNIC

Helioseismology: limits to the DM characteristics

Dark Sector (magnetic dipole dark matter): interaction between DM particle (with mass m_χ and magnetic dipole moment μ_χ) and a baryon, this leads to the following expression for cross section: $\sigma_{\chi n}(\ m_\chi, \mu_\chi\ , \ldots)$

Lopes, Kadota & Silk (2014)

Max $\delta c^2_{obs}\ [=(c^2_{obs}-c^2_{ssm})/c^2_{ssm}] \simeq\ 3\%$

Max $\delta c^2_{dm}\ [=(c^2_{dm}-c^2_{ssm})/c^2_{ssm}] \gtrsim\ 3\%$

μ_χ is the magnetic dipole moment

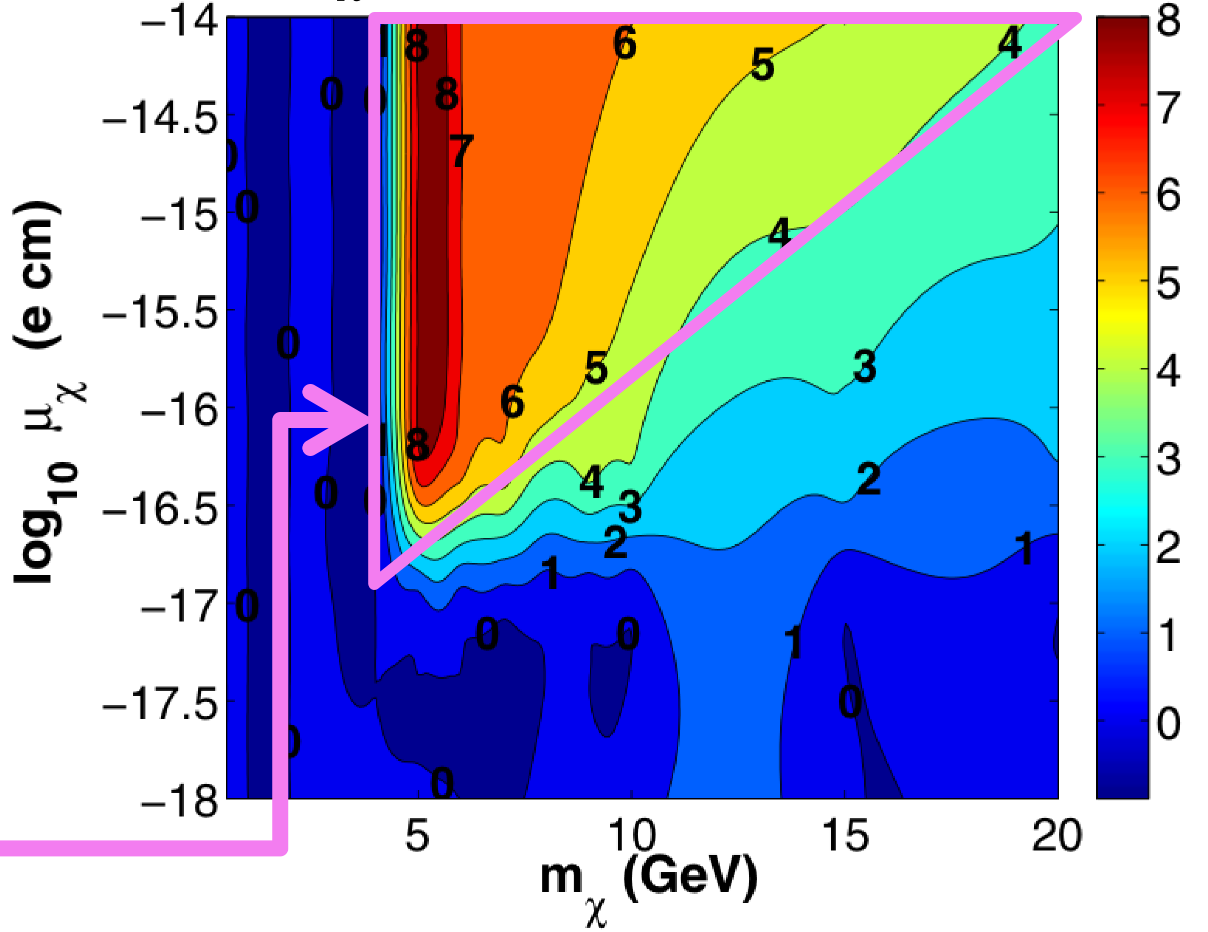

Helioseismology: The dipole interaction can lead to a sizable DM scattering cross section even for light DM, and asymmetric DM can lead to a large DM number density in the Sun. We find that solar model precision tests, using as diagnostic the sound speed profile obtained from helioseismology data, exclude dipolar DM particles with a mass larger than 4.3 GeV and magnetic dipole moment larger than $1.6\ \times\ 10^{-17}$ e cm.

TÉCNICO

Asteroseismology: limits to the DM characteristics

Dark Sector: ADM particle (point-like interaction) – interaction between a DM particle (with mass $\boldsymbol{m_\chi}$ and scattering cross-section $\boldsymbol{\sigma_{\chi p}}$) and a proton inside the star. Using the **the small frequency separations** the following constrains were obtained for **alpha centauri B.**

Casanellas & Lopes (2013)

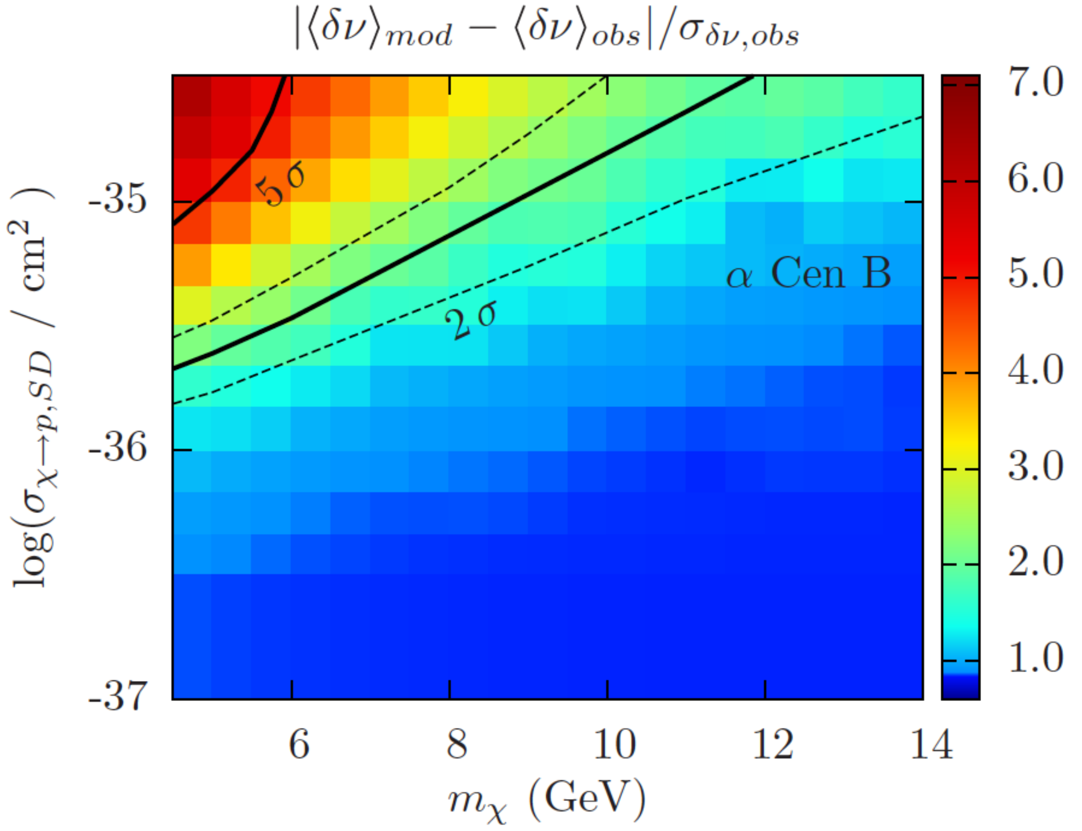

Asteroseismology: The presence of dark matter (asymmetric) changes the transport of heat energy inside these stars (decreasing the central temperature). Using the asteroseismology data of Alpha Cent B (0.9 Mo), DM particles with $m_\chi \sim 5$ GeV and $\sigma_{\chi p}^{SD} \geq 3\ 10^{-36}$cm^2 are excluded at 95% CL.

TÉCNIC

Asteroseismology: limits to the DM characteristics

Dark Sector: ADM particle (point-like interaction) - interaction between a DM particle (with mass $\boldsymbol{m_\chi}$ and scattering cross-section $\boldsymbol{\sigma_{\chi p}}$) and a proton inside the star. Using the **the small frequency separations** the following constrains were obtained for **alpha centauri B**.

Casanellas & Lopes (2013)

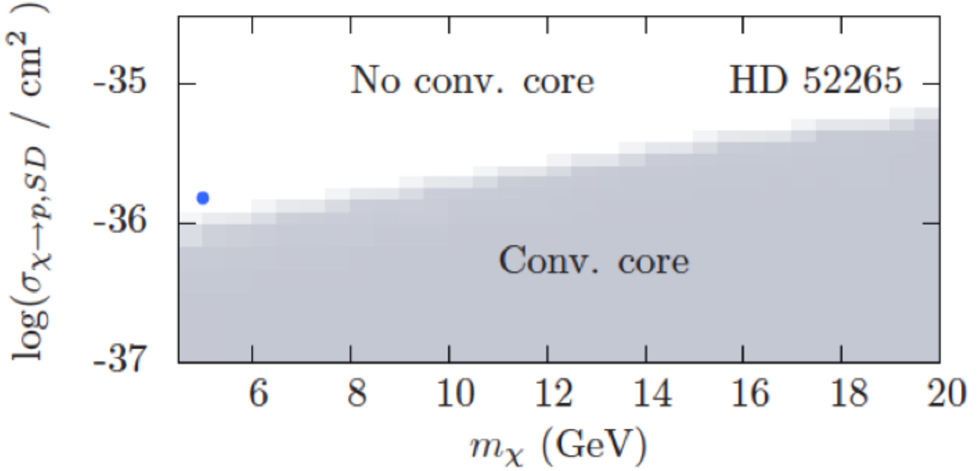

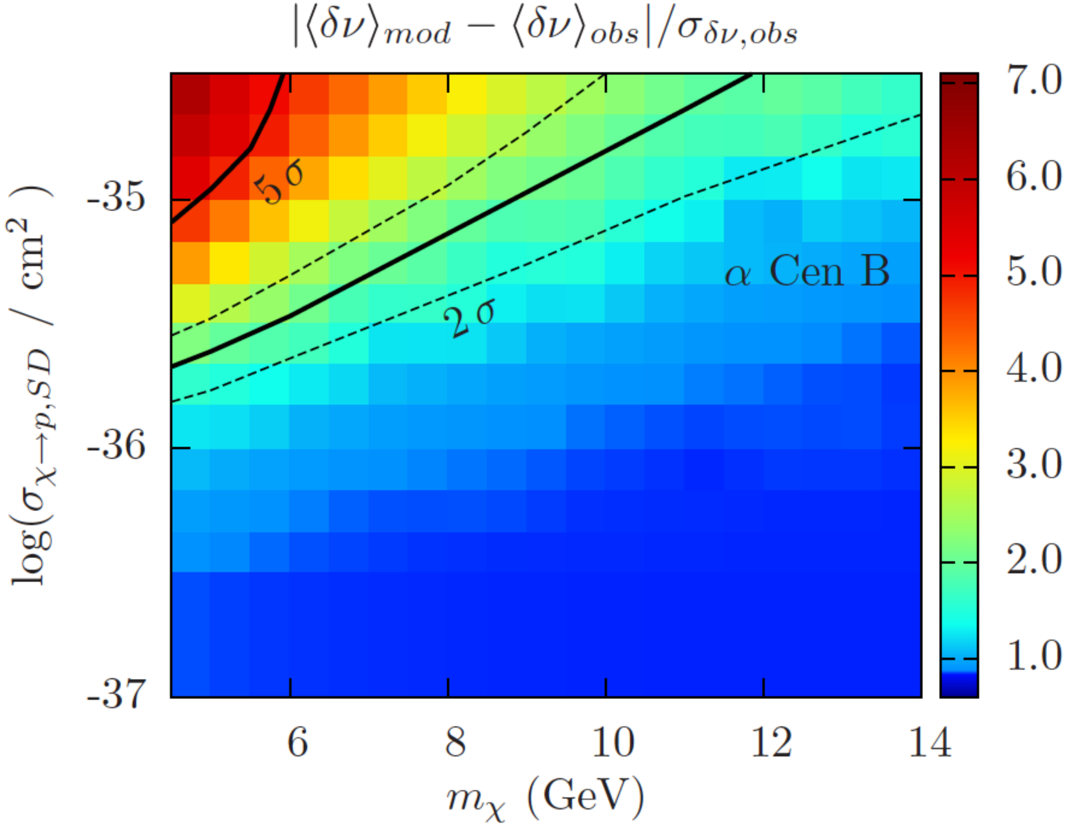

Asteroseismology: The presence of dark matter (asymmetric) changes the transport of heat energy inside these stars (decreasing the central temperature). Using the asteroseismology data of Alpha Cent B (0.9 Mo), DM particles with $m_\chi \sim 5$ GeV and $\sigma_{\chi n}^{SD} \geq 3\ 10^{-36}\mathrm{cm}^2$ are excluded at 95% CL.

Changes in the central temperatures and densities, leads to suppression of the convective core in 1.1-1.3 $M_\odot$ stars. This result was confirmed by Casanellas, Brandão & Lebreton 2015 using other stars.

Asteroseismology: limits to the DM characteristics

Dark Sector: ADM particle (point-like interaction) - interaction between a DM particle (with mass $\boldsymbol{m_\chi}$ and scattering cross-section $\boldsymbol{\sigma_{\chi p}}$) and a proton inside the star.. This model includes also a self-interaction cross section consistent with the constraint from self-interaction cross section ($\sigma_{\chi\chi}/m_\chi \lesssim 8.3 \times 10^{-25}$ cm^2/GeV) obtained from the galaxy bullet clusters (Harvey et al. 2015).

Martins, Lopes & Casanellas (2017)

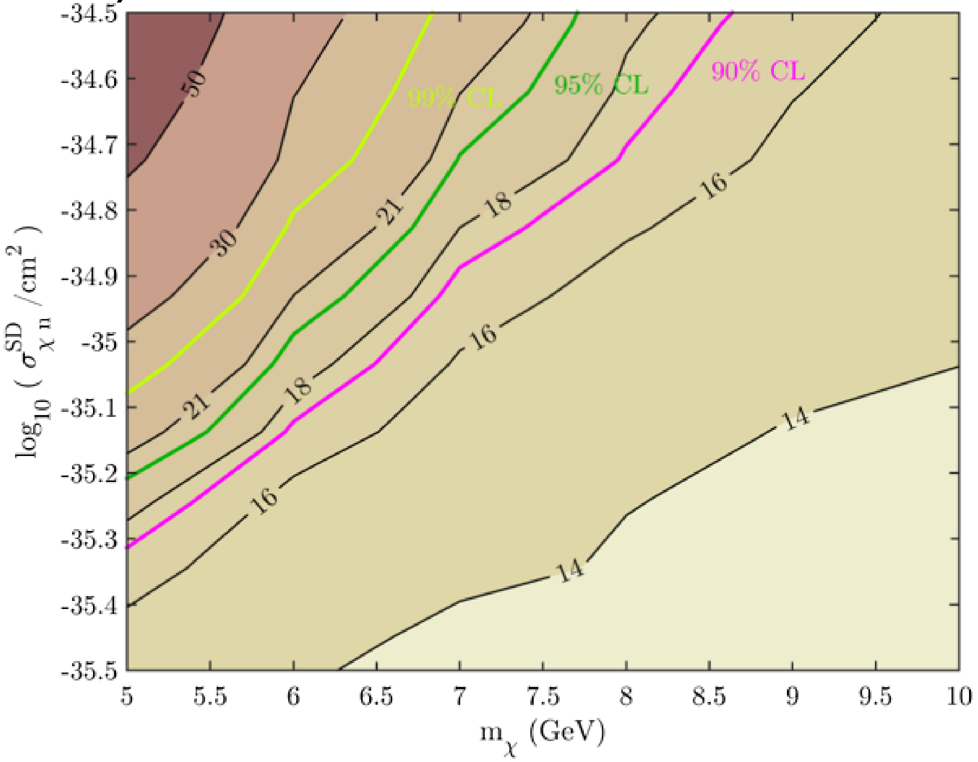

Asteroseismology: Sum of squared errors χ^2 for the r_{02} diagnostic of star KIC 8379927 **(1.12 M$_\odot$, 1.82 Gyr)** for these DM models with $\sigma_{\chi\chi} = 10^{-24}$ cm^2. Also shown are the 90%, 95%, and 99% C.L.'s corresponding to these χ^2's.

TÉCNIC

Asteroseismology: limits to the DM characteristics

Dark Sector: ADM particle (point-like interaction) - interaction between a DM particle (with mass $\boldsymbol{m_\chi}$ and scattering cross-section $\boldsymbol{\sigma_{\chi p}}$) and a proton inside the star.. This model includes also a self-interaction cross section consistent with the constraint from self-interaction cross section ($\sigma_{\chi\chi}/m_\chi \lesssim 8.3 \times 10^{-25}\ cm^2/GeV$) obtained from the galaxy bullet clusters (Harvey et al. 2015).

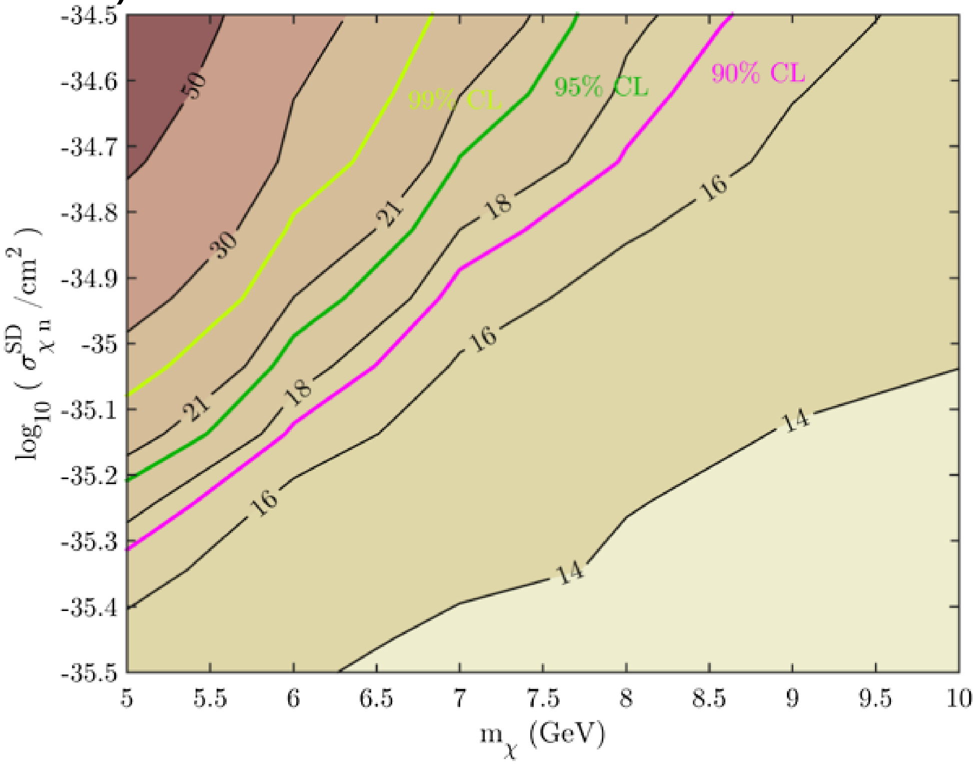

Martins, Lopes & Casanellas (2017)

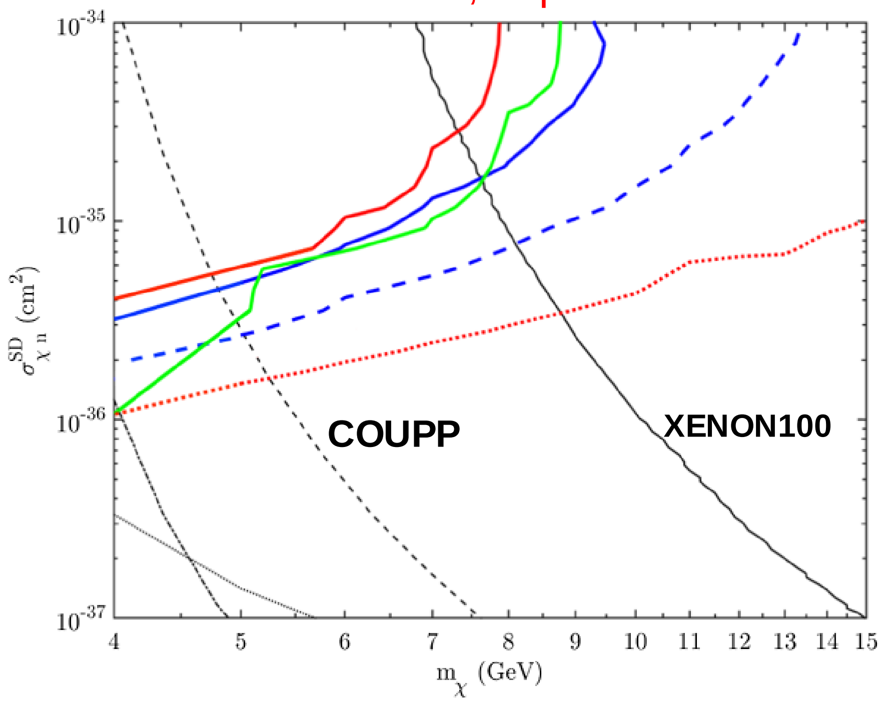

Asteroseismology: 90% C.L.'s ascertained from the ADM scenario for: Sun $\chi^2\ T_c$ (dotted red), Sun $\chi^2 r_{02}$ (solid red), KIC 8379927 $\chi^2 r_{02}$ (**solid blue**), and KIC 7871531 $\chi^2 r_{02}$ (solid green). The dashed blue line is the projected 90% C.L. corresponding to a **10% increase in precision for the mode frequencies**. For comparison, 90% C.L. limits from some direct detection experiments are also shown in black lines (like XENON100 and COUPP).

Constraints on Axion Like Particles

Asteroseismology

Impact of Axion Cooling on Stellar Evolution Asteroseismology subgiant star

Star's Detector: KIC 6933899 is a **late-type G0.5IV main-sequence star (sub-giant star)**with a mass between 1.10 and 1.14 solar masses, exhibiting **33 detected oscillation modes** with a precision of approximately **0.1 Hz.** This star displays acoustic behavior, as evidenced by its predominantly simple p-modes, which are sensitive to the physical properties of the stellar core.

Energy Production and Loss: Axions primarily produced near the star's center, affecting the hydrogen burning shell; Significant cooling effect from axionic energy loss competing with nuclear energy production.

Asteroseismic diagnostics: Changes in gravity-driven pulsation modes provide evidence of axion effects. Preliminary bounds on axion-photon coupling: $g_{a\gamma} \leq 1.38 \times 10^{-10} GeV^{-1}$ (95% CL) and $g_{a\gamma} \leq 0.98 \times 10^{-10} GeV^{-1}$ (68% CL)

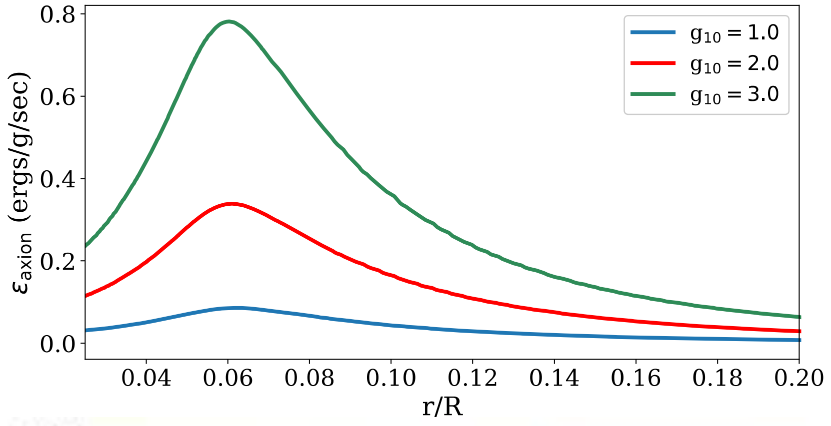

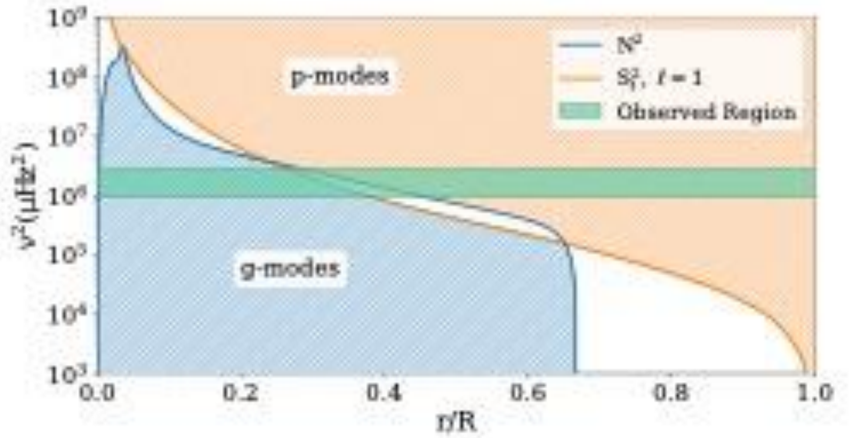

Fordham & Lopes (PRD,2024)

Asteroseismology: Axion cooling significantly impacts stellar evolution by modifying core temperatures, radiative regions, and pulsation modes. Precision tools like asteroseismology are crucial for detecting axionic effects in stars and refining constraints on axion properties.

Impact of Axion Cooling on Stellar Evolution Asteroseismology subgiant star

Star’s Detector: KIC 6933899 is a **late-type G0.5IV main-sequence star (sub-giant star)**with a mass between 1.10 and 1.14 solar masses, exhibiting **33 detected oscillation modes** with a precision of approximately **0.1 Hz.** This star displays acoustic behavior, as evidenced by its predominantly simple p-modes, which are sensitive to the physical properties of the stellar core.

Energy Production and Loss: Axions primarily produced near the star's center, affecting the hydrogen burning shell; Significant cooling effect from axionic energy loss competing with nuclear energy production.

Asteroseismic diagnostics: Changes in gravity-driven pulsation modes provide evidence of axion effects. Preliminary bounds on axion-photon coupling: $g_{a\gamma} \leq 1.38 \times 10^{-10} GeV^{-1}$ (95% CL) and $g_{a\gamma} \leq 0.98 \times 10^{-10} GeV^{-1}$ (68% CL)

Stars

Fordham & Lopes (2024)

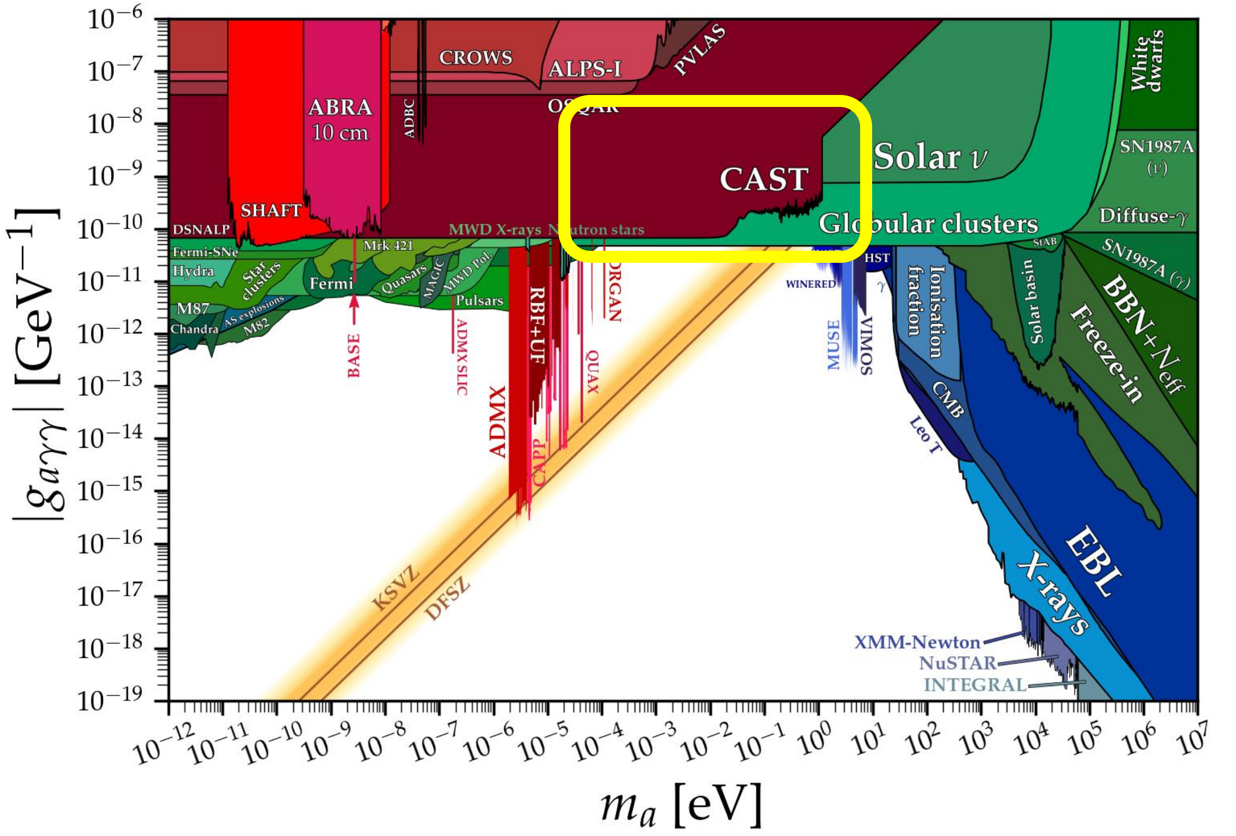

https://github.com/cajohare/AxionLimits/blob/master/docs/ap.md

Asteroseismology: Axion cooling significantly impacts stellar evolution by modifying core temperatures, radiative regions, and pulsation modes. Precision tools like asteroseismology are crucial for detecting axionic effects in stars and refining constraints on axion properties.

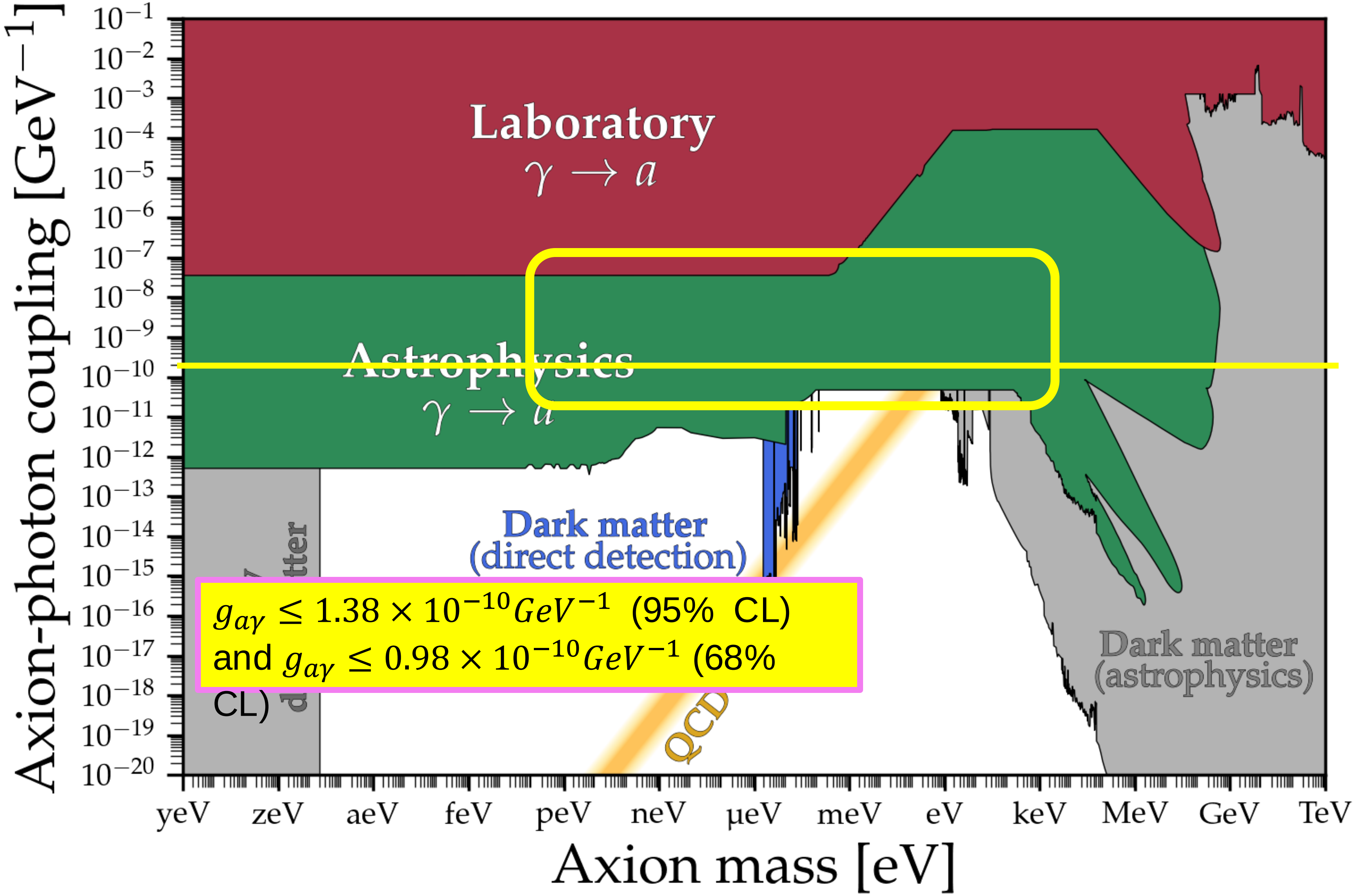

$g_{a\gamma} \leq 1.38 \times 10^{-10} GeV^{-1}$ (95% CL) and $g_{a\gamma} \leq 0.98 \times 10^{-10} GeV^{-1}$ (68% CL)

Impact of Axion Cooling on Stellar Evolution Asteroseismology red supergiant star

Star's Detector: Betelgeuse (Alpha Orionis) is an M2Iab red supergiant star with a mass between 16.5 and 19 solar masses, exhibiting oscillation periods of 416 and 185 days identified as the fundamental mode and the first overtone, respectively, displaying complex oscillatory behavior sensitive to the conditions in its convective and radiative layers.

Energy Production and Loss: Axions primarily produced near Betelgeuse's core affect the helium burning shell; significant cooling from axionic energy loss competes with nuclear energy production, resulting in increased luminosity and higher neutrino production.

Asteroseismic diagnostics: Changes in gravity-driven pulsation modes in Betelgeuse provide evidence of axion effects. Stellar models with an axion-photon coupling $2.0 \times 10^{-13}\mathrm{GeV}^{-1}$: $\leq g_{a\gamma} \leq 2 \times 10^{-10}\mathrm{GeV}^{-1}$ align with observational data. An upper limit will be $g_{a\gamma} \leq 3.0 \times 10^{-10}\mathrm{GeV}^{-1}$.

Stars

Severino & Lopes (2023)

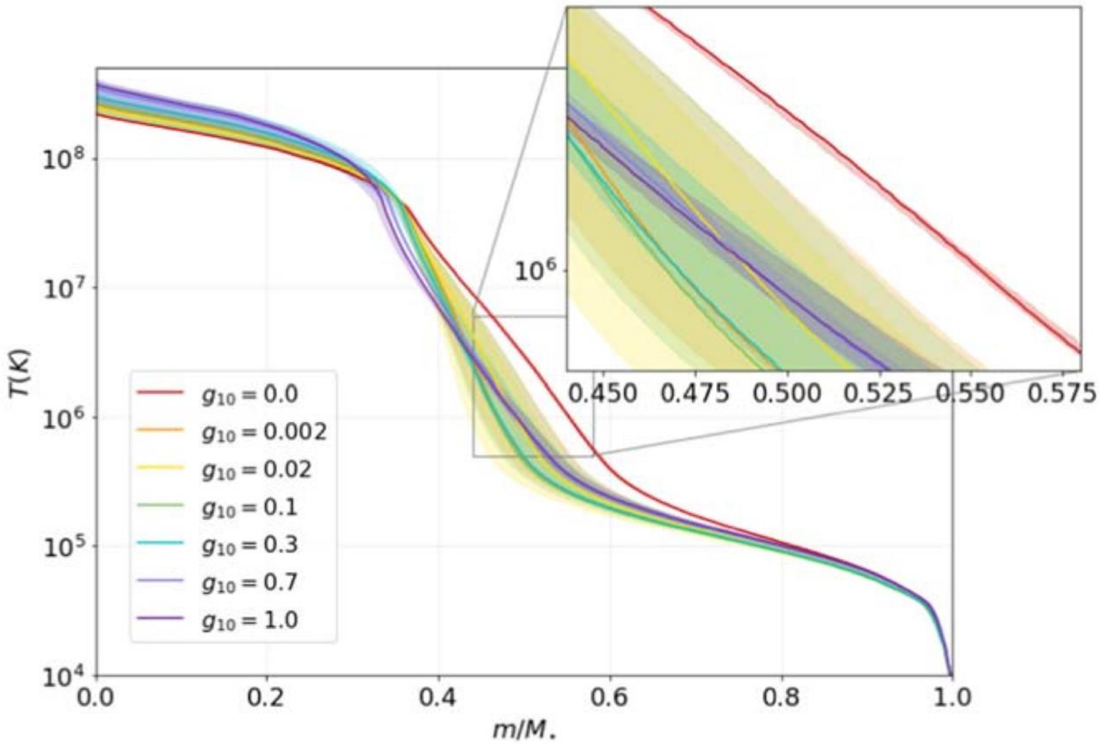

Temperature profiles of the α-Ori models. The solid lines correspond to the model that best represents the average behavior for the corresponding g10, while the shaded regions illustrate the uncertainty.

Asteroseismology: Axion cooling significantly impacts stellar evolution by modifying core temperatures, radiative regions, and pulsation modes. Precision tools like asteroseismology are crucial for detecting axionic effects in stars and refining constraints on axion properties.

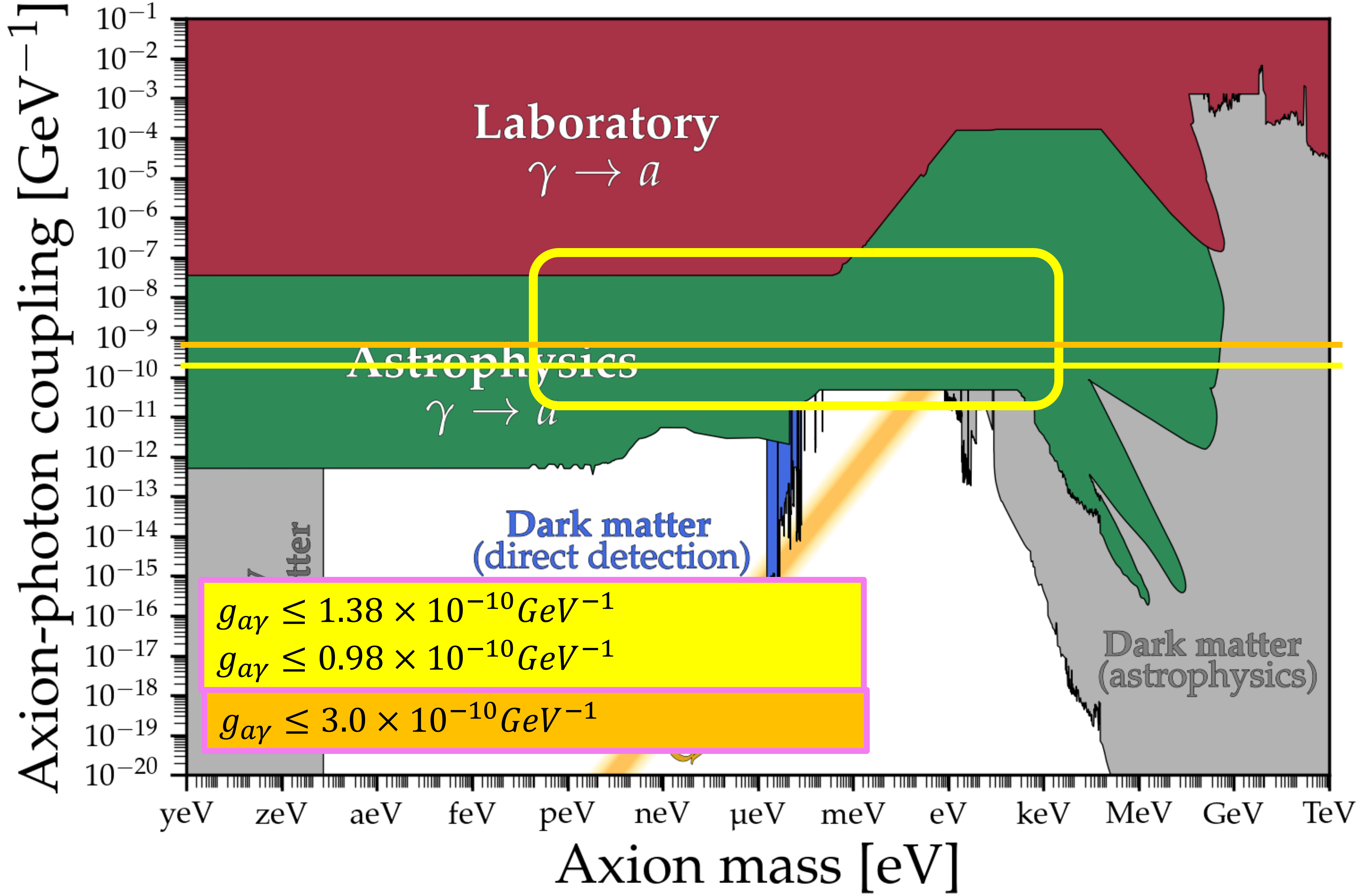
Axion-photon coupling [GeV^{-1}]
Axion mass [eV]
10^{-1} 10^{-2} 10^{-3} 10^{-4} 10^{-5} 10^{-6} 10^{-7} 10^{-8} 10^{-9} 10^{-10} 10^{-11} 10^{-12} 10^{-13} 10^{-14} 10^{-15} 10^{-16} 10^{-17} 10^{-18} 10^{-19} 10^{-20}
yeV zeV aeV feV peV neV μeV meV eV keV MeV GeV TeV
Laboratory
$\gamma \to a$
Astrophysics
$\gamma \to a$
Dark matter
(direct detection)
Dark matter
(astrophysics)
$g_{a\gamma} \leq 1.38 \times 10^{-10} GeV^{-1}$
$g_{a\gamma} \leq 0.98 \times 10^{-10} GeV^{-1}$
$g_{a\gamma} \leq 3.0 \times 10^{-10} GeV^{-1}$

Impact of Axion Cooling on Stellar Evolution
Asteroseismology red supergiant star

Star's Detector: Betelgeuse (Alpha Orionis) is an M2Iab red supergiant star with a mass between 16.5 and 19 solar masses, exhibiting oscillation periods of 416 and 185 days identified as the fundamental mode and the first overtone, respectively, displaying complex oscillatory behavior sensitive to the conditions in its convective and radiative layers.

Energy Production and Loss: Axions primarily produced near Betelgeuse's core affect the helium burning shell; significant cooling from axionic energy loss competes with nuclear energy production, resulting in increased luminosity and higher neutrino production.

Asteroseismic diagnostics: Changes in gravity-driven pulsation modes in Betelgeuse provide evidence of axion effects. Stellar models with an axion-photon coupling: $g_{a\gamma} \leq 1.38 \times 10^{-10}\mathrm{GeV}^{-1}$ align with observational data. No compatible models for a $g_{a\gamma} \geq 3.5 \times 10^{-10}\mathrm{GeV}^{-1}$.

Stars

Severino & Lopes (2023)

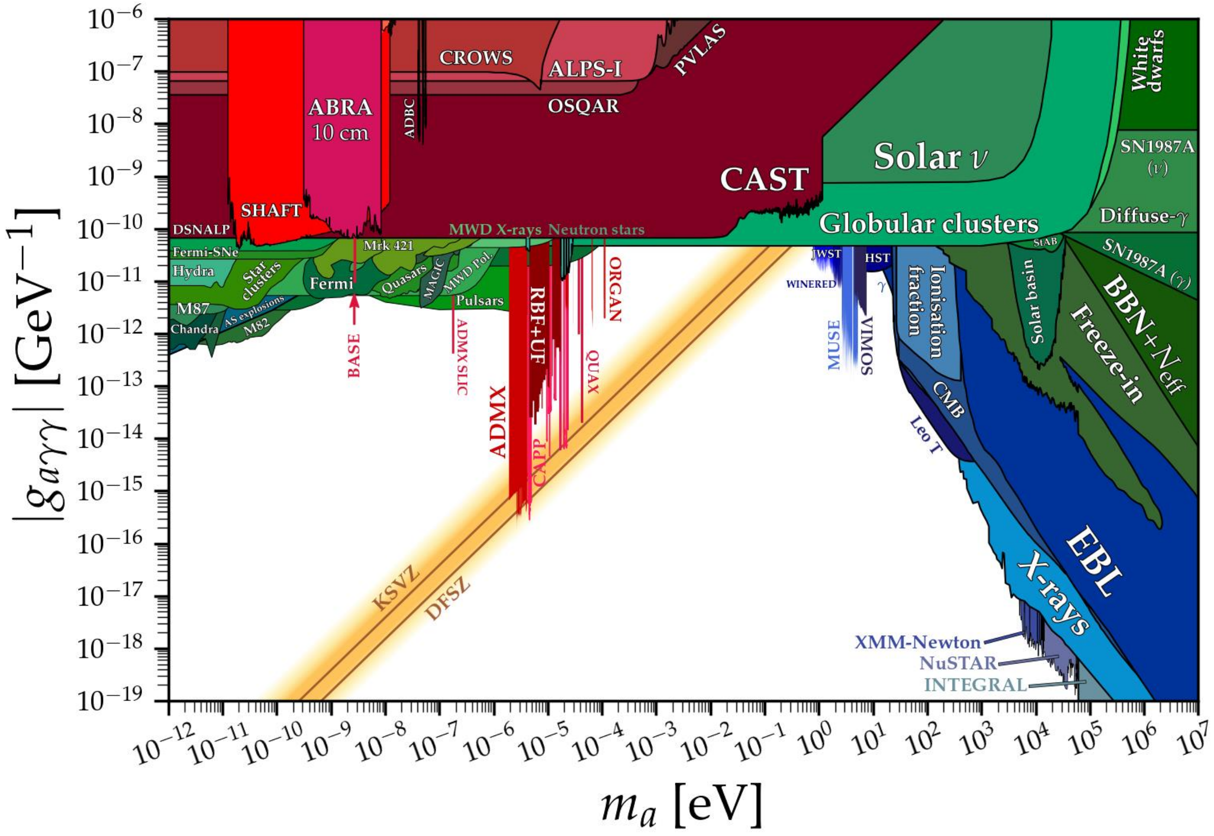

Asteroseismology: Axion cooling significantly impacts stellar evolution by modifying core temperatures, radiative regions, and pulsation modes. Precision tools like asteroseismology are crucial for detecting axionic effects in stars and refining constraints on axion properties.

Constraints on Annihilating Dark Matter

Stars in the Galactic Centre

TÉCNICO LISBOA

Stellar Cluster: limits to the DM characteristics

Dark sector: DM particle (point-like interaction) – an interaction between a DM particle (with mass $\boldsymbol{m_\chi}$ and scattering cross-section $\boldsymbol{\sigma_{\chi p}}$) and a proton inside a low-mass main-sequence star in the Milky Way's nuclear stellar cluster. **Lopes & Lopes (2019)**

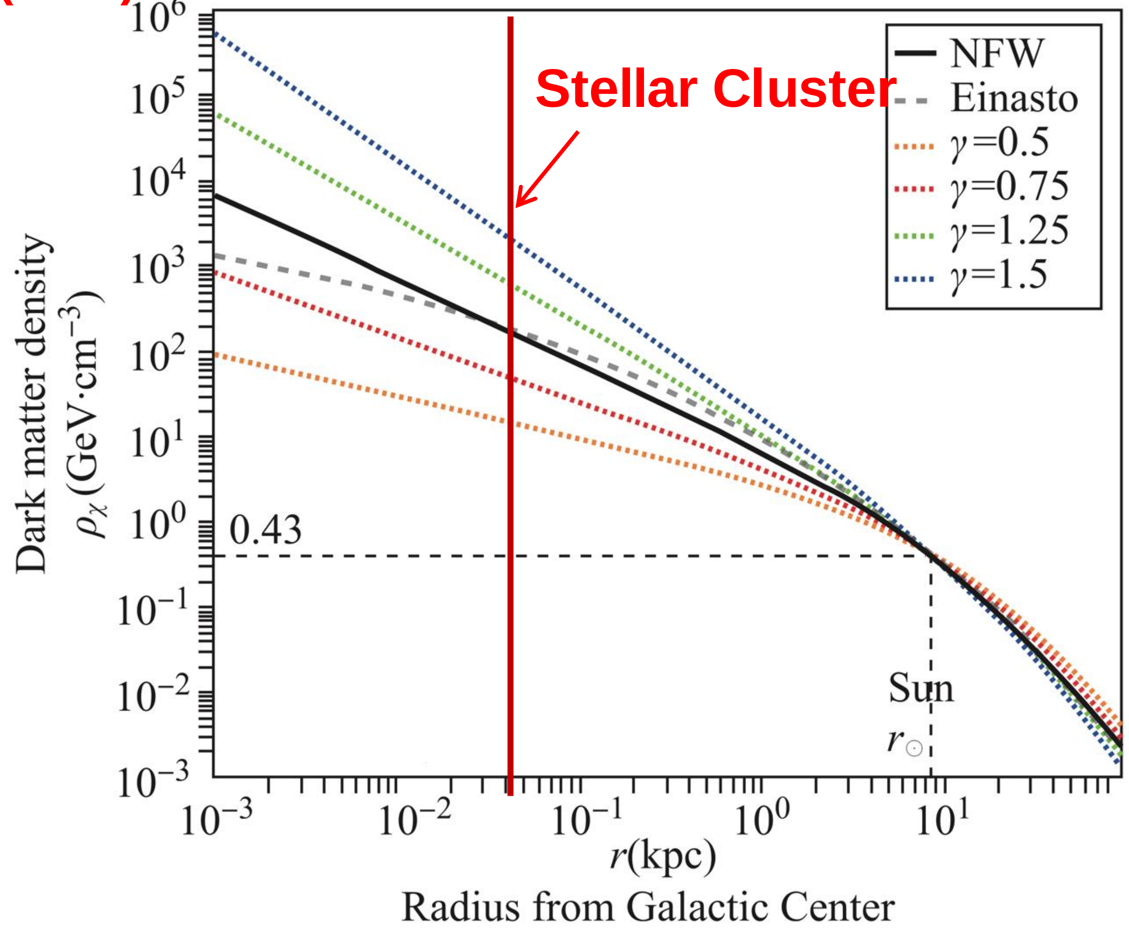

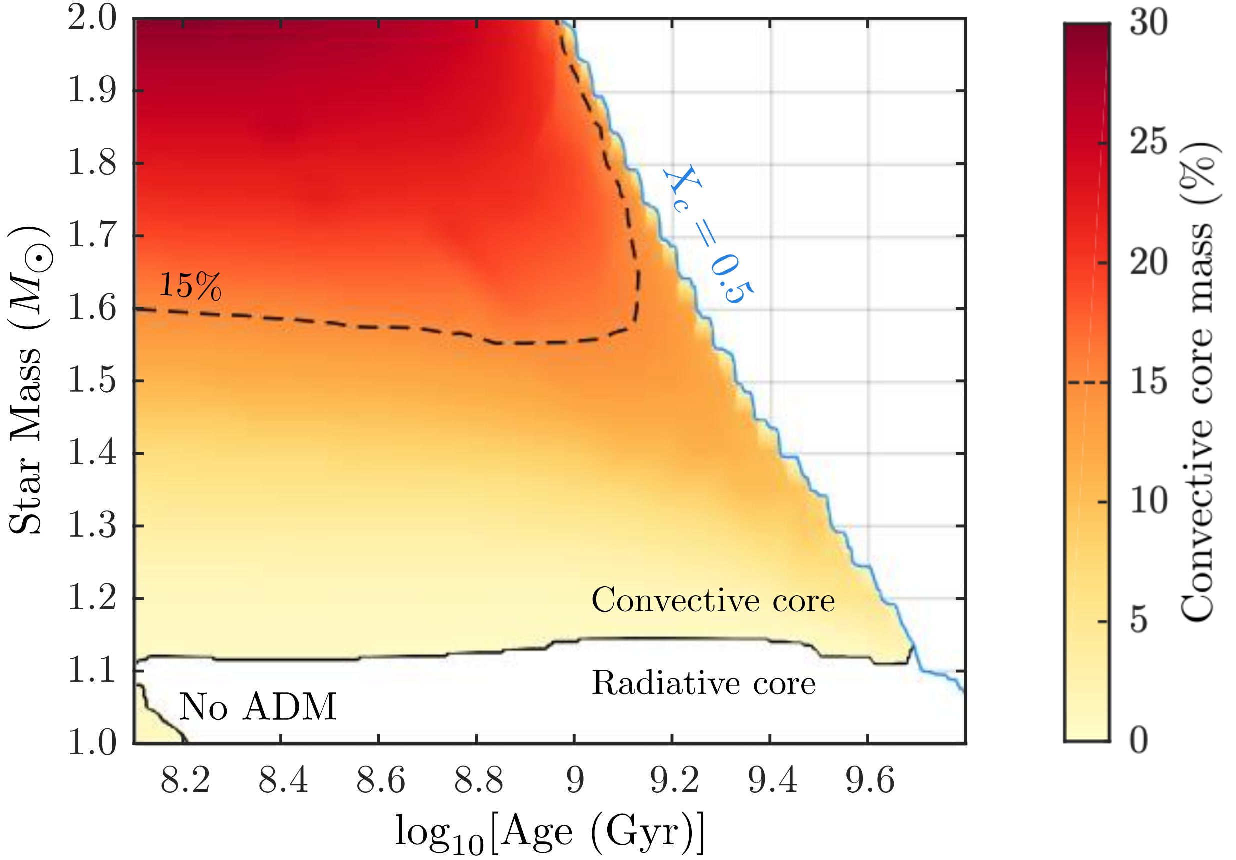

The solid black line separates stars with radiative core from stars with a convective core. We also show the contour (black dashed line) for which the mass of the convective region represents 15% of the total mass of the star.

Stellar Clusters: If we consider $\rho_\chi > 10^3$ **GeV cm^{-3}** (corresponding to the inner 5 pc of the Milky Way), stars lighter than the Sun will have a main-sequence lifespan comparable to the current age of the universe. Stars more massive than 2 $M_\odot$ are not sensitive to the dark matter particles.

Stellar Cluster: limits to the DM characteristics

Dark sector: DM particle (point-like interaction) – an interaction between a DM particle (with mass $\boldsymbol{m_\chi}$ and scattering cross-section $\boldsymbol{\sigma_{\chi p}}$) and a proton inside a low-mass main-sequence star in the Milky Way's nuclear stellar cluster. **Lopes & Lopes (ApJ, 2019)**

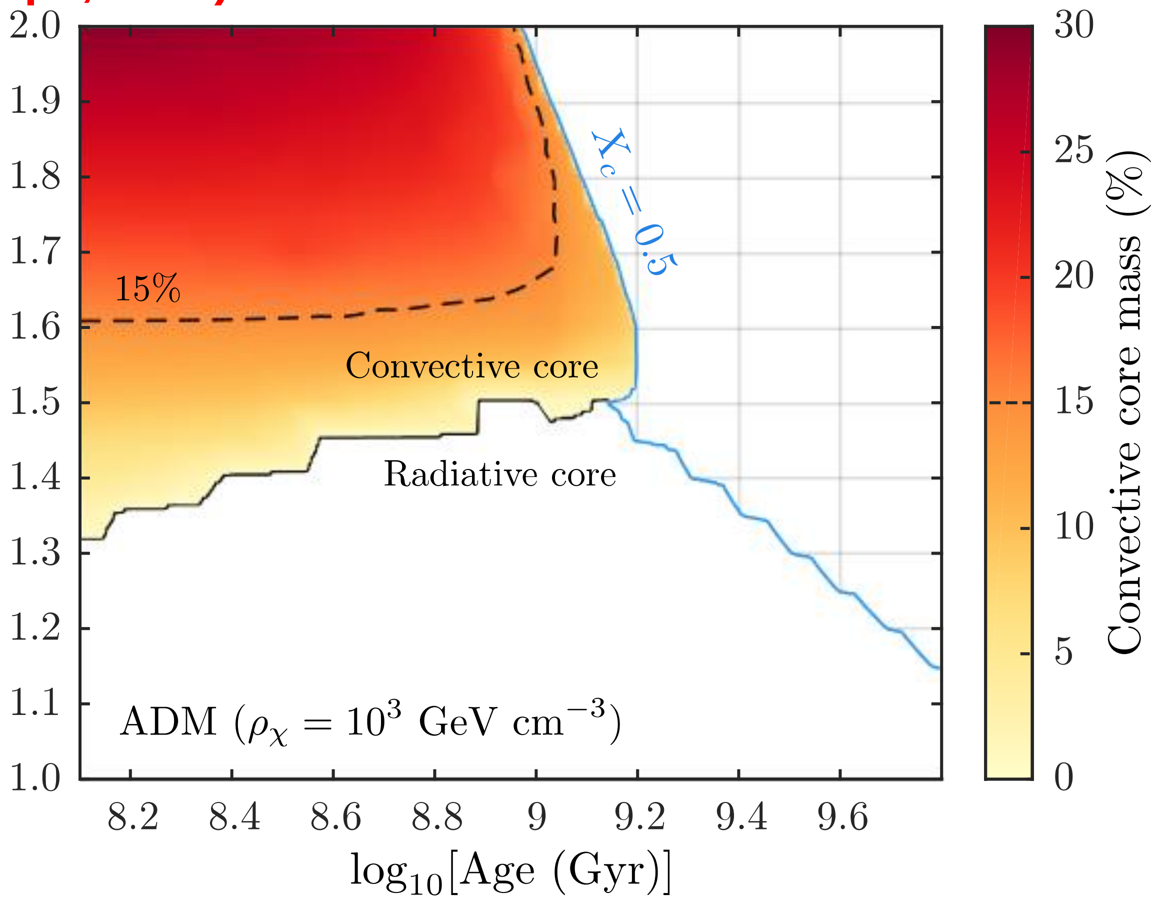

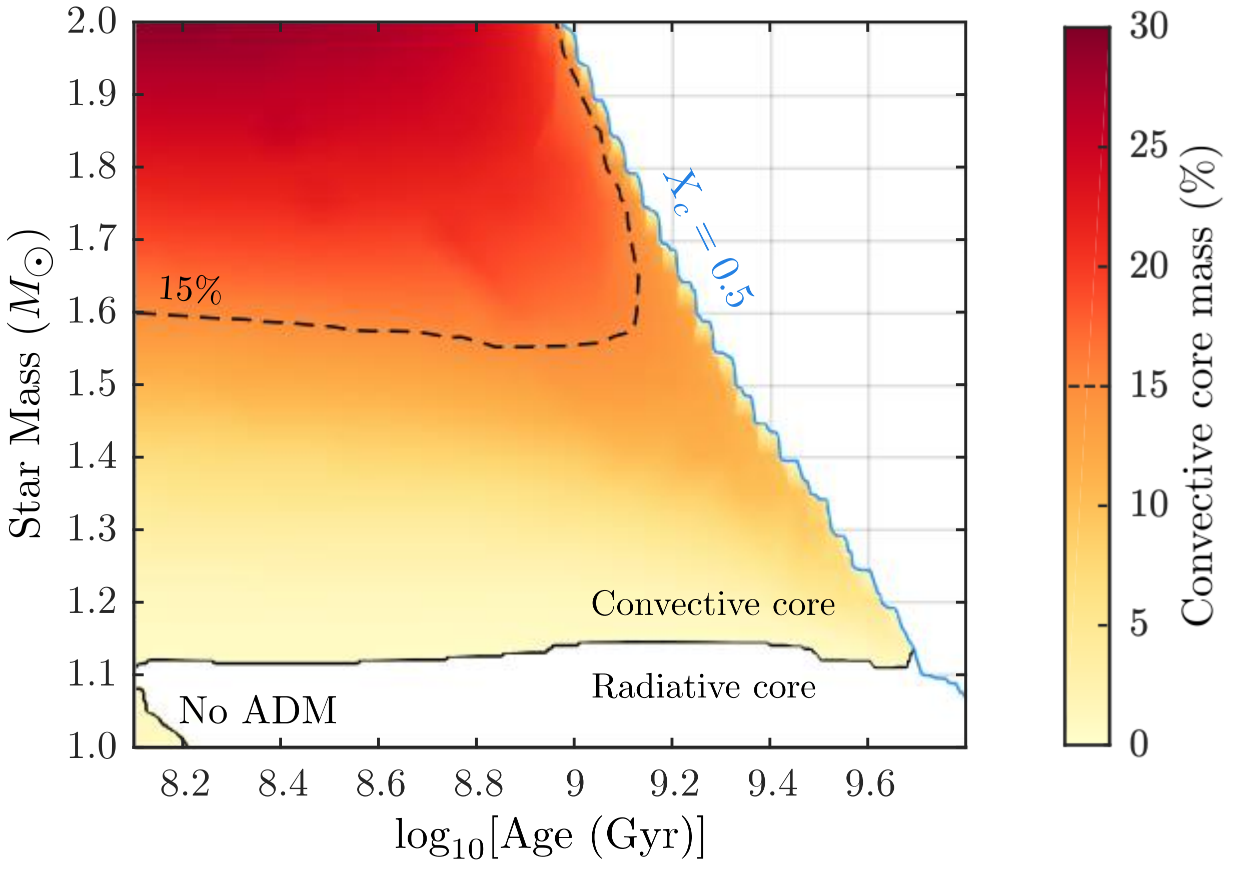

The solid black line separates stars with radiative core from stars with a convective core. We also show the contour (black dashed line) for which the mass of the convective region represents 15% of the total mass of the star.

Stellar Clusters: If we consider $\rho_\chi > 10^3$ **GeV cm^{-3}** (corresponding to the inner 5 pc of the Milky Way), stars lighter than the Sun will have a main-sequence lifespan comparable to the current age of the universe. Stars more massive than 2 $M_\odot$ are not sensitive to the dark matter particles.

Stellar Cluster: limits to the DM characteristics

Dark sector: DM particle (point-like interaction) – an interaction between a DM particle (with mass $\boldsymbol{m_\chi}$ and scattering cross-section $\boldsymbol{\sigma_{\chi p}}$) and a proton inside a low-mass main-sequence star in the Milky Way's nuclear stellar cluster. **Lopes & Lopes (ApJ, 2019)**

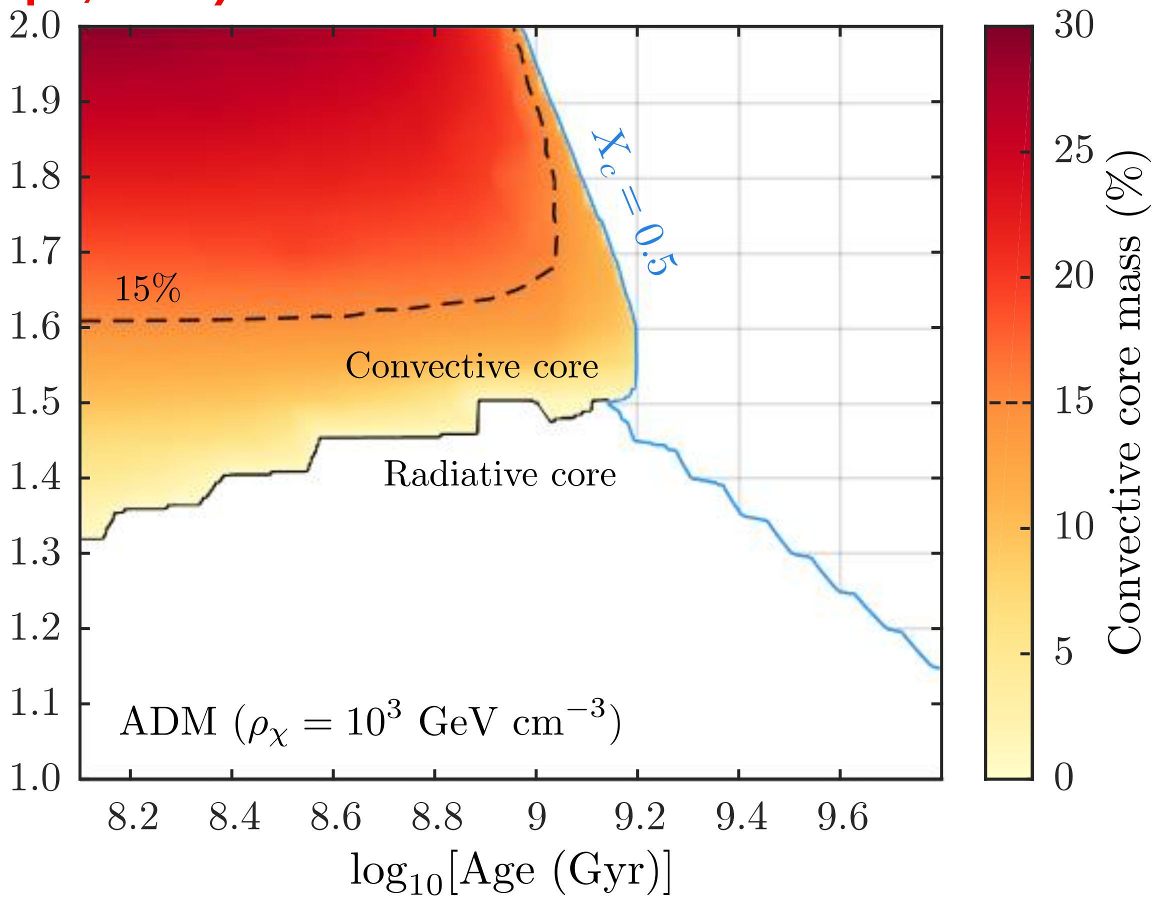

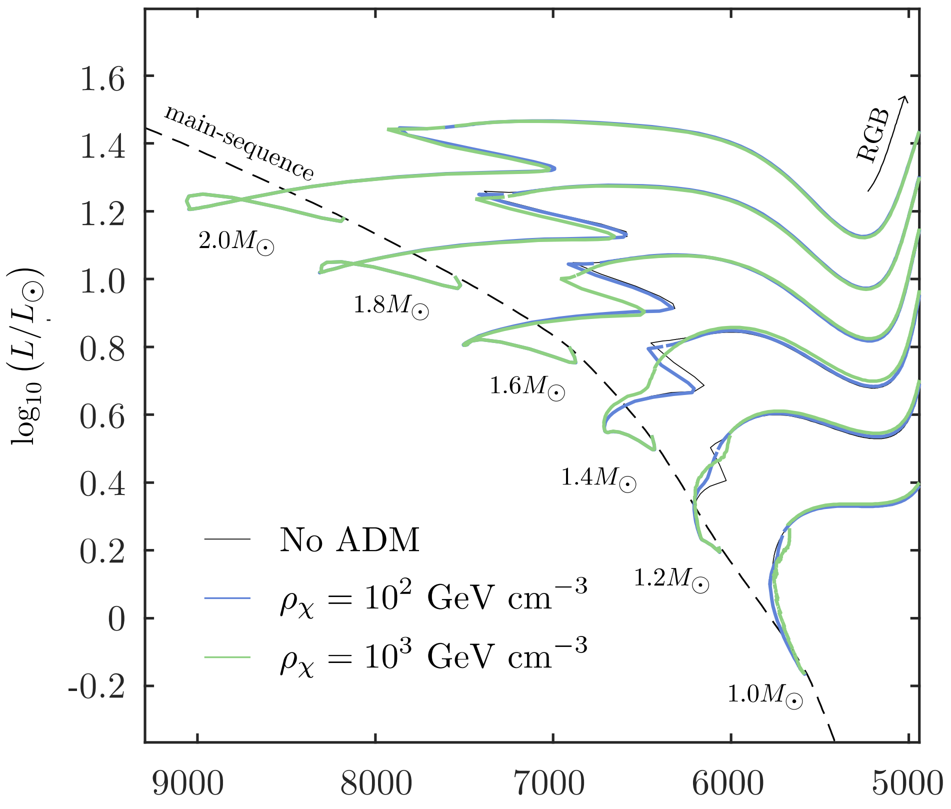

The solid black line separates stars with radiative core from stars with a convective core. We also show the contour (black dashed line) for which the mass of the convective region represents 15% of the total mass of the star.

Stellar Clusters: If we consider $\rho_\chi > 10^3$ **GeV cm**$^{-3}$ (corresponding to the inner 5 pc of the Milky Way), stars lighter than the Sun will have a main-sequence lifespan comparable to the current age of the universe. Stars more massive than 2 $M_\odot$ are not sensitive to the dark matter particles.

Stellar Cluster: limits to the DM characteristics

Dark sector: DM particle (point-like interaction) – Thermally produced DM particles in the mass range 4-10 GeV with spin-independent annihilation and scattering cross-sections that are close to the observational upper limits from direct detection experiments. **Lopes & Lopes, Silk (ApJL, 2019)**

Red Clump stars, in some cases with **$L \sim 10^2\ L_{sun}$**, can be observed throughout the galaxy and thus can give us insight into the DM conditions found in situ.

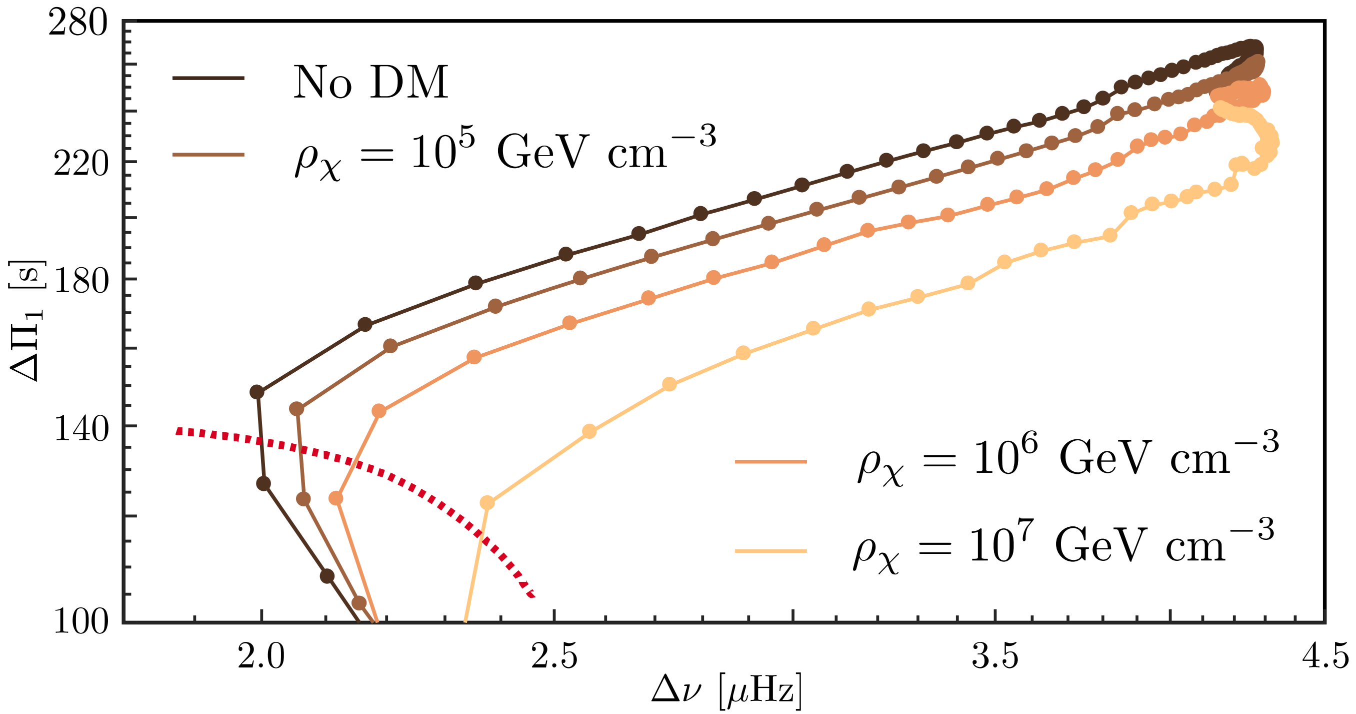

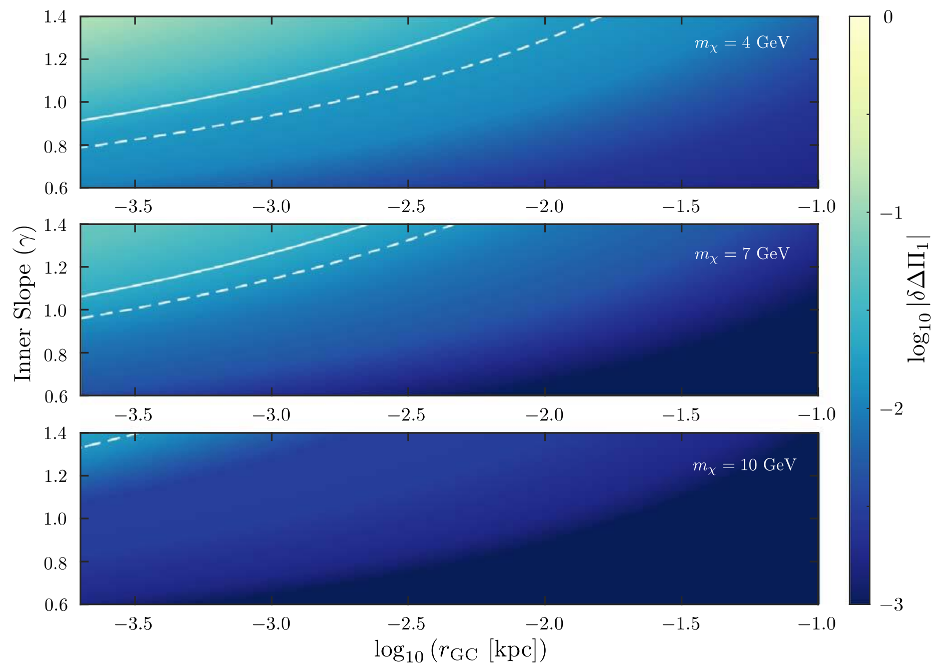

G-mode period spacing $\Delta\Pi_1$ vs. p-mode large frequency separation $\Delta\nu$ for an HB star with M=1.0 Msun from the ZAHB phase until the beginning of the asymptotic giant branch evolved in different DM densities. The considered DM particle has m_χ=4 GeV, σ χ,SI=10^{-39} cm2 and < σ v> = 3 10^{-26} cm^3 s^{-1}. The red dashed line flags the approximate region where the HB phase ends.

Stellar Clusters: "Asteroseismology of **Red Clump Stars** as a Probe of the Dark Matter Content of the Galaxy Central Region"

Constraints on Annihilating Dark Matter

Stars in the Galactic Centre

TÉCNICO LISBOA

Impact of DM Annihilation on Red Giant Stars

Dark sector: The research examines how WIMPs are captured, evaporated, and annihilated **in low-mass RG stars**, affecting their structure and evolution, $\boldsymbol{\rho_\chi = 10^4\ GeV cm^{-3}}$, $\boldsymbol{\sigma_\chi = 10^{-36}\ cm^2}$, $\boldsymbol{< \sigma v >_\chi = 10^{-26} cm^3 s^{-1}}$,**(Lopes & Lopes 2021).**

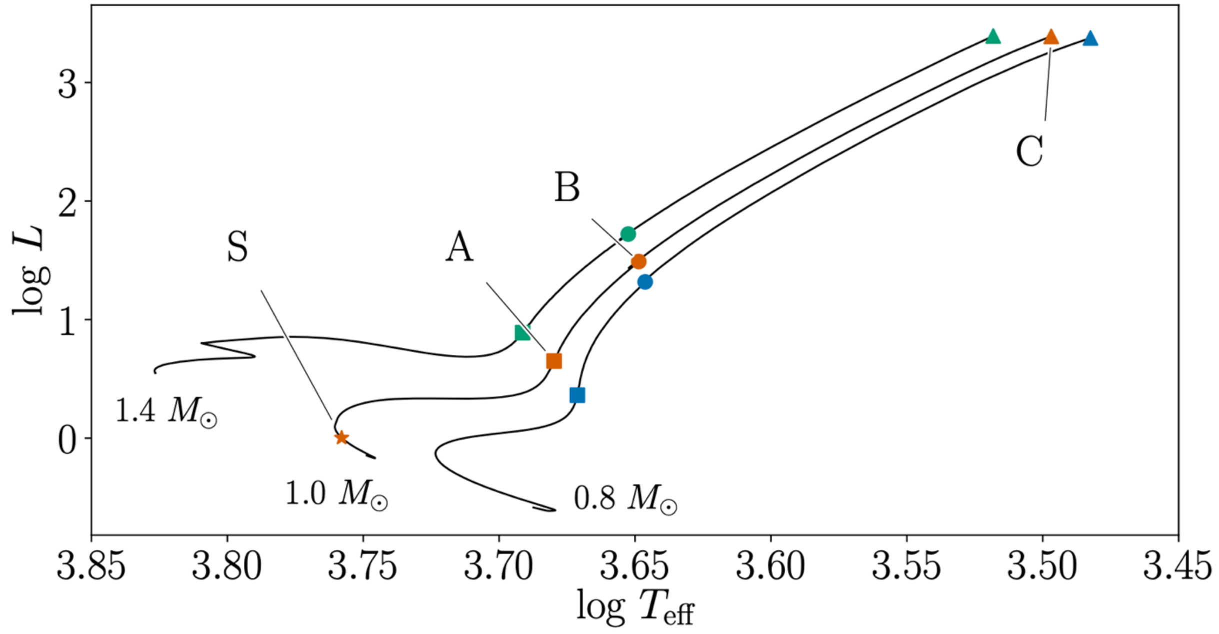

Hertzsprung-Russell (HR) diagram with the evolution of stars from the Zero Age Main Sequence (**ZAMS)** to the **Tip of the Red Giant Branch** (**TRGB**).

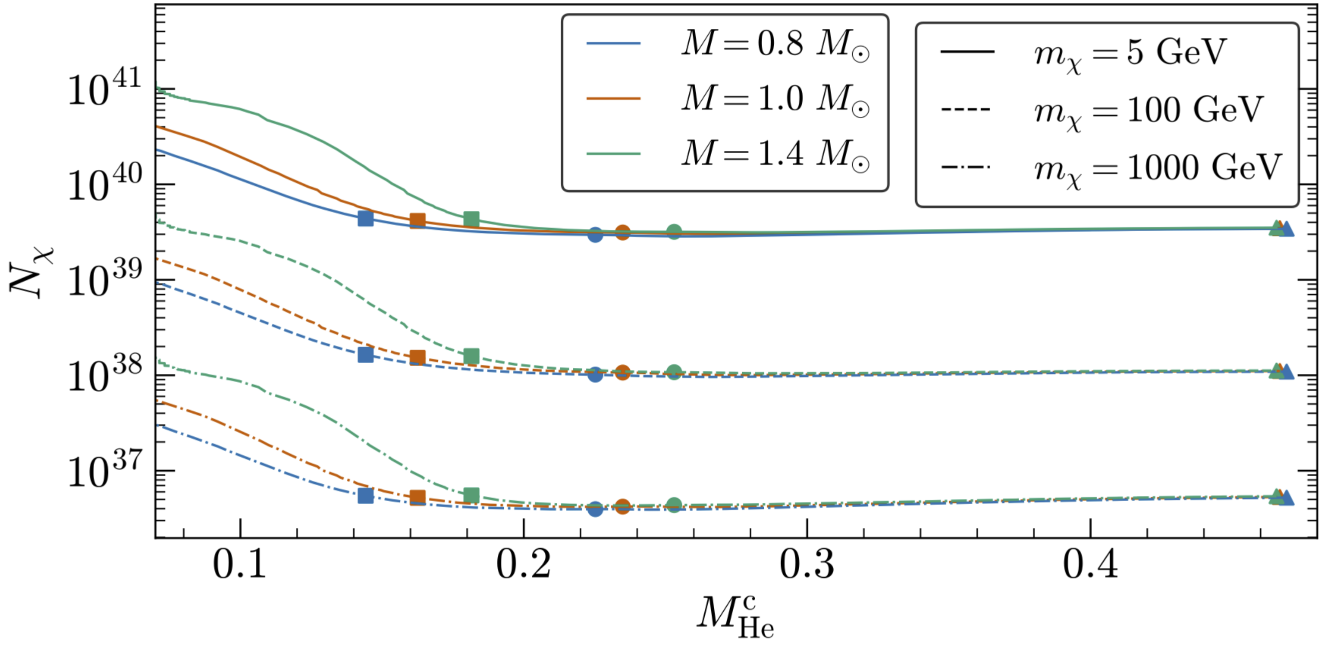

The total number of DM particles inside different stars with fixed metallicity during the RG branch phase, comparing stars of different masses and dark matter particle masses.

The helium core mass (M^c_{He}) is representative of the star's evolution during the RGB phase

Red Giant Star: The energy injected into the cores of low-mass red giant branch stars by the annihilation of WIMPs can trigger an early helium ignition, leading to a premature end of the RGB phase and a decrease in the luminosity at the TRGB, with significant deviations for light WIMPs in dense regions of the Milky Way.

It found that DM particles stay constant in these stars during the RGB phase, mostly independent of the star's mass and metallicity.

Impact of DM Annihilation on Red Giant Stars

Dark sector: The research examines how WIMPs are captured, evaporated, and annihilated **in low-mass RG stars**, affecting their structure and evolution, $\boldsymbol{\rho_\chi = 10^4\ GeV cm^{-3}}$, $\boldsymbol{\sigma_\chi = 10^{-36}\ cm^2}$, $\boldsymbol{<\sigma v>_\chi = 10^{-26} cm^3 s^{-1}}$,**(Lopes & Lopes 2021).**

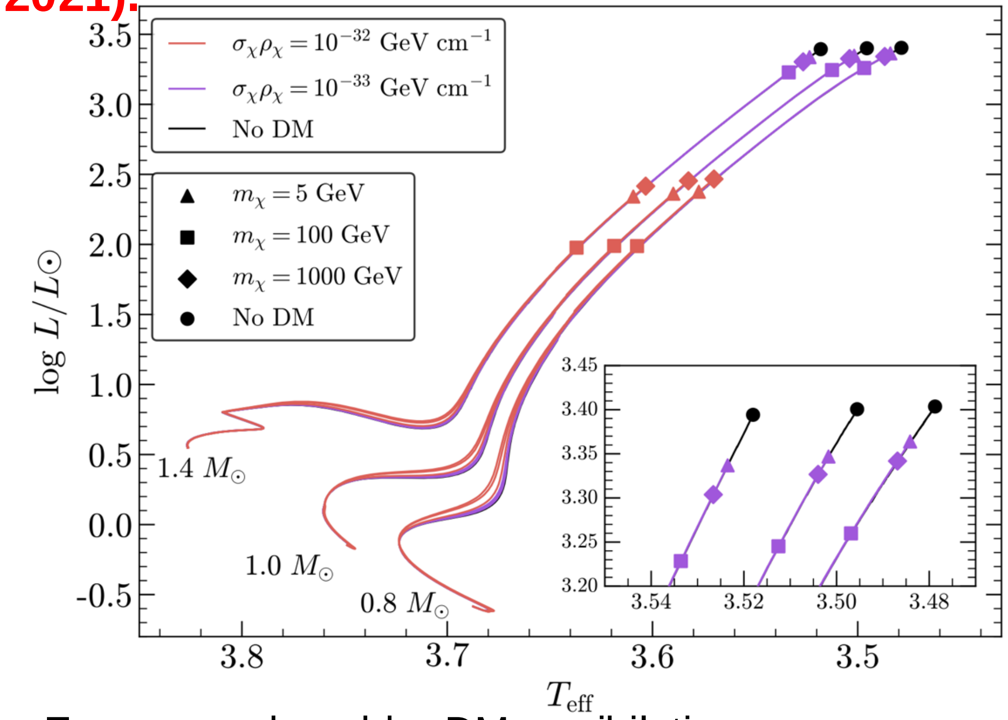

Energy produced by DM annihilation causes an early onset of helium ignition in the cores of RGB stars, resulting in a premature end to the RGB phase (**TRGB**).

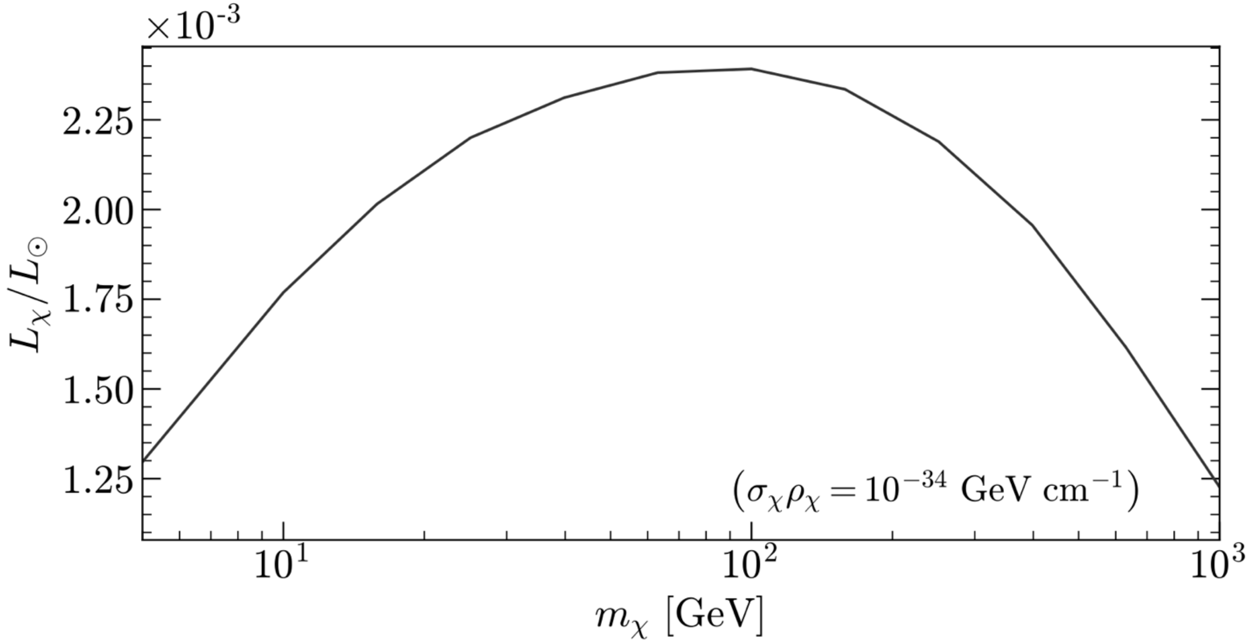

Relationship between the DM luminosity and the mass of DM particles for low-mass red giant branch (RGB) stars with the same luminosity $[Log\,(L/L_\odot) = 2]$.

Red Giant Star: DM particles accumulate inside low-mass red giant branch (RGB) stars, and the energy injected into the stellar core due to DM annihilation can promote conditions necessary for helium burning, leading to an early end of the RGB phase and a lower luminosity at the tip of the red giant branch (TRGB).

The most significant reduction in TRGB luminosity is observed for WIMPs with $\mathrm{m_\chi = 100\,GeV}$, which can cause the TRGB luminosity to be up to 76.4% lower than in the standard no-DM case.

Solar Neutrinos probe the Hidden Sector (dark matter and sterile neutrinos)

Standard Solar Model

Solar Neutrinos: limits to the hidden dark matter sector

Dark Sector (dark matter particle and sterile neutrino): interaction of DM particle and sterile neutrino with baryons, this leads to the following expression for cross section:

Asymmetric Dark Matter Model

Neutrino Model: $(\nu_e, \nu_\tau, \nu_\mu, \nu_s)$

Lopes (ApJ, 2018)

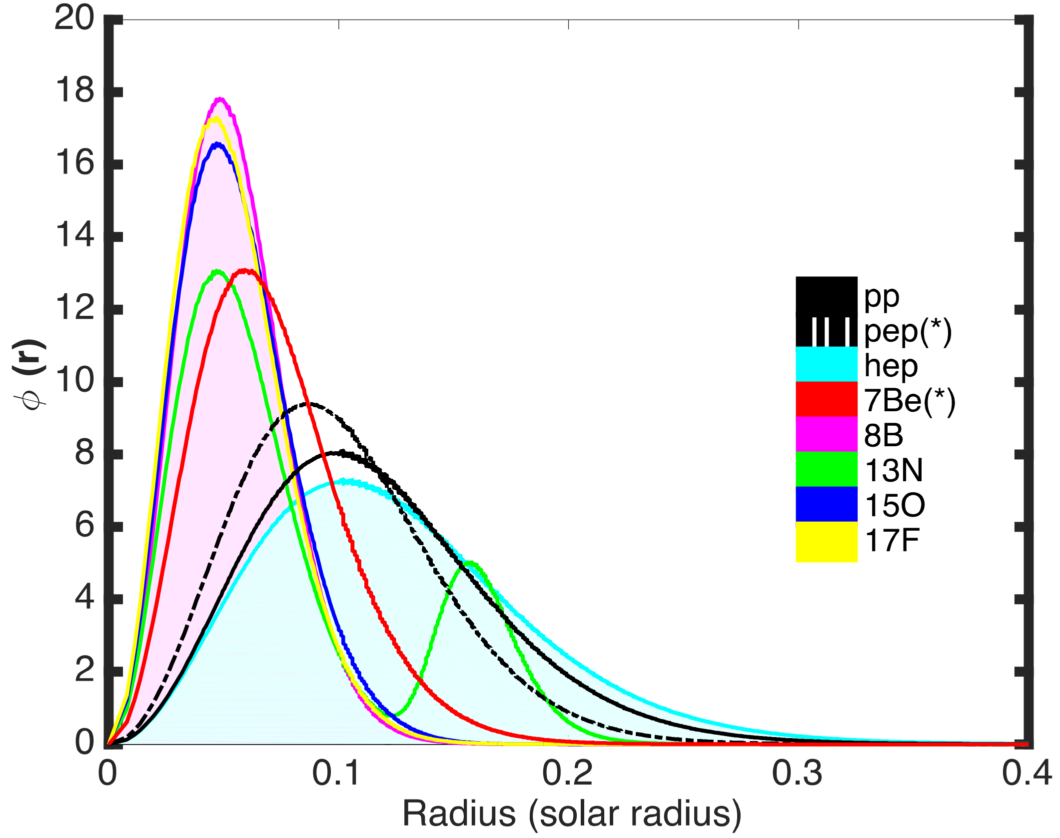

Helioseismology: The strength of the interaction of the dark matter particles with neutrinos depends on an effective coupling constant, $\mathbf{G}_\chi$, which is a Fermi constant analogue for the hidden sector. By using the latest 8B solar neutrino flux data, we found that $\mathbf{G}_\chi$, must be smaller than 0. 5 10^9 $\mathbf{G}_F$, for this particle physics model to be in agreement with the data.

Solar Neutrinos: limits to the hidden dark matter sector

Dark Sector (dark matter particle and sterile neutrino): interaction of DM particle and sterile neutrino with baryons, this leads to the following expression for cross section:

Lopes (ApJ, 2018)

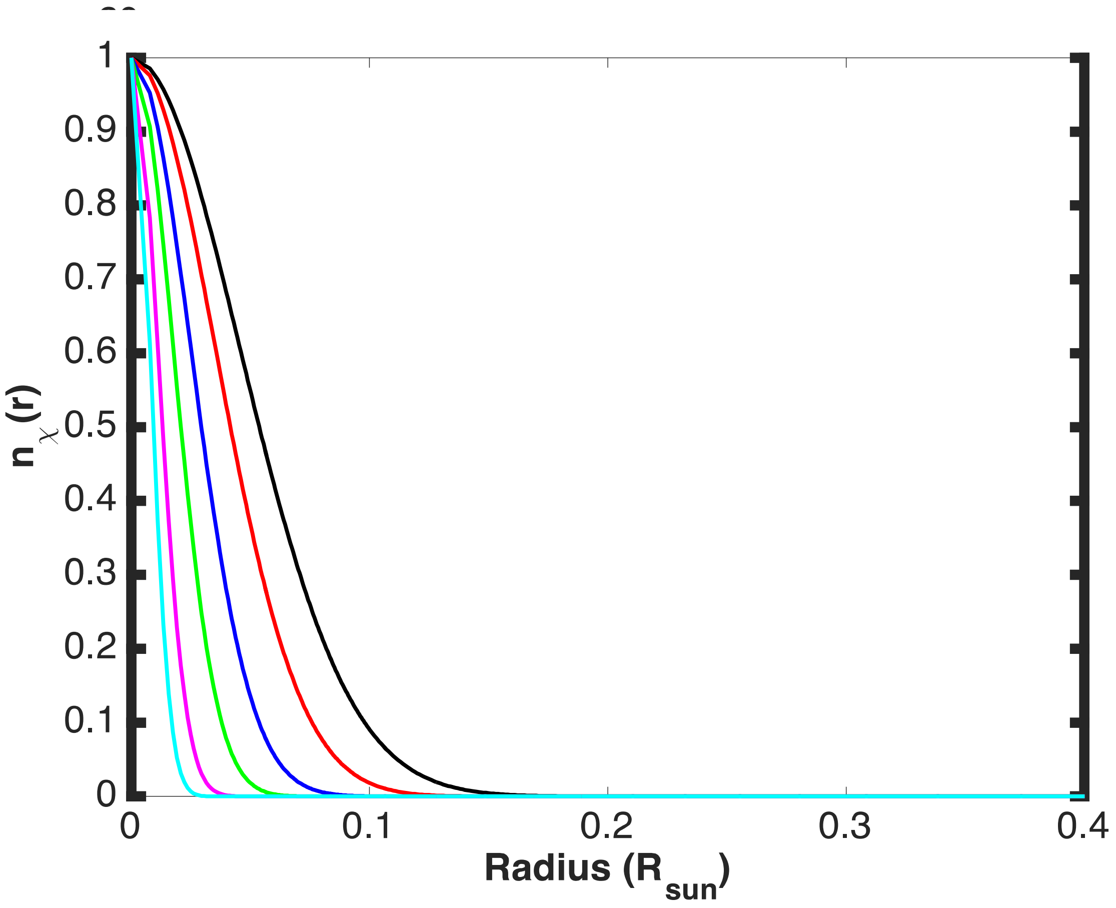

Asymmetric Dark Matter Model

Dark Matter density $n_\chi(r)$

Neutrino Model: (ν_e , ν_τ , ν_μ , ν_s)

Helioseismology: The strength of the interaction of the dark matter particles with neutrinos depends on an effective coupling constant, $\mathbf{G}_\chi$, which is a Fermi constant analogue for the hidden sector. By using the latest 8B solar neutrino flux data, we found that $\mathbf{G}_\chi$, must be smaller than 0. 5 10^9 $\mathbf{G}_F$, for this particle physics model to be in agreement with the data.

Solar Neutrinos: limits to the hidden dark matter sector

Lopes (ApJ, 2018)

Dark Sector (dark matter particle and sterile neutrino): interaction of DM particle and sterile neutrino with baryons, this leads to the following expression for cross section:

Asymmetric Dark Matter Model

Dark Matter density $n_{\chi}(r)$

Neutrino Model: (ν_e , ν_τ , ν_μ , ν_s)

MSW Matter oscillations n_e (r) and n_n(r)

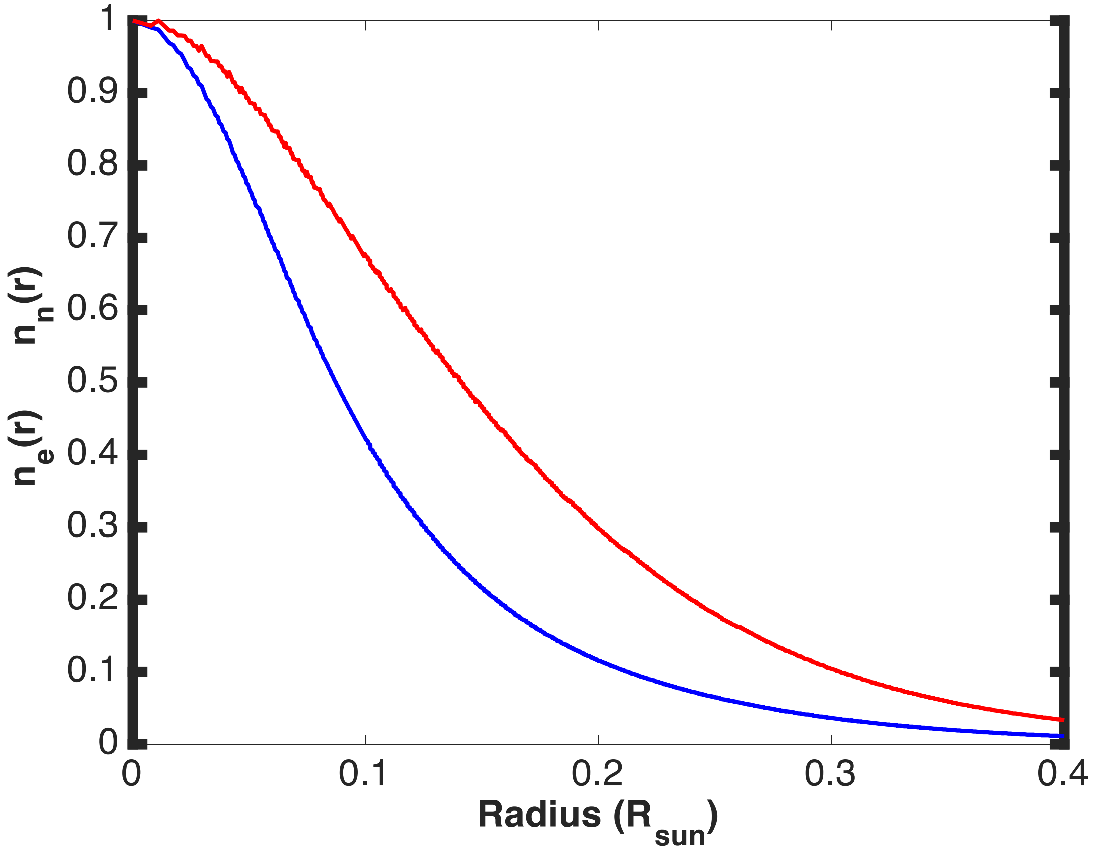

Helioseismology: The strength of the interaction of the dark matter particles with neutrinos depends on an effective coupling constant, $\mathbf{G_\chi}$, which is a Fermi constant analogue for the hidden sector. By using the latest 8B solar neutrino flux data, we found that $\mathbf{G_\chi}$, must be smaller than 0. 5 10^9 $\mathbf{G}_F$, for this particle physics model to be in agreement with the data.

Solar Neutrinos: limits to the hidden dark matter sector

Lopes (ApJ, 2018)

Dark Sector (dark matter particle and sterile neutrino): interaction of DM particle and sterile neutrino with baryons, this leads to the following expression for cross section:

Asymmetric Dark Matter Model

Dark Matter density $n_{\chi}(r)$

Neutrino Model: $(\nu_e, \nu_\tau, \nu_\mu, \nu_s)$

MSW Matter oscillations $n_e(r)$ and $n_n(r)$

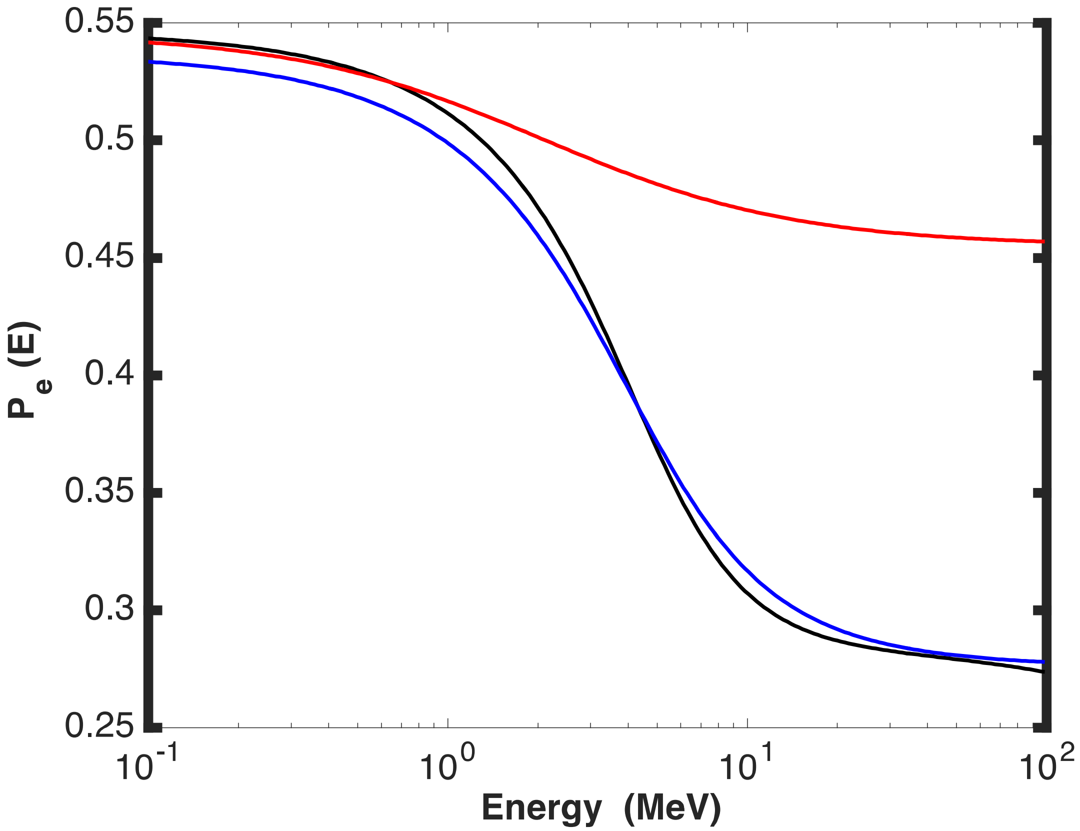

Helioseismology: The strength of the interaction of the dark matter particles with neutrinos depends on an effective coupling constant, $\mathbf{G}_{\chi}$, which is a Fermi constant analogue for the hidden sector. By using the latest 8B solar neutrino flux data, we found that $\mathbf{G}_{\chi}$, must be smaller than 0. 5 10^9 $\mathbf{G}_F$, for this particle physics model to be in agreement with the data.

Solar Neutrinos: limits to the hidden dark matter sector

Dark Sector (dark matter particle and sterile neutrino): interaction of DM particle and sterile neutrino with baryons, this leads to the following expression for cross section:

Lopes (ApJ, 2018)

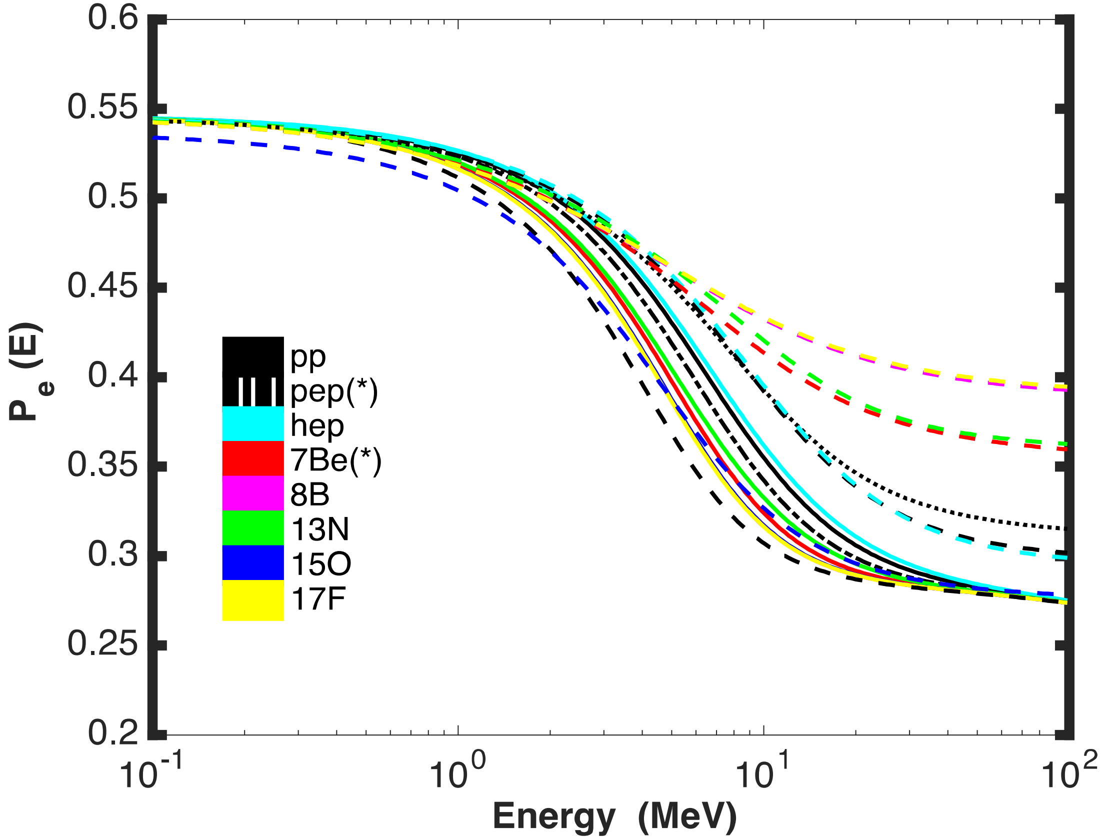

Asymmetric Dark Matter Model

Dark Matter density $n_{\chi}(r)$

Neutrino Model: $(\nu_e, \nu_\tau, \nu_\mu, \nu_s)$

MSW Matter oscillations $n_e(r)$ and $n_n(r)$

Helioseismology: The strength of the interaction of the dark matter particles with neutrinos depends on an effective coupling constant, $\mathbf{G}_\chi$, which is a Fermi constant analogue for the hidden sector. By using the latest 8B solar neutrino flux data, we found that $\mathbf{G}_\chi$, must be smaller than 0. 5 10^9 $\boldsymbol{G_F}$, for this particle physics model to be in agreement with the data.

Solar Neutrinos: limits to the hidden dark matter sector

Dark Sector (dark matter particle and sterile neutrino): interaction of DM particle and sterile neutrino with baryons, this leads to the following expression for cross section:

Asymmetric Dark Matter Model

Dark Matter density $n_\chi(r)$

Neutrino Model: $(\nu_e, \nu_\tau, \nu_\mu, \nu_s)$

MSW Matter oscillations $\mathrm{n_e(r)}$ and $\mathrm{n_n(r)}$

Lopes (ApJ, 2018)

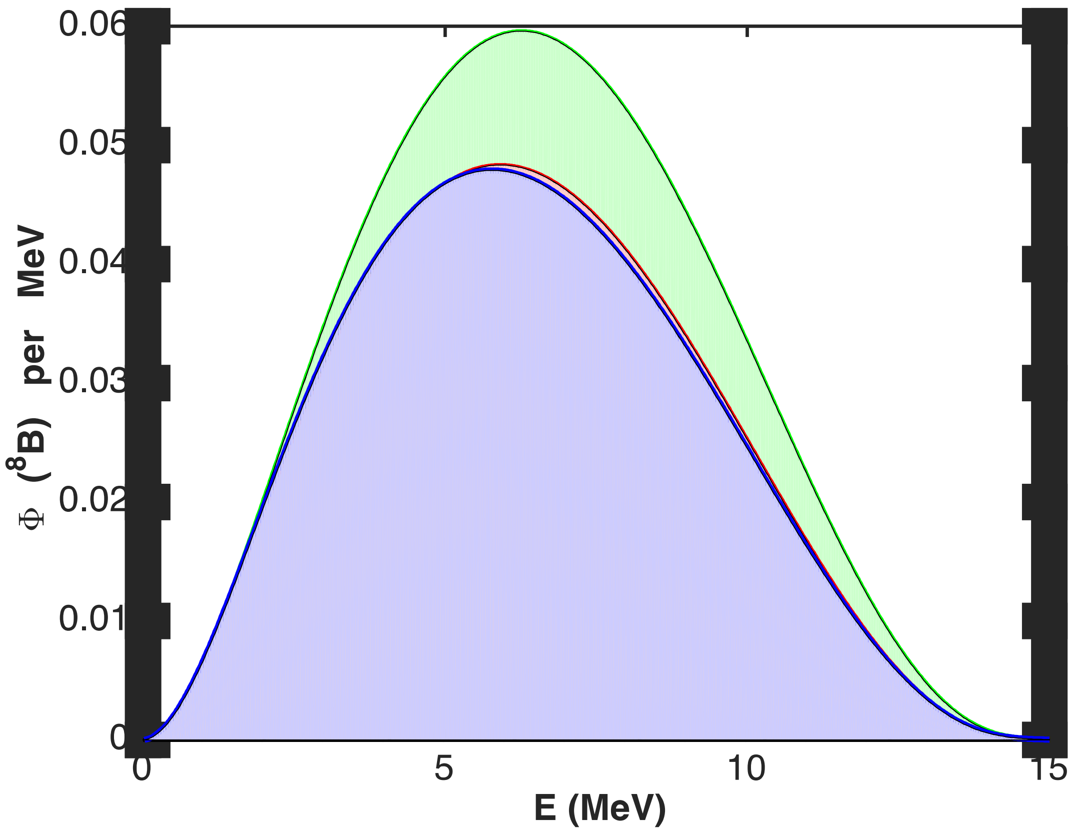

Helioseismology: The strength of the interaction of the dark matter particles with neutrinos depends on an effective coupling constant, $\mathbf{G_\chi}$, which is a Fermi constant analogue for the hidden sector. By using the latest 8B solar neutrino flux data, we found that $\mathbf{G_\chi}$, must be smaller than 0. 5 10^9 $\mathbf{G_F}$, for this particle physics model to be in agreement with the data.

Solar Neutrinos: limits to the hidden dark matter sector

Lopes (ApJ, 2018)

Dark Sector (dark matter particle and sterile neutrino): interaction of DM particle and sterile neutrino with baryons, this leads to the following expression for cross section:

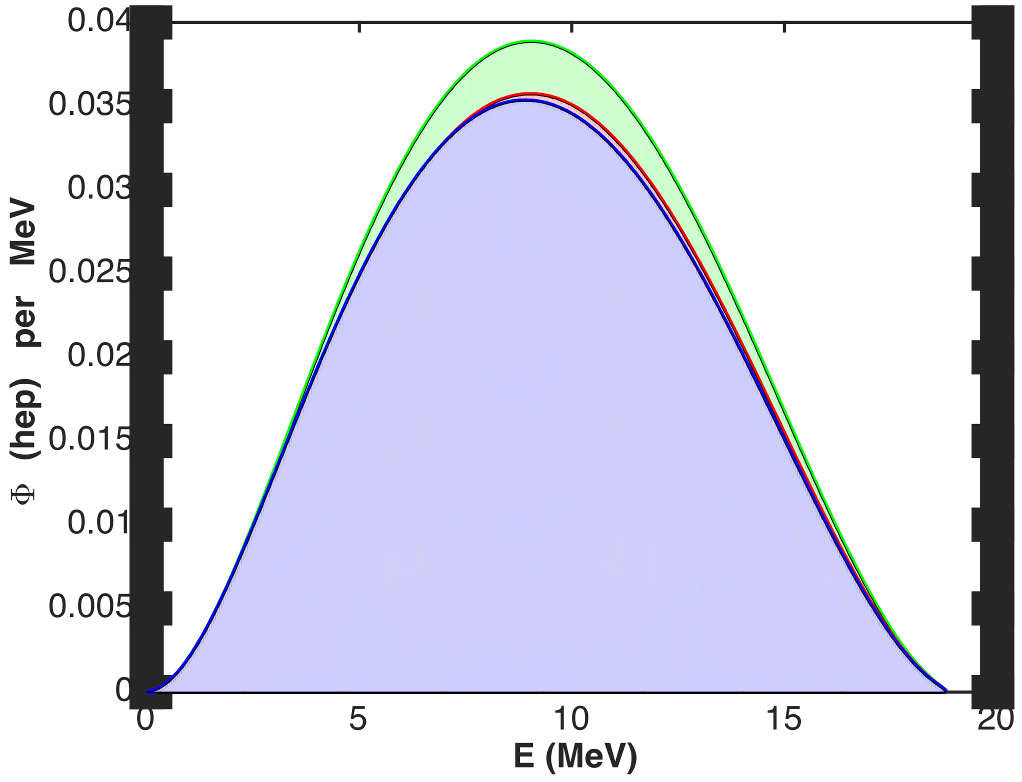

Asymmetric Dark Matter Model

Dark Matter density $n_\chi(r)$

Neutrino Model: $(\nu_e, \nu_\tau, \nu_\mu, \nu_s)$

MSW Matter oscillations $n_e(r)$ and $n_n(r)$

Helioseismology: The strength of the interaction of the dark matter particles with neutrinos depends on an effective coupling constant, $\mathbf{G}_\chi$, which is a Fermi constant analogue for the hidden sector. By using the latest 8B solar neutrino flux data, we found that $\mathbf{G}_\chi$, must be smaller than 0. 5 10^9 $\mathbf{G}_F$, for this particle physics model to be in agreement with the data.

Solar Neutrinos: limits to the hidden dark matter sector

Lopes (ApJ, 2018)

Dark Sector (dark matter particle and sterile neutrino): interaction of DM particle and sterile neutrino with baryons, this leads to the following expression for cross section:

Asymmetric Dark Matter Model

Dark Matter density $n_\chi(r)$

Neutrino Model: $(\nu_e, \nu_\tau, \nu_\mu, \nu_s)$

MSW Matter oscillations $n_e(r)$ and $n_n(r)$

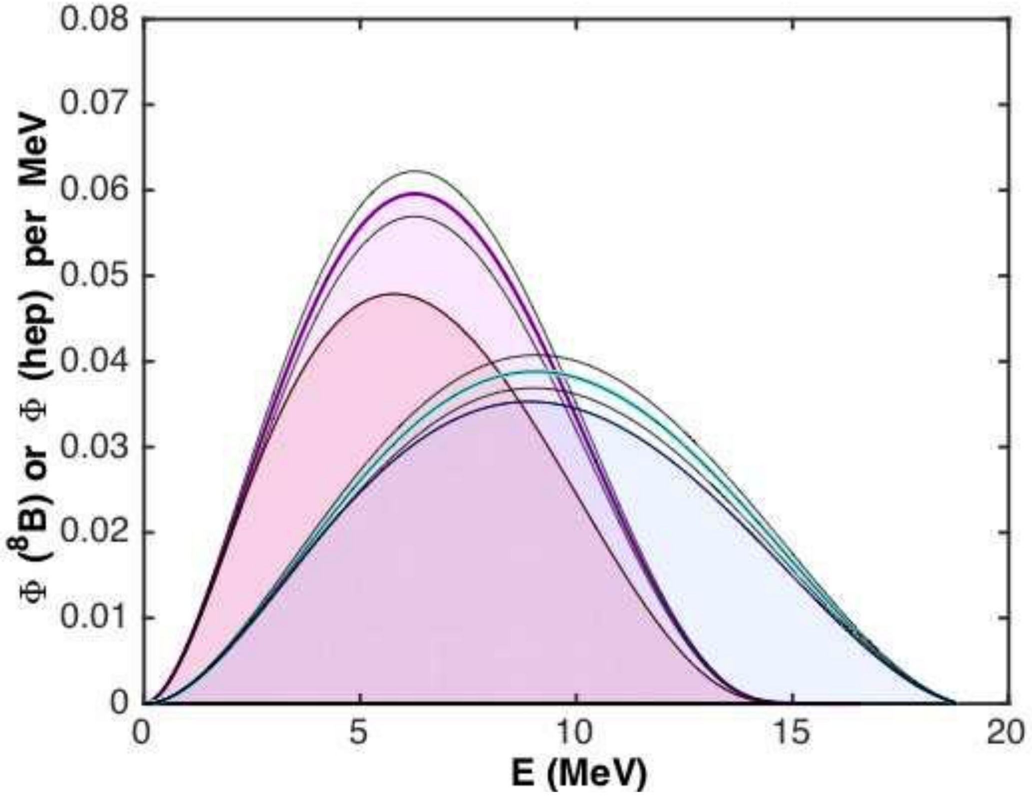

Helioseismology: The strength of the interaction of the dark matter particles with neutrinos depends on an effective coupling constant, $\mathbf{G}_\chi$, which is a Fermi constant analogue for the hidden sector. By using the latest 8B solar neutrino flux data, we found that $\mathbf{G}_\chi$, must be smaller than 0. 5 10^9 $\mathbf{G}_F$, for this particle physics model to be in agreement with the data.

Neutrinos from annihilating Dark Matter present in the Sun’s core

Helioseismology

TÉCNICO LISBOA

Limits on Thermally Annihilating Dark Matter from Neutrino Telescopes

Dark Sector : Neutrino flux (including neutrino flavour oscillations) resulting from the WIMP annihilation (with the annihilation rate $\langle \sigma v \rangle$) of two DM particles in the Sun is given by

I. Lopes, J. Lopes (2016)

$$\Phi_\nu = \frac{\Gamma_A}{4\pi r^2} \sum_i \mathrm{BR}_i \int \frac{dN_\nu}{dE_\nu} dE_\nu$$

$$\langle \sigma v \rangle (\mathrm{v}) = a + b \langle v^2 \rangle$$

p-wave annihilation

s-wave annihilation (standard)

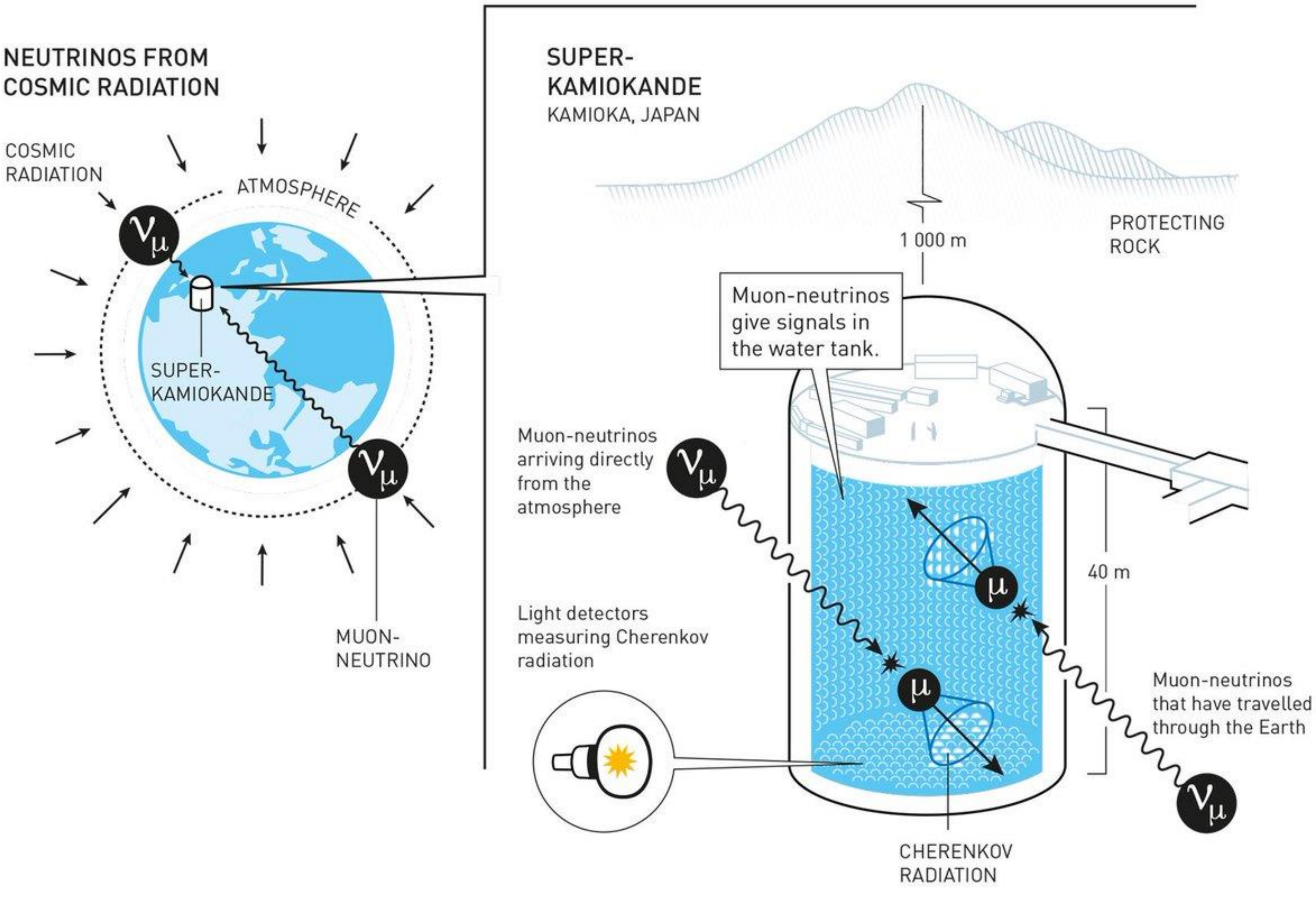

Illustration: © Johan Jarnestad/The Royal Swedish Academy of Sciences

Limits on Thermally Annihilating Dark Matter from Neutrino Telescopes

Dark Sector : Neutrino flux (including neutrino flavour oscillations) resulting from the WIMP annihilation (with the annihilation rate $\langle\sigma v\rangle$) of two DM particles in the Sun is given by

$$\Phi_\nu = \frac{\Gamma_A}{4\pi r^2}\sum_i \mathrm{BR}_i \int \frac{dN_\nu}{dE_\nu} dE_\nu$$

$$\langle\sigma v\rangle(\mathrm{v}) = a + b\,\langle v^2\rangle$$

p-wave annihilation

s-wave annihilation (standard)

Limits in the $\sigma_{\chi n}^{SD}$ scattering cross-section placed by the Super-Kamiokande and IceCube neutrino detectors.

I. Lopes, J. Lopes (2016)

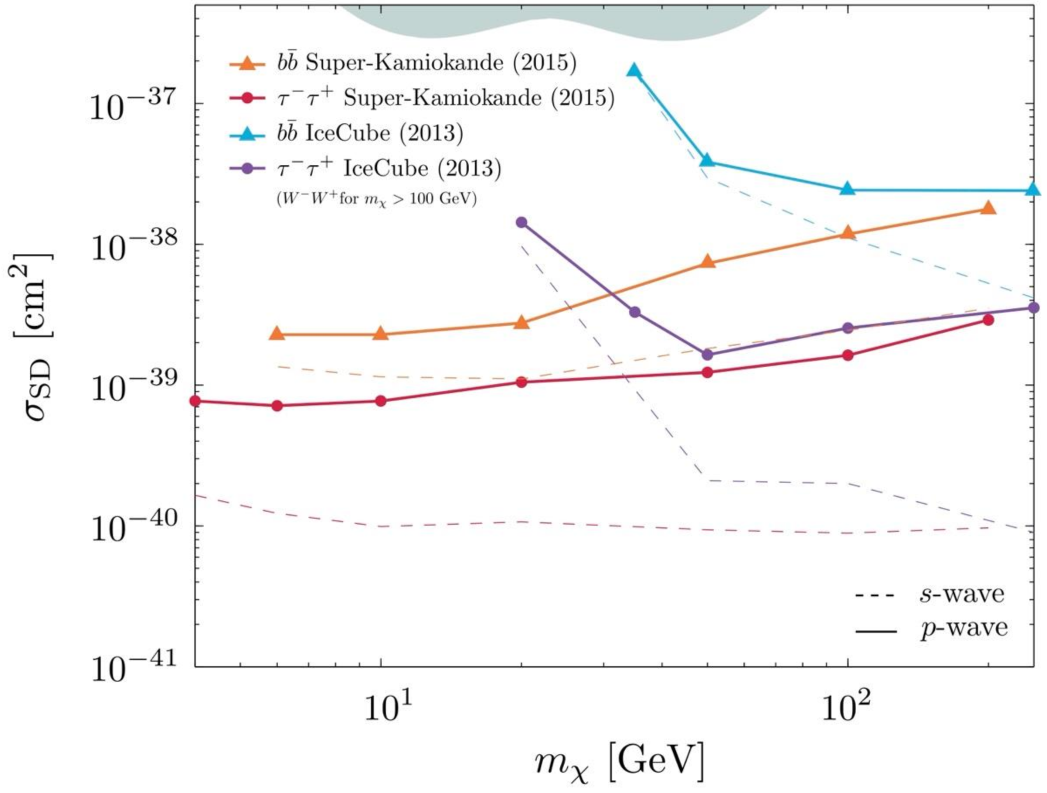

Spin dependent

Limits on Thermally Annihilating Dark Matter from Neutrino Telescopes

Dark Sector : Neutrino flux (including neutrino flavour oscillations) resulting from the WIMP annihilation (with the annihilation rate $\langle\sigma v\rangle$) of two DM particles in the Sun is given by

$$\Phi_\nu = \frac{\Gamma_A}{4\pi r^2}\sum_i \mathrm{BR}_i \int \frac{dN_\nu}{dE_\nu} dE_\nu$$

$\langle\sigma v\rangle(\mathrm{v}) = a + b\,\langle v^2\rangle$ p-wave annihilation

s-wave annihilation (standard)

Limits in the $\sigma_{\chi n}^{SD}$ and $\sigma_{\chi n}^{SI}$ scattering cross-section placed by the Super-Kamiokande and IceCube neutrino detectors.

I. Lopes, J. Lopes (2016)

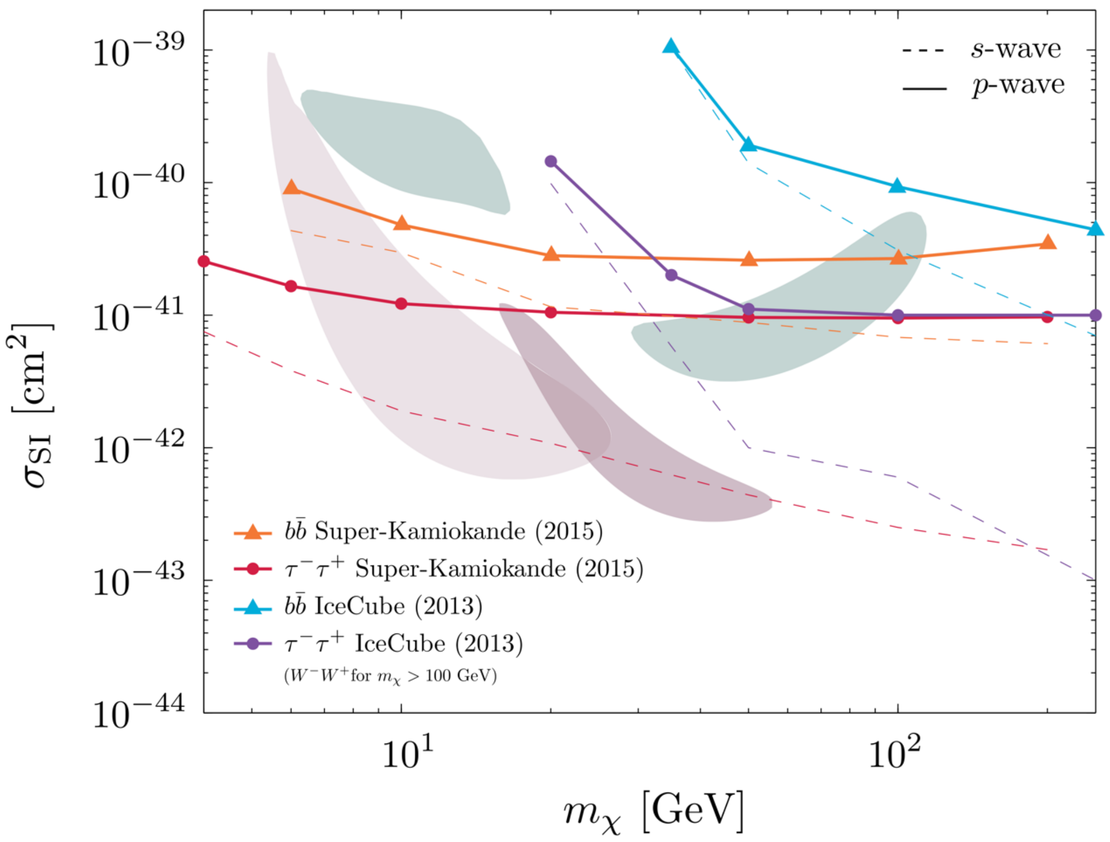

Spin independent

Limits on Thermally Annihilating Dark Matter from Neutrino Telescopes

Dark Sector : Neutrino flux (including neutrino flavour oscillations) resulting from the WIMP annihilation (with the annihilation rate $\langle\sigma v\rangle$) of two DM particles in the Sun is given by

$$\Phi_\nu = \frac{\Gamma_A}{4\pi r^2} \sum_i \mathrm{BR}_i \int \frac{dN_\nu}{dE_\nu} dE_\nu$$

$$\langle\sigma v\rangle(\mathrm{v}) = a + b\,\langle v^2\rangle$$

p-wave annihilation

s-wave annihilation (standard)

Limits in the $\sigma^{SD}_{\chi n}$ and $\sigma^{SI}_{\chi n}$ scattering cross-section placed by the Super-Kamiokande and IceCube neutrino detectors.

I. Lopes, J. Lopes (2016)

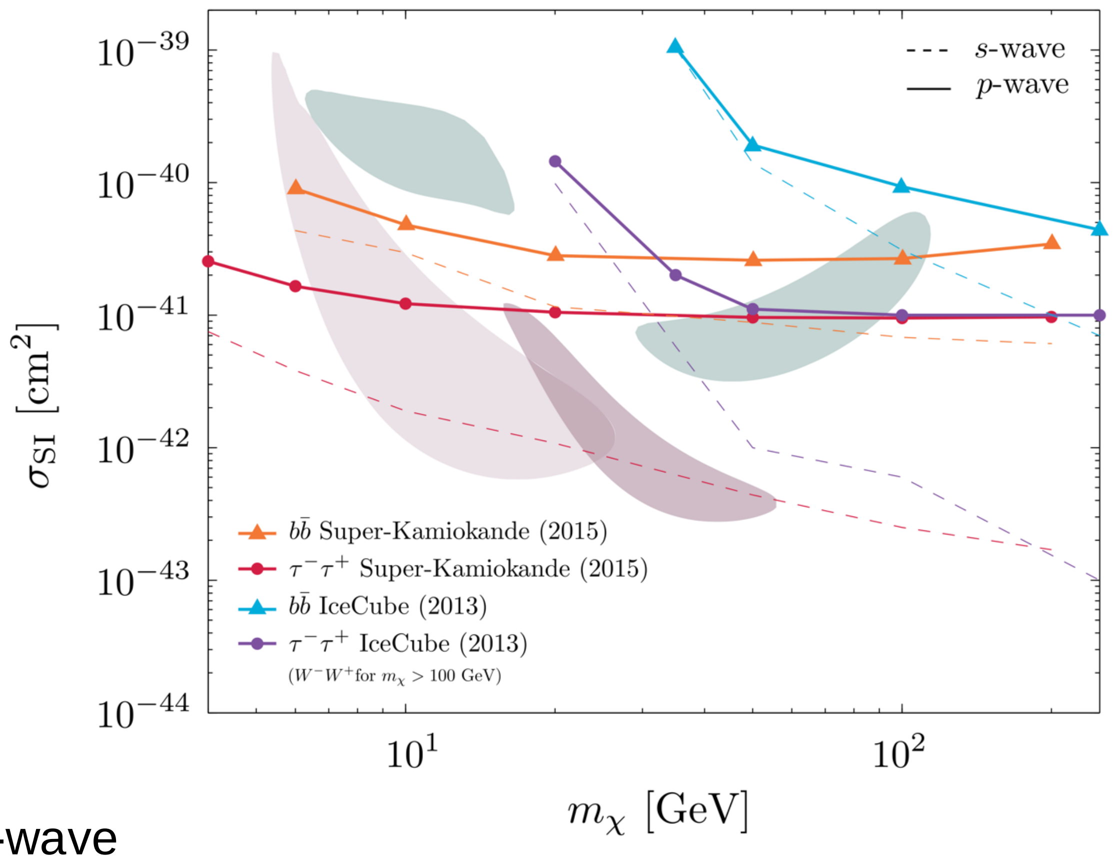

Spin independent

Helioseismology: Limits on the scattering cross-section for WIMPs for s-wave (dashed) and p-wave (dotted) annihilations, obtained from the IceCube (Aartsen et al. 2013) and Super-Kamiokande (Choi et al. 2015). The regions of interest obtained by direct detection experiments are also shown.

Limits on Thermally Annihilating Dark Matter from Neutrino Telescopes

Dark Sector : Neutrino flux (including neutrino flavour oscillations) resulting from the WIMP annihilation (with the annihilation rate $\langle\sigma v\rangle$) of two DM particles in the Sun is given by

$$\Phi_\nu = \frac{\Gamma_A}{4\pi r^2}\sum_i \mathrm{BR}_i \int \frac{dN_\nu}{dE_\nu} dE_\nu$$

$$\langle\sigma v\rangle(\mathrm{v}) = a + b\,\langle v^2\rangle$$

p-wave annihilation

s-wave annihilation (standard)

Limits in the $\sigma^{\mathrm{SD}}_{\chi n}$ and $\sigma^{\mathrm{SI}}_{\chi n}$ scattering cross-section placed by the Super-Kamiokande and IceCube neutrino detectors.

I. Lopes, J. Lopes (2016)

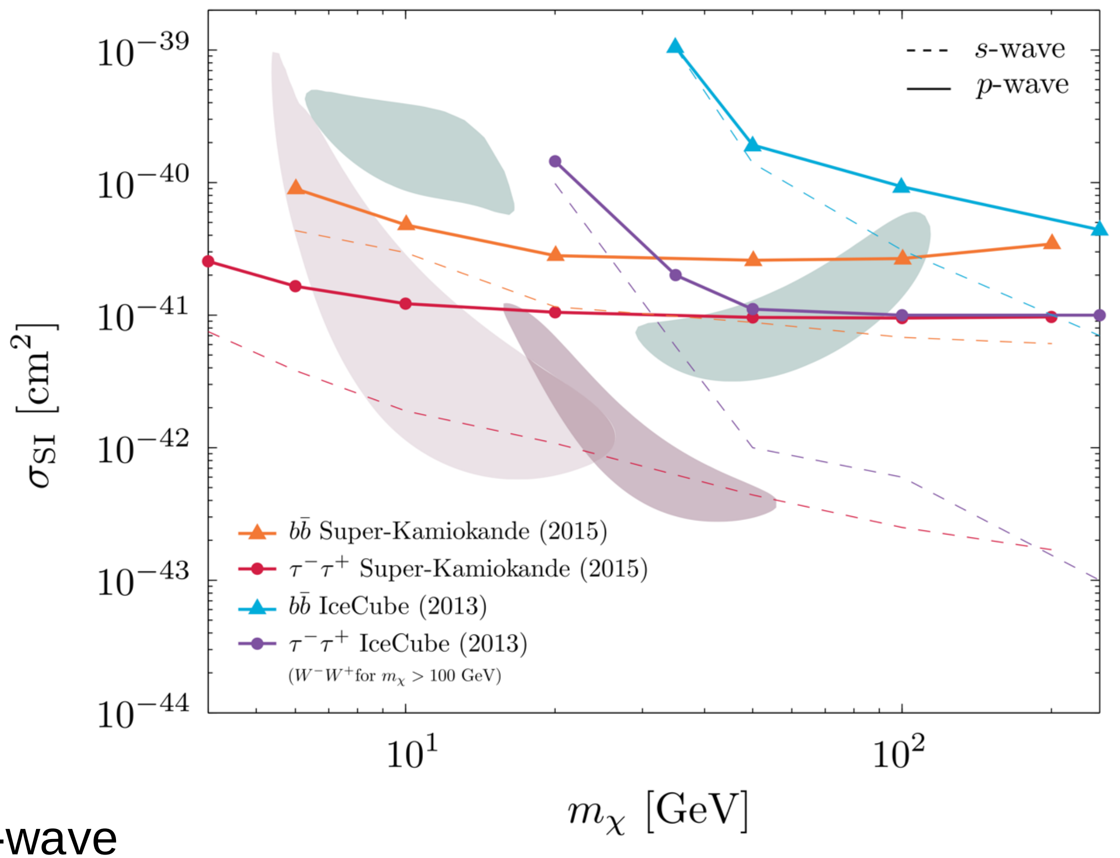

Spin independent

Helioseismology: Limits on the scattering cross-section for WIMPs for s-wave (dashed) and p-wave (dotted) annihilations, obtained from the IceCube (Aartsen et al. 2013) and Super-Kamiokande (Choi et al. 2015). The regions of interest obtained by direct detection experiments are also shown.

The favoured regions from different direct detection are also shown. **Pink: CDMS II Si** at 2σ C.L. (Agnese et al. 2013); **Green: DAMA/LIBRA** at 3σ C.L. (Bernabei et al. 2008); **Purple: CRESST**II at σ C.L. (Angloher et al. 2012).

Conclusion

Conclusion

The resolution of the dark matter problem will possibly be achieved through the development of an extension to the standard model of elementary particles, i.e., a dark matter sector made of one or more particles (stable and unstable) with their own set of rules.

A final resolution will be possible, not through efforts by a single field of research only, but more likely through an interdisciplinary approach to this problem, where the Stars can play an important **complementary role** to Cosmology and Particle Physics.

Thank You

Athens Symposium 2024

TÉCNICO LISBOA

centra
30th Anniversary